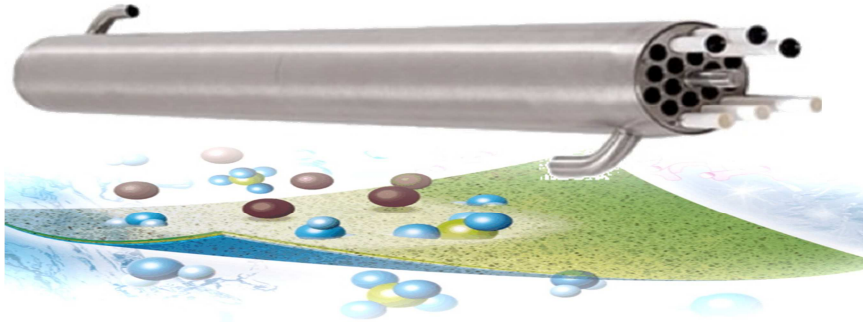




TÉCNICO
LISBOA



Evaluation of High Pressure Effects on Ultrafiltration Process Applied to Aqueous Inkjet Colorant

Inês Sofia Zambujo Pé-Leve

Dissertação para obtenção de Grau de Mestre em **Engenharia
Química**

Júri

Presidente: Prof^o José Madeira Lopes

Orientador IST: Prof^ª Maria Norberta de Pinho

Orientador *Fujifilm Imaging Colorants*: Mr. Gary Cuthbertson

Vogal: Prof^ª Ana Maria de Figueiredo Brites Alves

Novembro 2012

Acknowledgements

I am very grateful for the opportunity given to me by the Chemical Engineering Department of IST, and for being part of such a great company as Fujifilm Imaging Colorants. It was a very important experience for me both professionally and personally. I would like to thank to a few people who made this experience possible and who helped me to finish this important step in my life.

To **Mr. Gary Cuthbertson**, for all the help before and during my placement. For all the teaching and confidence in my work. And finally, for all the guidance, support and patience during the elaboration of my report.

To **Professor Maria Norberta de Pinho**, for all the guidance and for being willing to help me, despite my detachment.

To all the people in Process Technology Department, for receiving me very well and for helping me integrate into the team. In particular, to **Justin Harrison**, for all the teaching in the laboratory, all the support of my work and all the help with misfortunes at work. To **George McLay**, for being always willing to help me and for being such a good company in the lab. To **Tomonori Ogata**, for helping me to integrate since the very beginning and for sharing with me his experience as an engineer. To all, for being good friends.

To **Mrs. Margaret Symon**, for receiving me so well into her house and for treating me as family.

To my Portuguese friends, who always kept very close during my stay in Scotland, for their presence and encouragement.

To all my closer family, and especially to my parents and my sister, for encouraging and helping me to make this internship. For all the support and patience they offered me during the whole time.

Resumo

A purificação e concentração de uma solução aquosa de corante de impressão a jacto é realizada por ultrafiltração associada a diafiltração, usando módulos de membranas tubulares. O grau de pureza da tinta é determinante na qualidade do produto final e, conseqüentemente, na satisfação dos clientes.

Com o objectivo de melhorar a qualidade do produto e o rendimento do processo, foi feita a avaliação do impacto do aumento da pressão de operação nos principais parâmetros, quer do produto quer do processo. Foram processadas amostras em laboratório à pressão de produção em larga escala, 30 bar, e à pressão testada de 40 bar. Posteriormente foram comparados os resultados relativamente ao fluxo de permeado, à rejeição de impurezas, ao rendimento do processo, ao tempo de operação e à quantidade de água consumida.

O estudo demonstrou que o aumento da pressão levou ao aumento médio do fluxo de permeado em 6%. Os resultados sugerem que, operar a 40 bar, não apresenta benefícios relativamente à remoção de impurezas. Foi registada uma taxa de remoção de impurezas, em média, inferior à observada a 30 bar. Em particular, a rejeição ao ião metálico aumentou em média 3%. O fenómeno de polarização por concentração e os agregados moleculares, formados pelo polímero de base da tinta, contribuem para estes resultados. O rendimento obtido a 40 bar foi menor, e as perdas no permeado aumentaram 25%. Nestas condições há maior consumo de água durante a diafiltração. Concluiu-se que o aumento de pressão não traz vantagens relevantes ao processo.

Palavras-chave: Ultrafiltração, Diafiltração, Pressão, Polarização por concentração, Rejeição, Corante de impressão a jacto.

Abstract

An aqueous inkjet colorant is purified and concentrated by an ultrafiltration process with diafiltration, using tubular membrane modules. The purity of the colorant is determinant in the final product quality, to meet the final target specifications.

The aim is to improve the efficiency of the membrane process and it is proposed to evaluate how an increase in pressure will affect the main parameters of the product and the process. Samples were processed on a pilot membrane unit at 30 bar pressure, which corresponds to the pressure applied in the large scale production, and at the increased pressure, 40 bar. The permeate flux rates, impurities rejection, process yield, cycle time and number of wash volumes during diafiltration were compared and discussed.

The results showed that the increase in the pressure led to an increase in the permeate flux, on average, by 6%. The results suggest that, operating at 40 bar offers no benefits on the impurities removal. In general, it was observed a lower impurities removal rate at 40 bar pressure. In particular, the metal ion rejection increased, on average, by 3%. The concentration polarisation phenomenon and the molecular aggregates formed by the dye on the membrane surface contribute to the results observed. At 40 bar, the process yield obtained was lower, with an increase of 25% in the permeate colour losses. Under these conditions, the water consumption during diafiltration is higher. In conclusion, the results indicate that the increased pressure does not bring significant benefits to the process.

Keywords: Ultrafiltration, Diafiltration, Pressure, Concentration Polarization, Rejection, Inkjet Colorant.

Index of Contents

1	Thesis Introduction	1
1.1	Placement at Fujifilm Imaging Colorants	1
1.1.1	Overview of Fujifilm Group	1
1.1.2	Overview of Fujifilm Imaging Colorants	2
1.2	Process Development	4
1.3	State of Art	5
1.3.1	Membrane Technology	5
1.3.2	Membrane Filtration Technology in the Dye Industry	6
1.3.2.1	Purification and Concentration by Ultrafiltration.....	6
1.3.3	Ultrafiltration with Diafiltration Process	7
1.4	Objectives of the Thesis	10
2	Overview of Membrane Science and Technology	12
2.1	History of membranes: Science and Process.....	12
2.2	Membrane Processes	14
2.2.1	Pressure Driven Processes.....	16
2.2.1.1	Reverse Osmosis	17
2.2.1.2	Nanofiltration.....	18
2.2.1.3	Ultrafiltration	19
i.	Membrane Characterisation.....	20
ii.	Molecular Weight Cut-Off.....	20
iii.	Basic Working Principles of Ultrafiltration.....	20
iv.	Membrane Fouling	21
v.	Concentration Polarisation.....	22
vi.	Effect of Concentration Polarisation on Retention	23
vii.	Effect of Concentration Polarisation on the Membrane Flux.....	24
viii.	Diafiltration	26
2.2.1.4	Microfiltration.....	27
2.2.1.5	Applications of Pressure Driven Membrane Processes.....	28
2.2.2	System Design.....	29
2.2.3	Membrane Types and Materials	30
2.2.3.1	Microporous Membranes.....	30
2.2.3.2	Homogeneous Membranes.....	31
2.2.3.3	Asymmetric Membranes	31
2.2.3.4	Composite Membranes	32
2.2.4	Membrane Modules.....	32
2.2.4.1	Plate and Frame Modules.....	33
2.2.4.2	Spiral Wound Modules	34

2.2.4.3	Tubular Modules.....	34
2.2.4.4	Hollow Fibre Modules.....	35
3	Experimental Apparatus	36
3.1	Experimental Description.....	36
3.1.1	Material Processed	36
3.1.2	Membranes and Module.....	36
3.1.3	Membrane Unit.....	37
3.2	Experimental Procedure.....	40
i.	Initial CWF measurement.....	40
ii.	Ultrafiltration and Diafiltration Process.....	41
iii.	Final CWF measurement.....	42
iv.	Cleaning.....	43
3.3	Analytical Methods.....	43
3.3.1	Determination of Dye Strength by UV/Vis Spectroscopy.....	43
3.3.2	Determination of Metal Content by HPLC	44
3.3.3	Water Analysis.....	45
4	Results and Discussion.....	46
4.1	Membrane Characterisation	46
i.	Membrane Performance before and after a Cyan processing.....	46
ii.	Temperature Effect on the Flux Rate	49
4.2	Cyan Trials	50
4.2.1	Monitored Parameters and Mass Balance of a Cyan Trial.....	51
4.2.2	Comparison Between Trials at 30 and 40 bar Pressure	55
4.2.2.1	Permeate Conductivity Profile.....	55
4.2.2.2	Temperature Profile.....	56
4.2.2.3	Flux Rate Profile.....	56
4.2.2.4	Mass Balance to the Dye	59
4.2.2.5	Permeate Colour Losses	61
4.2.2.6	Impurities Removal	62
i.	Metal Ion Removal	62
ii.	Solvent Removal.....	67
iii.	EDTA Removal	69
4.2.2.7	Cycle Time and Wash Volumes.....	70
4.2.2.8	Membrane Performance and Limitations.....	73
4.2.2.9	Summary of Results Obtained at 30 and 40 bar	75
5	Conclusions.....	76
5.1	Further Work Proposals.....	78

Index of Tables

Table 1.1 - FFIC current activities ^[4]	3
Table 2.1 - Summary of general characteristics of some of the most industrial important membrane processes ^{[5][25]}	15
Table 2.2 – Principal differences between RO, NF, UF and MF ^{[8][25]}	16
Table 2.3 – Basic working principles of ultrafiltration ^[32]	21
Table 2.4 - Examples of Applications of pressure driven membrane processes ^{[9][33]}	28
Table 3.1 - Membranes characteristics.	36
Table 3.2 – Method of dye strength determination.	44
Table 3.3 - Specifications of DI water.	45
Table 4.1 - Hydraulic permeabilities at different temperatures, and R-squared for each linear relation.	47
Table 4.2 - Percentage of flux increase, from 30 to 40 bar, registered for pure water and for the Cyan-X.	59
Table 4.3 – Measurements for the mass balance of the Cyan-X run, at 30 bar.	59
Table 4.4 – Measurements for the mass Balance of Cyan-X run at 40 bar pressure.	60
Table 4.5 - Guidelines to avoid or minimise compaction applied to the experimental conditions.	74
Table 4.6 - Summary of the results compared at 30 and 40 bar pressure.	75
Table A.1 - Water characterisation at three different pressures, before a run of cyan.	81
Table A.2 - Water characterisation at three different pressures, after a run of cyan.	81
Table A.3 - Water characterisation at three different pressures, after the chemical cleaning.	81
Table B.1 - Experimental results of the Cyan-X run carried out at 30 bar pressure, used for the comparison in section 4.2.2.	82
Table B.2 - Experimental results of the Cyan-X run carried out at 40 bar pressure, used for the comparison in section 4.2.2.	83
Table C.1 - Results of free metal content in the permeate and concentrate samples collected during the runs.	84
Table C.2 - Results of solvent content in the permeate and concentrate sample collected during the runs.	84
Table C.3 - Results of ETDA content in the permeate samples collected during the runs.	85
Table C.4 - Measurements of strength of the permeate samples collected during the runs.	85

Index of Figures

Figure 1.1 - Breakdown Fujifilm Group revenue, year ended 31 March 2012 ^[1]	1
Figure 1.2 – The Fujifilm Group’s history ^[4]	2
Figure 1.3 - Relative sizes of common components in ink jet fluids ^[11]	7
Figure 1.4 – A typical trend of flux versus TMP for a tangential flow filtration process.	9
Figure 2.1 - Professor Sidney Loeb and engineer Ed Selover remove newly manufactured reverse osmosis membrane from plate-and-frame production unit ^[21]	12
Figure 2.2 - First spiral wound element, in 1953 ^[22]	13
Figure 2.3 - Milestones in membrane development.....	13
Figure 2.4 - Illustration of a semi-permeable membrane filtration process.....	14
Figure 2.5 - Filtration Spectrum ^[26]	16
Figure 2.6 - Relative size exclusion for reverse osmosis ^[27]	17
Figure 2.7 – Schematic representation of flow as function of applied pressure ^[28]	17
Figure 2.8 - Illustration of hydrostatic pressure causing reverse osmosis.....	17
Figure 2.9 – Relative size exclusion for nanofiltration ^[27]	18
Figure 2.10 - Relative size exclusion for ultrafiltration ^[27]	19
Figure 2.11 - Ultrafiltration flux as function of time of an electrocoat paint latex solution ^[24]	22
Figure 2.12 - Schematic drawing of the relationship between flux and applied pressure in ultrafiltration ^[28]	23
Figure 2.13 - Concentration polarization in ultrafiltration.....	24
Figure 2.14 – Effect of pressure on ultrafiltration flux for bovine serum albumin solutions ^[31]	26
Figure 2.15 – Cross-flow ultrafiltration system ^[9]	26
Figure 2.16 - Schematic continuous diafiltration operation.....	27
Figure 2.17 - Relative size exclusion for microfiltration ^[27]	27
Figure 2.18 – Filtration operating in cross-flow.....	29
Figure 2.19 – Filtration operating in dead-end flow.....	29
Figure 2.21 - General classification of synthetic membranes.....	30
Figure 2.20 – Comparison of flux rates and layer thickness.....	30
Figure 2.22 – Polyethersulphone molecular structure ^[23]	32
Figure 2.23 - Cross-section of ultrafiltration membrane. Asymmetric membrane ^[35]	32
Figure 2.24 - Plate and frame module ^[34]	33

Figure 2.25 - Spiral wound module [24].....	34
Figure 2.26 – Tubular membrane module [8].....	35
Figure 2.27 – Tubular ultrafiltration system with 30 tubes in series [24].....	35
Figure 2.28 - Hollow fibre module [24].	35
Figure 3.1 - Cross flow tubular membranes.	36
Figure 3.2 – Module and membranes used in the ultrafiltration experiments.	37
Figure 3.3 - PCI unit.	38
Figure 3.4 – Flow diagram of membrane filtration process in the PCI unit.....	39
Figure 3.5 – Flow diagram of the system in recirculation.	40
Figure 3.6 - Flow diagram of the system during concentration.	41
Figure 3.7 - Flow diagram of the system during diafiltration.....	42
Figure 3.8 - Schematic chromatogram.	45
Figure 4.1 - Linear representation of the water flux rate versus applied pressure, at constant temperature, before the Cyan-X processing.....	47
Figure 4.2 - Linear representation of the flux rate versus applied pressure, at constant temperature, after the Cyan-X processing.....	47
Figure 4.3 - Comparison of the flux rates for pure water before and after (including after cleaning) a run of Cyan-X.....	48
Figure 4.4 - Percentage of membrane performance obtained after the run and after the cleaning, at 30 and 40 bar.	49
Figure 4.5 – Representation of the flux rate versus temperature, at constant pressure.....	50
Figure 4.6 - Molecular structure of CuPC [37].	50
Figure 4.7 - Spreadsheet of a typical run in PCI.	51
Figure 4.8 - Permeate conductivity profile versus time, of a Cyan-X run.....	52
Figure 4.9 – Temperature profile versus time, of a Cyan-X run.....	52
Figure 4.10 - Flux rate profile versus time, of a Cyan-X run.....	53
Figure 4.11 - Mass balance of the filtration process.....	54
Figure 4.12 - Measurements of the optical density of the permeate samples, of the referred trial.....	54
Figure 4.13 - Permeate conductivity profiles at 30 and 40 bar pressure.....	55
Figure 4.14 - Temperature profiles at 30 and 40 bar pressure.....	56
Figure 4.15 - Comparison of the flux rates at 30 and 40 bar pressure.	56

Figure 4.16 - Comparison of the flux rates showing the different stages of the filtration. R – recirculation, C – concentration, W – washing.	58
Figure 4.17 - Effect of pressure on Cyan - X ultrafiltration.	58
Figure 4.18 - Mass balance of Cyan-X run at 30 bar.	60
Figure 4.19 - Mass balance of Cyan-X run at 40 bar pressure.	60
Figure 4.20 - Colour loss rate through the permeate of the runs at 30 and 40 bar.....	61
Figure 4.21 - Colour loss rate at 30 and 40 bar, showing the different stages of the filtration process.	62
Figure 4.22 - Metal content profile in the concentrate and permeate, during UF process.	63
Figure 4.23 - Copper content profile in the concentrate.	63
Figure 4.24 - Copper content profile in the permeate.....	63
Figure 4.25 - Copper rejection and transmission at 30 bar pressure.....	64
Figure 4.26 - Copper rejection and transmission at 40 bar pressure.....	64
Figure 4.27 - Metal rejection at 30 and 40 bar pressure, showing the different stages of the filtration process.....	65
Figure 4.28 - Model of the aggregate formed by the dye molecules ^[38]	66
Figure 4.29 - Model of the CuPc molecule, CuC ₃₂ N ₈ H ₁₆	66
Figure 4.30 - Solvent content profile in the permeate and concentrate, during UF process.	67
Figure 4.31 - Solvent content in the concentrate, at 30 and 40 bar.	67
Figure 4.32 - Solvent content in the permeate, at 30 and 40 bar.	67
Figure 4.33 - Solvent removal rate, at 30 and 40 bar pressure.....	68
Figure 4.34 - Molecular structure of EDTA.	69
Figure 4.35 - EDTA content profile in the permeate, at 30 and 40 bar.....	69
Figure 4.36 - Rate of EDTA removal at 30 and 40 bar.....	70
Figure 4.37 - Overview of the cycle time of some runs of Cyan-X, at 30 and 40 bar.....	71
Figure 4.38 - Comparison of the cycle time, showing the different filtration stages, at 30 and 40 bar, runs PCI/1283 and 1284.....	71
Figure 4.39 - Comparison of wash volumes required at 30 and 40 bar pressure, differentiating the filtration stages.	72
Figure 4.40 - Initial CWF measurements of several runs on PCI. Experimental conditions: 30 or 40 bar pressure, temperature of 25°C, pump speed 5.....	73
Figure D.1 – Example of one of the measurements of free metal by HPLC.....	86

List of Abbreviations

RO – Reverse Osmosis

NF – Nanofiltration

UF – Ultrafiltration

DF - Diafiltration

MF - Microfiltration

CuPc – Copper phthalocyanine

DI – De-ionised

CWF – Cold water flux

PES – Polyethersulphone

OD – Optical density

HPLC – High-performance liquid chromatography

TMP – Transmembrane pressure

WV – Wash volumes

MW – Molecular weight

MWCO – Molecular weight cut off

EDTA – Ethylenediamine tetraacetic acid

Nomenclature

J – Permeate Flux

$v_{p,w}$ – Pure water flux

ΔP – Pressure differential

$\Delta \pi$ – Osmotic pressure differential

L_p – Hydraulic permeability coefficient

μ_w – Water viscosity

μ_s – Solute viscosity

C – Concentration

V - Volume

C_b – Bulk concentration

C_m – Concentration on the membrane surface

$C_{f,s}$ – Feed concentration of solute s

$C_{p,s}$ – Permeate concentration of solute s

R_s – Rejection to component s

R_m – Membrane resistance

R_s – Resistance due the deposition of the solute

k – Overall mass transfer coefficient

A – Absorbance

I_0 – Incident radiation

I_1 – Transmitted radiation

1 Thesis Introduction

1.1 Placement at Fujifilm Imaging Colorants

1.1.1 Overview of Fujifilm Group

Fujifilm Holdings Corporation is the holding company of the Fujifilm Group having three operating companies: Fujifilm Corporation, Fuji Xerox Co. Ltd. and Toyama Chemical Co. Ltd. and a shared services company, Fujifilm Business Expert Corporation [1].

Fujifilm Group has, in addition to the conventional business field of “Imaging and Information”, become a company that contributes to the development of culture, science, technology and industry, as well as improving health and environmental concerns across society. The three business fields are the Imaging Solutions, Information Solutions and Document Solutions.

The breakdown of group business revenue, year ended 31 March 2012, is displayed in Figure 1.1

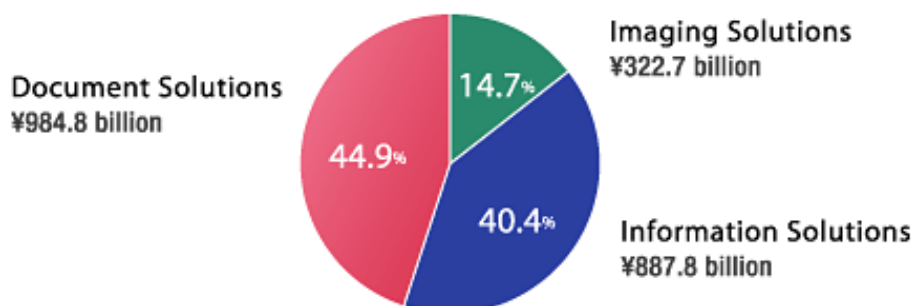


Figure 1.1 – Breakdown of Fujifilm Group revenue, year ended 31 March 2012 [1].

Fujifilm Group has wide range of chemical synthesis knowledge, which has been refined over the years through the development of photographic technology, advanced nanotechnology and unique drug development capability.

Recently, the priority business fields have been: the medical/life sciences such as medical equipment, pharmaceuticals, functional skin care cosmetics and nutritional supplements; graphic arts such as printing materials and equipment; documents such as office equipment/printing; optical devices such as camera phone lens units; highly functional materials such as LCD materials; digital imaging such as digital cameras, digital printing, and photobooks.

Regarding the corporate history, the group was established in 1934 with the aim of producing photographic films. Over the decades Fujifilm has expanded in several markets and acquired some groups.

During this growth into a global corporation, there is also history of innovation, which extends from photography and printing to medicine life science.

After the first 10 years of being established, in the 1940s, the group expanded into markets such as the optical glasses, lenses and equipment, having also penetrated the medical and electronic imaging fields. In 1962, Fuji Xerox Co. Ltd. was established as joint venture with U.K.-based Rank Xerox Limited. In the 1980s, the group expanded its production overseas, both in Europe and in USA. In the last 10 years, with the increase in digital technology, the group implemented management reforms transforming its business structures. A summary of the history of the group is shown in Figure 1.2.

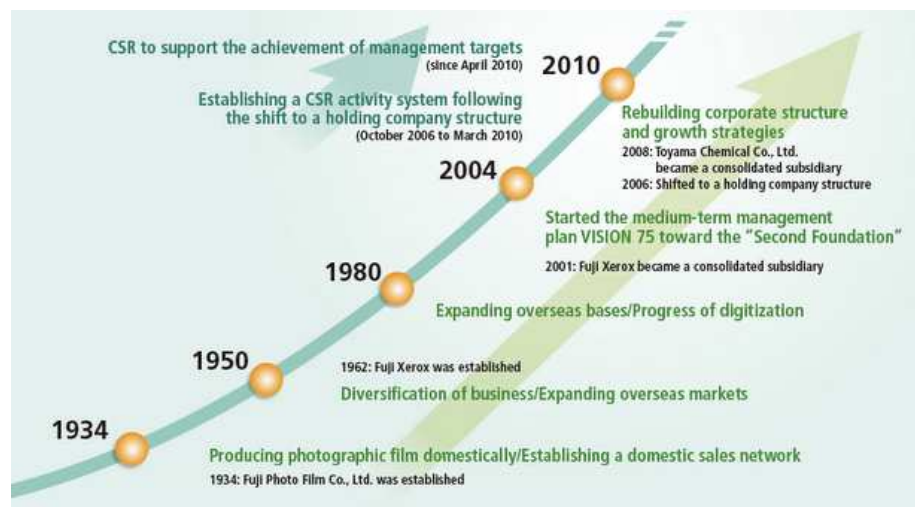


Figure 1.2 – The Fujifilm Group’s history [4].

1.1.2 Overview of Fujifilm Imaging Colorants

Fujifilm Imaging Colorants was formed when Avecia Inkjet, a spin-off from ICI, was acquired by Fujifilm in February 2006. However, the business started in the 1920’s with the invention, development and production of aqueous dyes for textile applications, run at the time by Imperial Chemical Industries (ICI). Later, in the 1980s, the R&D in inkjet became more significant and it continued growing under Zeneca management. The Inkjet business then became the market leader between 1999 and 2006, after having been acquired by Avecia.

At £150 million, it was an excellent investment opportunity for Fujifilm, who have invested significantly in its further development, since the acquisition [2].

Nowadays, Fujifilm Imaging Colorants (FFIC) is a world leader in the development and supply of high performance colorants for the global digital printing market. This achievement is based on a 25-year track record of product innovation, a strong proprietary technology and patent portfolio, complemented

by extensive development and manufacturing capabilities. All of this has been followed by the highest standards of safety, health & environmental performance.

The main activities developed by Fujifilm Imaging Colorants are described in the Table 1.1. The first three products are for inkjet printing, the chemical toners for laser printers and photocopiers and finally infrared absorbers for special applications.

Table 1.1 - FFIC current activities ^[4].

Pro-Jet™ Aqueous Dye-Based Liquids	Custom designed for ink jet printing and suitable for a wide variety of ink, substrates and image quality requirements.
Pro-Jet™ Aqueous Inks	Based in competencies in organic chemistry, resin/polymer chemistry, allows aqueous inkjet progress into new applications.
Pro-Jet™ Aqueous Pigment Dispersions	FFIC's proprietary reactive dispersant technology has produced a step change in pigment dispersion performance for aqueous ink formulators.
Pro-Color™ Chemically Produced Toners	Patented technology provides base or formulated toners to meet specific printer or copier requirements for the electrophotographic industry.
Pro-Jet™ Infrared Absorbers	Applications in laser imaging, automatic identification, polymer laser welding, and fuel marking.

FFIC comprises of two legal entities, Fujifilm Imaging Colorants Limited and Fujifilm Imaging Colorants, Inc. operating as an independent organization within the Fujifilm Industrial Products Group. It employs more than 250 people across three principal sites ^[4]:

- Blackley, Manchester, England
- Grangemouth, Scotland
- New Castle, Delaware, USA

The manufacture of the PRO-JET™ and PRO-COLOR product ranges is carried out in Grangemouth and New Castle, Delaware, USA.

Although FFIC holds a leading position, the market is increasingly dynamic and competitive, which leads to a constant need for research and development activity.

FFIC Grangemouth, in addition to manufacturing capabilities, has invested in process development, with the contribution of staff technologically trained, with a high proportion of employees holding PhDs. At Grangemouth, 65 employees are involved in new product development and receipt of R&D. The company enjoys excellent relations with UK's major universities, and also with international scientists, especially from countries where the chemical industry is less established [4].

The plant at Grangemouth manufactures the primary dye colorants – cyan, magenta, yellow and black, supported by the laboratories, located in Process Technology Department, where the inks are developed, tested and contribute to troubleshooting of plant problems.

Due to the effort put into safety, health and environmental issues, FFIC at Grangemouth has been rewarded with five Gold Award from the Royal Society for the Prevention of Accidents, supporting a well developed occupational health and safety management systems culture.

1.2 Process Development

The placement at FujiFilm Imaging Colorants lasted for 6 months, plus an extension of 6 additional months. All the work carried out was in the Membrane Technology Team responsibility, which has a significant role within the Process Technology (PT) Department, in both R&D projects and as support to the large scale production unit. The placement involved membrane processing as part of the development projects and for supply of samples to costumers. Gathering of data from the trials and appropriate report were an important contribution for the studies carried out in PT.

The work carried out involved two different products, aqueous inkjet colorants and aqueous pigment dispersions, although most of the work focused in the former one, and it was the product on which this thesis study was made.

The study presented for this thesis is about one specific colorant but the work in the laboratory involved the processing of several different types of products and their corresponding formulations.

1.3 State of Art

1.3.1 Membrane Technology

The process industries produce a wide variety of chemicals and components, which in most cases requires separation, concentration, or purification of a range of materials. These species include reagents, chemicals used in manufacture, intermediates, products and undesirable products. One of the biggest challenges is providing an efficient separation process for those industrial chemical processes, some are absolutely critical, such as: to obtain high-grade products in the food and pharmaceutical industries, to supply communities and industry with high-quality water, or to remove or recover toxic or valuable components from products.

Conventional separation techniques, like distillation, precipitation, crystallization, extraction, adsorption, ion-exchange, etc., have been replaced and/or complemented by processes with membranes as separation barriers^[5].

The benefits of membrane technology can be summarised as follows: separation can be carried out continuously, energy consumption is generally low, membrane processes can easily be combined with other separation processes (hybrid processing), separation can be carried out under mild conditions, up-scaling is easy, membrane properties are variable and can be adjusted.

The large-scale industrial utilisation began around 1970 with the production of potable and high quality industrial water. Since then, membranes have gradually become an option in process engineering, with a significant technical and commercial impact.

Today, membranes are used on a large scale in different areas, and are the separation process chosen for the production of a wide variety of products. Membrane technology is used to produce potable water from sea and brackish water, to clean industrial effluents and recover valuable constituents, to concentrate, purify, or fractionate macromolecular mixtures in the food and drug industries, and to separate gases and vapours in petro chemical processes. They are still a key component in energy conversion and storage systems, in chemical reactors, in artificial organs and in drug delivery devices.

The industrial areas where membrane technology is used are: food and beverages, metallurgy, pulp and paper, textile, pharmaceutical, automotive, dairy, biotechnology, chemical industry, etc. Water treatment, either for domestic or industrial water supply and environmental applications are also very important membrane processes.

The progress achieved with the research on membrane processes efficiency, has led to the development of new membrane based unit operations in process engineering, such as membrane contactors and membrane reactors^[6].

1.3.2 Membrane Filtration Technology in the Dye Industry

Membrane filtration is routinely used by a wide variety of process industries to concentrate, purify and improve final product quality. Its popularity within the dye industry is growing as dye manufacturers discover that this technique is a reliable and cost effective mean of improving yield and product quality, where repeatable purification and concentration are required [7].

The technology is now being applied widely for dye manufacturing and textile colorants. The largest application in the dye industry is dye desalting and concentration of the finished product, which is most commonly applied to reactive dyes, but can also be used on other products such as sulphur and direct dyes. Desalting is the process that removes salts in the manufacture of both powder and liquid dyestuffs. The dye, retained by the membrane, is desalted and concentrated, increasing its strength by reducing the inorganic content and the amount of water.

Membranes are also used with the many types of aqueous dyes. In this case the technology can be utilised for concentration and purification.

In dye production there are the following main uses for membranes: improvements in the quality of the finished product, increase yield, savings in raw materials, recovery of product from waste, and increase dryer capacity.

In the dye manufacture and application there is a continual search for production methods that will improve product yield and reduce manufacturing costs and membrane technology is an important contributor [8].

1.3.2.1 Purification and Concentration by Ultrafiltration

Many dyes are too small to be retained by a UF membrane, but aggregated dyes are an exception. Whether recovered by UF or RO, it has been established that recovered dyes can be reused in dyeing operations with no issues meeting all colour specifications. UF has also been evaluated as a method for purification of aggregated dyes. As expected, these dyes are rejected completely by the membrane [9].

It has been found that when a feed solution made up of an aqueous colorant of molecular weight above 1000 Daltons (colorant, colorant precursors, colorant degradation products, salts and impurities of molecular weight below 1000 Daltons) is pumped through a semipermeable membrane under ultrafiltration conditions in a diafiltration mode, it is obtained: a permeate enriched in impurities and a retentate enriched in colorant of MW above 1000 Daltons [10].

Ink jet fluids are comprised of components and contaminants of various sizes. Figure 1.3 shows the relative sizes of components and contaminants commonly found in ink jet fluids.

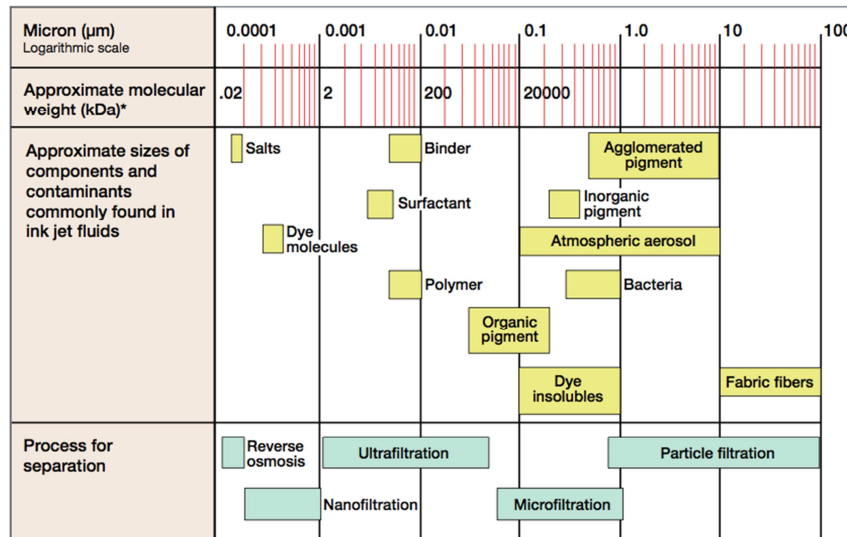


Figure 1.3 - Relative sizes of common components in ink jet fluids [11].

Cross flow technology can be used to separate these components and contaminants in the following applications: removal of impurities from pigmented aqueous colorants, classification of pigmented dispersion for inks and colorants, dye purification and waste stream management [11].

1.3.3 Ultrafiltration with Diafiltration Process

Diafiltration is a tangential flow filtration that can be performed in combination with any of the other categories of separation, namely ultrafiltration, to enhance both product yield and purity [12]. Constant-volume diafiltration is the more commonly used control mode. To perform a constant-volume DF, a solvent, mainly water, is added to the recycle tank at the same rate that the filtrate is removed. The total volume of the retentate remains constant throughout the process, thus this mode of operation requires some method of level control that will meter the addition of water. The other common mode of diafiltration is the batch DF. These processes are used for clarifying, concentrating and purifying proteins [12].

Membrane diafiltration is a well established technique and has found many applications in the food and beverage, chemical, biotechnological and pharmaceutical industries. Batch system design is of both industrial and academic interest, including active areas on purification of oligosaccharides, recovery of high-value product from process waste stream, fractionation of whey proteins, diafiltration of milk, desalting of dye and pigments, recovery of products from fermentation broth, removal of humic substances, etc [13].

Diafiltration results in the dilution of the retentate and thus hereby alleviates the problems associated with the built-up concentration boundary layer on the membrane surface. It has been reported that diafiltration combined with membrane separation could be an efficient tool to enhance the purity of

the retained stream without any mechanical enhancement of the membrane module ^[14]. Also, the addition of pure solvent avoids an excessive concentration of the retentate, which would cause an increase in the effects of concentration polarisation and fouling, leading to a decrease of the permeate flux. This process can also cause a positive effect due to the reduction in viscosity of the retentate, facilitating its pumping through the system.

The use of diafiltration is now a state of art technique in food and beverage, biotechnology and pharmaceutical industries. It was shown that diafiltration in conjunction with cross-flow filtration significantly enhances the purity of the separation of proteins by employing a continuous washing of the retained solutes on the membrane. Studies by Arabelle et al. ^[14] have employed ultrafiltration to separate α -lactalbumin from casein whey applying different modes of diafiltration in conjunction with UF.

In a study, developed in 2012, to optimize the production of soy protein filtration with low phytic acid content by membrane separation, it was determined that the most promising means to effect the purification is tangential flow ultrafiltration and diafiltration ^[15].

Another industry where UF and DF are applied is the dairy industry. The conventional method of whey concentration is by thermal evaporation, but it has several drawbacks related with energy consumption and the high content of ashes and lactose that remain in the concentrate. Ultrafiltration is a very attractive alternative method, which has been used in the dairy industry in the recovery and fractionation of milk components, allowing a more economical concentration process. Diafiltration is used for the production of whey-protein concentrate with a high protein content. DF is used for protein purification to eliminate problems associated with high concentrations in the retained product, generating high purification, while retaining good membrane performance ^[16].

One of the biggest problems of ultrafiltration with diafiltration, and of all the membrane processes, is the decline of permeate flux with time. Previous studies show that this decrease is caused by the accumulation of feed components in the membrane pores (membrane fouling) and also on the membrane surface (concentration polarisation and gel layer) ^[17]. Some researchers have attempted to describe the mechanism of transport through a membrane in different pilot scale systems. Analysis of permeate flux is mainly carried out by using one of the models: gel-polarisation model, osmotic pressure model or resistance in series model. The gel-polarisation model is used to describe the case that the transmembrane pressure is large enough to form a gel layer on the membrane surface and the membrane permeation rate is limited without the influence of further increasing the TMP. In the osmotic pressure model, during the ultrafiltration of macromolecules, the osmotic pressure is constantly rising due to an increasing surface concentration. At constant TMP, this increase in osmotic pressure as a function of surface concentration leads to lower fluxes. Falling permeate flux in the resistance in series model is owing to the resistances caused by fouling or solute adsorption and concentration polarisation.

Therefore, reducing the fouling is always a major challenge in applications of membrane filtration. A number of methods have been investigated. The concept of critical flux, first introduced by Field et al., is a hydrodynamic manipulation method that is intended to avoid severe fouling of the membrane. The application of critical flux theory during membrane filtration has been reviewed by Pollice et al. and Bacchin et al. [18]. At a critical flux condition, the drag forces on solute molecules concentrated over the membrane surface are equal to the dispersive forces by flow shear stress near the membrane surface, and this leads to a nearly constant long-term flux with negligible fouling. A number of researches have demonstrated that critical flux may increase with enhancing cross flow rate and decrease with increasing feed concentration. Since feed concentration may be diluted by adding solvent during diafiltration, it is possible to operate diafiltration in the critical flux condition to remove most permeable solutes without severe fouling, and diluted feed could also reduce the fouling load during post-concentration [18].

Regarding the optimisation of ultrafiltration/diafiltration tangential flow systems, operating parameter selection has a very significant impact as the process is scaled to full-scale manufacturing levels. The goal is to obtain a process with the following success criteria: superior product quality, consistent and high product yield, reproducible process flux and time and a cleaning regime that allows extended membrane reuse. Thus, one of the experiments that should be considered during the processing methodology is the impact of transmembrane pressure and feed flow on process flux and contaminants retention [19].

The optimisation guide to ultrafiltration/diafiltration developed in 2003 by *Millipore* [12], defines the optimal TMP for protein concentration as described in Figure 1.4.

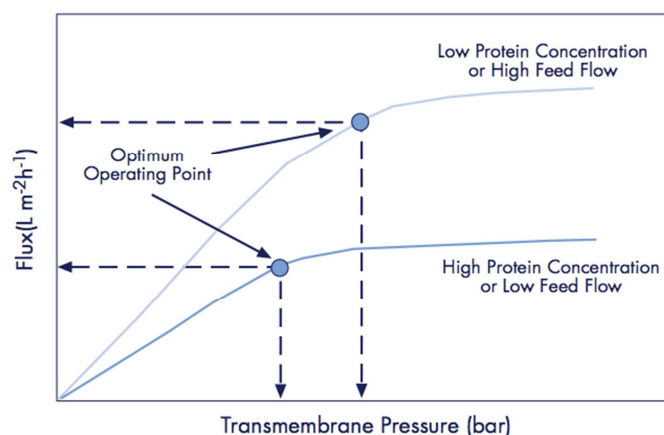


Figure 1.4 – A typical trend of flux versus TMP for a tangential flow filtration process.

In a tangential flow filtration unit operation, permeate flux increases with increasing pressure up to a point and then it levels off. The first part of the curve, where the flux increases with pressure, is the

pressure dependent regime. In this regime the main limiting flux factor is the fouled membrane resistance. The second part of the curve is the pressure independent regime. Here the concentration of solute at the membrane surface is high and a significant part of the applied pressure is working against the osmotic pressure. As the feed concentration increases or feed flow rate decreases, the TMP at which the flux stabilises decrease.

Running the process in the pressure independent regime, maximum flux is achieved and this minimises the required membrane area. However, the solute wall concentration is high and could exceed a solubility limitation, leading to yield losses. On the other hand, running the process in the pressure dependent regime, fluxes are lower and more membrane area is required. Therefore, for a standard UF/DF process, the optimum pressure at which to run a process is at the knee of the curve, where nearly the highest flux is achieved without exerting excessive pressure or reaching exceedingly high solute wall concentration.

1.4 Objectives of the Thesis

Ultrafiltration processes with diafiltration have widely been applied in pharmaceutical, food, dairy and chemical industries. However, there are very few studies that include the effects of variables (pressure, temperature, feed circulation rate, etc) on the ultrafiltration process in the dye industry context. Therefore, the main objective of this thesis is to study the overall high pressure effects on ultrafiltration process applied to an aqueous inkjet colorant. This study will allow on understanding of the actual applied pressure on the process if it is the optimum operation pressure or if it can be further optimised. Inkjet colorants are high value products, thus the optimisation should be carefully investigated fully.

As previously indicated, the high solute wall concentration is a characteristic phenomenon of UF/DF processes. Besides that, the filtration of the aqueous inkjet colorant studied in this thesis, is characterised by the formation of molecular aggregates on the membrane surface, which affect the removal of impurities. In different circumstances, these impurities would easily permeate an UF membrane. Therefore, this thesis aims to study the effect of increased pressure for these specific conditions.

The production of the aqueous inkjet colorant, namely the Cyan dye, includes a filtration stage. The solution of colorant that is feed to the filtration unit, is constituted of the colorant itself, water, organic solvent, metal ions and EDTA. The impurities, which are the organic solvent, metal ions and the EDTA, are removed in the permeate and the dye is concentrated by ultrafiltration with diafiltration using cross-flow tubular membranes. The diafiltration is crucial to allow high impurities removal, in order obtain a highly purified final product.

In the large scale production of Cyan, the membrane modules operate at 30 bar pressure, but according to the membrane supplier, these membranes can operate up to 40 bar. These values of

operating pressure are uncommonly high and it became necessary to study the increase pressure effects in order to optimise the final product quality and the process yield. Additionally there are no restrictions related with the feed pumps. The following aims of the thesis can be detailed as follows:

Pressure effects on the product quality:

- Study of the impurities removal rates at 30 and 40 bar, giving more relevance to the rejection of a specific metal ion.

Pressure effects on the process yield:

- Comparison of mass balance;
- Measurement of the permeate colour losses.

Pressure effects on the process parameters:

- Study the pressure effects on the permeate flux, temperature, permeate conductivity, number of wash volumes required during diafiltration and cycle time of the operation.

Pressure effects on the membrane performance:

- Study the membrane performance drop at 30 and 40 bar pressure, predicting the pressure effect on the membranes damage.

With successful achievement of these aims, the results will contribute to an overall evaluation of advantages and disadvantages of increased applied pressure in the purification and concentration process of an aqueous inkjet colorant.

2 Overview of Membrane Science and Technology

2.1 History of membranes: Science and Process

Membranes and membrane processes are not a recent invention, as they have been part of our daily life for a long time. The early studies on membrane permeation were carried out using natural materials. In 1752 Nollet recognised a relation between a semipermeable membrane and the osmotic pressure, recording the first studies about the discovery of osmosis. He discovered that a pig's bladder passes preferentially ethanol, when it is used as a barrier between a water/ethanol mixture and pure water.

In the following century studies arose about permeability and artificial preparation of membranes. A very important step in membrane science and technology was achieved with the development of a reverse osmosis membrane based on cellulose acetate, which granted high salt rejection and high fluxes at moderate hydrostatic pressures [Reid et al., 1959; Loeb et al., 1964] [6]. This represented the major advance towards the application of membranes as an effective technique for the production of potable water from the seawater.

In 1958 Sidney Loeb joined Sourirajan in a project that later, in 1962, would lead to the practical large-scale use of membranes in osmosis reverse. Researchers considered that, among the commercially available flat sheet membranes, the membrane developed by Loeb and Sourirajan held the most promise for osmosis because it offers the highest permeation flux for a given osmotic driving force [20]. This membrane had an asymmetric structure with a dense skin at the surface, which determined the membrane selectivity and the flux, and with highly porous substructure that provided the mechanical strength.



Figure 2.1 - Professor Sidney Loeb and engineer Ed Selover remove newly manufactured reverse osmosis membrane from plate-and-frame production unit [21].

Rapidly, other synthetic polymers such as polyamide, polyacrylonitrile, polysulphone, polyethylene, etc were used as basic material for the preparation of synthetic membranes.

The first membranes produced for reverse osmosis desalination and other applications were flat sheets and then installed in a spiral wound module. After the development of efficient membranes, appropriate membrane housing devices, the modules, were created. The design of the modules were devised in order to get high membrane packing density, reliability, ease of replacement, control of concentration polarisation effects and low cost. Membranes were produced in three different configurations: as flat sheet, as hollow fibre and as a tube.



Figure 2.2 - First spiral wound element, in 1953 [22].

Advances in materials development along with computer modeling and simulation have contributed greatly to this field, allowing for improved design and manufacture of selective membrane as critical components for such energy and environmental systems as gas processing, ion transport, osmosis and filtration. The demands of sustainable energy production and clean industry continue to drive membrane development toward the goal of simple, efficient and easily integrated systems that offer low-cost, reliable processing and operation [23].

The Figure 2.3 illustrates, summarily, the main developments on membranes technology history ¹.

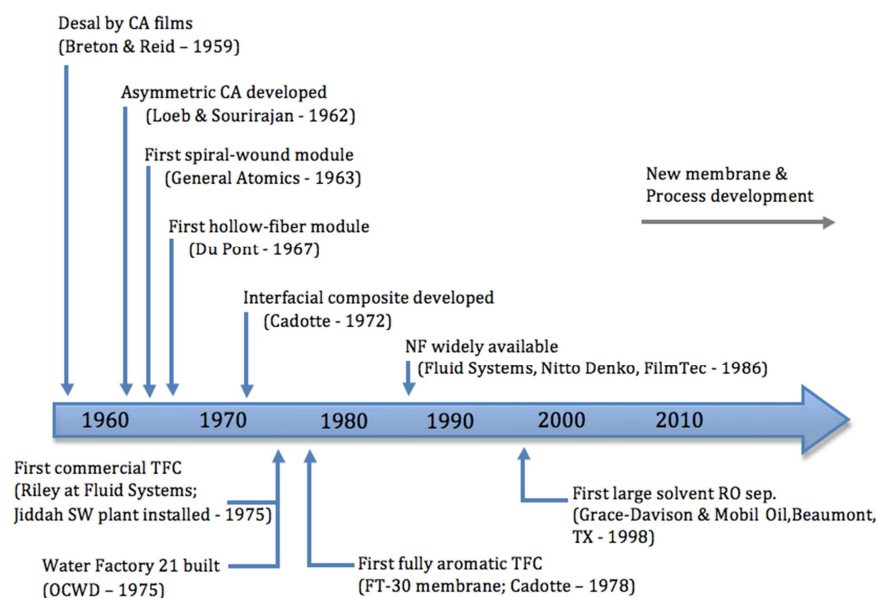


Figure 2.3 - Milestones in membrane development.

¹ Adapted from [24]

2.2 Membrane Processes

In a generic way, membranes carry out a separation by passing materials selectively. Membranes can be defined essentially as a barrier that separates two phases and restricts transport of different components in a selective manner. A wide range of materials can work potentially as membranes. They can be homogenous or heterogeneous, symmetric or asymmetric in structure, solid or liquid, can carry positive or negative charge, or can be neutral or bipolar.

The mass transfer can be performed by convection or by diffusion of individual molecules induced by one of the following gradients: electric field, concentration, pressure or temperature. In addition, membranes can physically or chemically modify the permeating species, so they can be active or passive depending of their ability to change the chemical species.

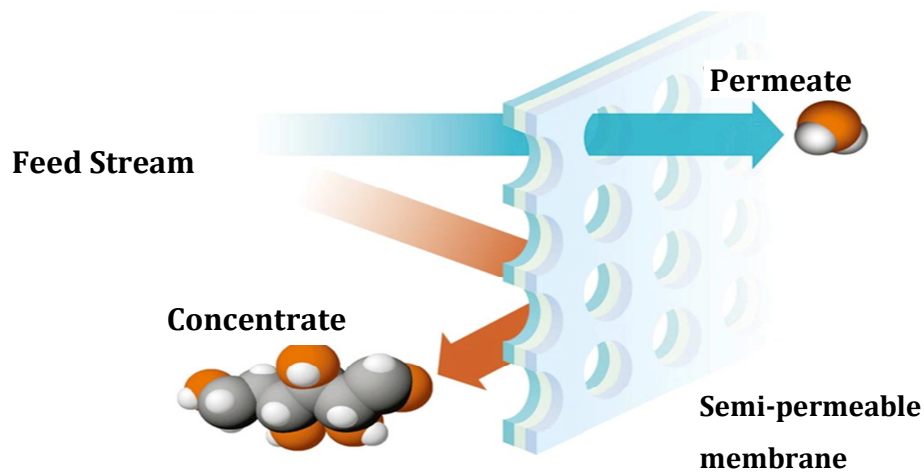


Figure 2.4 - Illustration of a semi-permeable membrane filtration process.

To carry out the separation, the porous membranes discriminate according to the size of particles, and non-porous membranes discriminate according to the chemical affinities between components and membrane materials.

The flux through the membrane is generally expressed by equation (1). It depends linearly of both permeability and driving force, and the membrane can be categorised in terms of an appropriate permeability coefficient ^[25].

$$Flux = \frac{MembranePermeability}{MembraneThickness} (DrivingForce) \quad (1)$$

The variety of the membranes structure combined with the different driving forces, leads to a considerable number of membrane processes. Some of them are summarized in Table 2.1.

Table 2.1 - Summary of general characteristics of some of the most industrial important membrane processes ^{[5][25]}.

Driving Force	Membrane Process	Membrane type	Membrane Material	Applications
Pressure difference	Reverse Osmosis (10 – 100 bar)	Asymmetric skin type	Polymers, Cellulosic acetate, Aromatic polyamide	Separation of salts and microsolute from solutions
	Nanofiltration (10 – 70 bar)	Asymmetric thin-film membranes	Cellulosic acetate and aromatic polyamide	Partial separation of salts and organics
	Ultrafiltration (1 – 10 bar)	Asymmetric microporous	Polysulphone, polypropylene, nylon 6, PVC, acrylic copolymer	Separation of macromolecular solutions
	Microfiltration (0.5 – 2 bar)	Symmetric microporous	Cellulose nitrate/acetate, polyamides, polysulphones	Sterilisation, clarification
	Gas separation	Asymmetric homogeneous polymer	Polymers and copolymers	Separation of gas mixtures
	Pervaporation ²	Asymmetric homogeneous polymer (non-porous membrane)	Polyacrylonitrile, polymers	Separation of mixtures of volatile liquids
Concentration difference	Dialysis	Non-porous and microporous	Polymers	Macromolecular purification, protein concentration
Electrical Potential difference	Electrodialysis	Ion exchange membrane	Sulphonated polystyrene	Desalting of ionic solutions
Temperature difference	Membrane distillation	Microporous	Polymers	Separation of water from non-volatile solutes

² The driving force can be both concentration gradient or vapour pressure.

2.2.1 Pressure Driven Processes

The most common pressure driven membrane processes are distinguished by the hydraulic pressure applied, to speed up the transport process and by the size range of the particles that are separated. The use of driving force as a mean of classification is not completely satisfactory because different membranes processes can be applied to the same separation. Thus, from the applications point of view, classification in terms of suspended solids, colloids, dissolved solutes, etc. is preferable.

Reverse osmosis is essentially a dewatering technique, while ultrafiltration is simultaneously used for purifying, concentrating and fractionating macromolecules. Nanofiltration is the intermediate of UF and RO, excluding the particles that are in the order of 1 nanometre. Microfiltration is a clarification process based on size and solubility of the molecules. Figure 2.5 shows the filtration spectrum of the pressure driven membrane filtration processes, and the Table 2.2 presents their main differences.

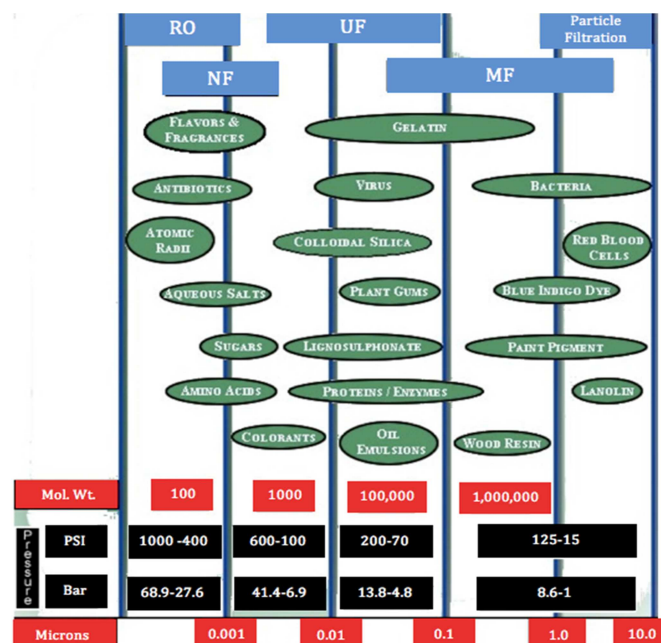


Figure 2.5 - Filtration Spectrum [26].

Table 2.2 – Principal differences between RO, NF, UF and MF³ [8][25].

Membrane Process	Pressure (bar)	Cross Flow (m/s)	Process flux (L/m ² .hr)	Particle characteristics
Reverse Osmosis	30 to 50	2 to 3	5 to 40	Ionic
Nanofiltration	20 to 40	2 to 3	20 to 80	Ionic to molecular
Ultrafiltration	5 to 25	3 to 4	3 to 200	Molecular to macromolecular
Microfiltration	1 to 5	3 to 8	50 to 500	Macromolecular to cellular

³ Values from the membranes supplier used in the work developed.

2.2.1.1 Reverse Osmosis

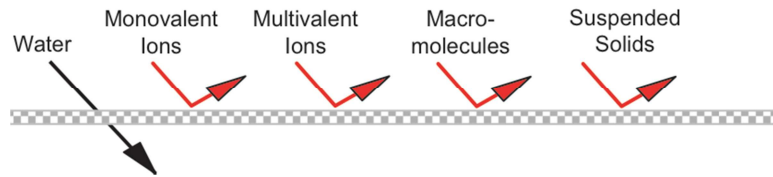


Figure 2.6 - Relative size exclusion for reverse osmosis [27].

Reverse osmosis is a high pressure process for dewatering process streams, concentrating low molecular weight substances in solution or purifying wastewater. It can also be used to concentrate dissolved and suspended solids and it is widely used for desalination.

Reverse osmosis and normal osmosis (dialysis) are directly related processes. Using the following example to desalinate the sea water it is necessary to create a flow through the membrane, so the water passes from the salt side to the fresh side. To reverse the natural process of osmosis, pressure must be applied on the first side, to overcome osmotic pressure equilibrium and to create extra pressure that leads to the water transport.

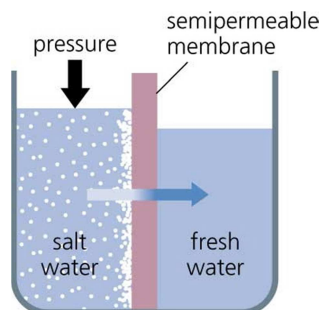


Figure 2.7 - Illustration of hydrostatic pressure causing reverse osmosis.

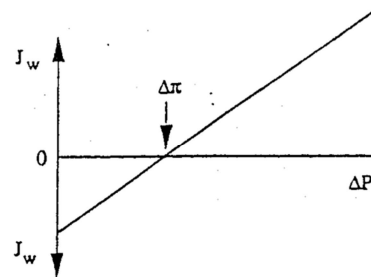


Figure 2.8 – Schematic representation of flow as function of applied pressure [28].

Salt and water permeate reverse osmosis membranes by the solution-diffusion model. The water flux is linked to the pressure and concentration gradients across the membrane.

RO has some advantages over the conventional separation processes, since it is a pressure driven process and no additional (potentially expensive) energy sources are needed, it is simple design and simultaneous separation and concentration are possible, it can be used in a hybrid process, combined with, for example, distillation.

2.2.1.2 Nanofiltration

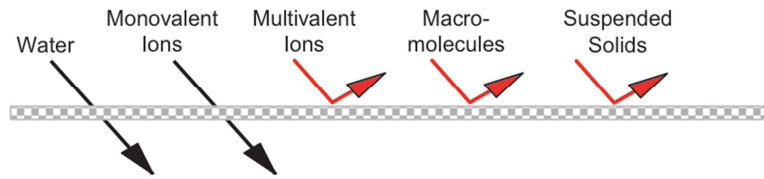


Figure 2.9 – Relative size exclusion for nanofiltration [27].

The high pressure used in reverse osmosis results in a considerable energy cost, but the quality of the permeate obtained is very good. Thus, membranes with lower rejections of dissolved components and higher water permeability were necessary and those are nanofiltration membranes [29].

Some types of nanofiltration membranes can be considered as RO membrane, as they are similar processes. NF membranes are applied in the area between the separation capabilities of RO and UF membranes.

Typically, NF membranes have NaCl rejections between 20 and 80% and molecular weight cut-off for dissolved organic solutes of 200-1000 dalton. These properties are intermediate between RO membranes (with a salt rejection of more than 90% and molecular weight cut-off of less than 50) and UF membranes with a salt rejection of less than 5% [24].

These membrane processes have found wide applications for the treatment of aqueous based systems involving material recovery, reuse and for pollution prevention. One of the main applications is water softening. However, the improvement of solvent stability of NF membranes has opened a wide range of potential applications in the chemical and pharmaceutical industry [23]. NF membrane separations already have significant industrial applications in the separation of inorganic salts from dye solutions

2.2.1.3 Ultrafiltration

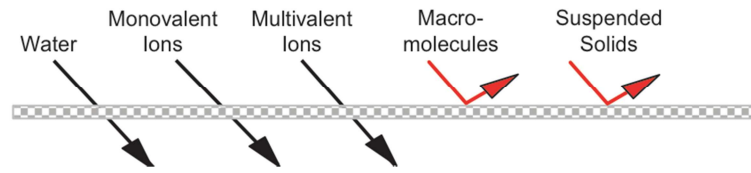


Figure 2.10 - Relative size exclusion for ultrafiltration [27].

Ultrafiltration is a permeability-based membrane separation technique, mainly used to remove particles in the size range 0.002 – 0.1 μm . Solvents and salts of low molecular weight pass through the membranes whilst larger molecules, such as proteins, pigments and surfactants are retained [30]. The principal application of UF is in the separation of macromolecules with a molecular weight range 1000 – 100,000 Dalton. UF operates at a pressure range of 1 – 10 bar but in some cases up to 25-30 bar has been utilised. The typical membrane materials are polysulphone, polyethersulphone and polyacrylonitrile [5].

UF is based on a sieving separation mechanism (and electrostatic interactions also have influence), where an increase in applied pressure increases the flux rate. However, UF membranes are very sensitive to the fouling phenomenon and to concentration polarisation. The dynamics of the fluid processed must be studied carefully to control the material transfer on the membrane-liquid interface. Fouling and polarisation concentration are more detailed in sections iv and v.

The effect of the concentration polarisation phenomenon puts an upper limit on practical flow rates. Concentration polarisation arises from a build-up of solute concentration on the feed side of the membrane and this boundary layer formation results in an additional resistance. At high pressures, jellification of the macromolecules can occur and a thin gel layer forms at the membrane surface. Membrane fouling also leads to a gradual decline in flux with time and it is attributed to changes in the chemical nature of the gel layer such as crosslinking and compaction [5].

Some techniques have been known to help achieve high permeate flux in ultrafiltration, such as: periodic backflushing of the membrane using the permeate, creation of turbulence on the feed side by using flow inserts and baffles, introduction of gas bubbles into the membrane module for membrane cleaning and the creation of turbulence [29].

i. Membrane Characterisation

The performance of ultrafiltration membranes is commonly quoted by manufactures in terms of the pure water flux and the so-called “cut-off”.

The pure water flux through ultrafiltration membranes is directly proportional to the driving force (ΔP), and the proportional coefficient (L_p) is called the hydraulic permeability coefficient, which determines the membrane ability for water permeation.

$$v_{p,w} = L_p \Delta P \quad (2)$$

Since the water flux measured at different temperatures is inversely proportional to the viscosity (μ_w), it is useful to define a “standard” permeability coefficient L_p^* by the equation (3).

$$v_{p,w} = \frac{L_p^* \Delta P}{\mu_w} \quad (3)$$

The standard permeability coefficient is characteristic of the system membrane/water and is independent of the pressure and temperature [31].

ii. Molecular Weight Cut-Off

The cut-off is a parameter that identifies the membrane’s separating capacity. However, it is important to note that the cut-off is only an indicative measurement with no correlation with the real porosity of the membrane [30]. The cut-off of ultrafiltration membranes is usually characterized by solute molecular weight.

UF membranes are tested with dilute solutions of well-characterized macromolecules to determine the molecular weight cut off. Membranes characteristics usually include MWCO, for specifying the solute retention property. The convention established by AMICON states that MWCO of the membrane is defined as the smallest molecular weight species for which the membrane has more than 90% rejection [9].

iii. Basic Working Principles of Ultrafiltration

There are two main parameters in ultrafiltration processes, the permeate flux and the selectivity. The volumetric permeate flux is the volume of permeate collected per unit time per unit membrane area. The relationship between the applied ultrafiltration pressure and the rate of permeation (flux) for a pure

solvent feed flowing under laminar conditions may be described by the Carman-Kozeny equation (4). The general approach to describe ultrafiltration in the presence of a solute is given by the equation (5). The flux in ultrafiltration is affected by several factors, such as transmembrane pressure, feed temperature and solute concentration.

Selectivity is a measure of the relative permeation rates of different components through the membrane and is given by the retention factor. This is defined as the fraction of solute in the feed that is retained by the membrane, equation (6).

Table 2.3 – Basic working principles of ultrafiltration [32].

<p>Carman-Kozeny equation</p>	$J = \frac{ \Delta P }{\mu R_m} \quad (4)$ <p>Where: J – flux Δp – transmembrane pressure difference μ – solvent viscosity R_m – membrane resistance</p>
<p>Flux in the presence of a solute</p> <p>Comment – osmotic pressure is negligible for macromolecules⁴</p>	$J = \frac{\Delta P - \Delta \pi}{\mu(R_m + R_s)} \quad (5)$ <p>Where: Δπ – osmotic pressure difference R_s – resistance due the deposition of solute (gel layer)</p>
<p>Retention factor for solute s</p>	$R_s = \left(1 - \frac{C_{p,s}}{C_{f,s}}\right) \times 100 \quad (6)$ <p>Where: C_{p,s} – solute concentration in the permeate C_{f,s} – solute concentration in the feed.</p>

iv. Membrane Fouling

It is known that the permeation rate is not limited in a constant manner. When an ultrafiltration module is operated under limiting conditions over long periods (the usual industrial situation), the flux

⁴ Not all the authors consider that the osmotic pressure of macromolecules is negligible.

decreases steadily with time. This observation is not only explained in terms of concentration polarisation but rather is due to chemical modifications occurring in the layer of concentrated solution or gel at the membrane surface. The hydraulic resistance of this layer increases with time and reduces the effective permeability of the membranes, so that the permeation rate through the membrane declines [31].

Membrane fouling can be defined as the (ir)reversible deposition of retained particles, colloids, emulsions, suspensions, macromolecules, salt, etc on the membrane. This includes adsorption, pore blocking, precipitation and cake formation. Fouling depends of the physical and chemical parameters such as concentration, temperature, pH, ionic strength and specific interactions [28].

For most applications there is a gradual flux decay with the time due to the material accumulation on the membrane surface, which no longer participate in the mass transport, to or away from the membrane. Often preventive measures maybe taken to avoid fouling the membrane, such as pre-treatment, high cross flow velocities and low pressures [9].

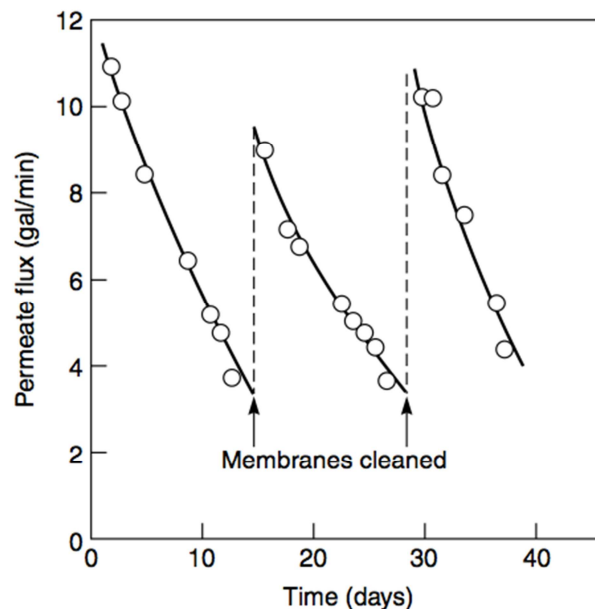


Figure 2.11 - Ultrafiltration flux as function of time of an electrocoat paint latex solution [24].

v. Concentration Polarisation

The separation of solute and solvent takes place at the membrane surface where the solvent passes through the membrane and the retained solute causes a local concentration increase. This effect is called concentration polarisation. Therefore a concentration profile is established within a boundary film generated by the hydrodynamic conditions.

With the higher concentration at the membrane surface, there is a tendency of solute to diffuse back into the bulk solution according to Fick's Law of Diffusion. A solute mass balance above the membrane surface at steady state condition, gives the rate of convective transport of solute towards the

membrane surface. The equation (7) is obtained from the mass balance, and gives the flux taking in account the effect of the polarisation concentration [32].

$$J = k_s \ln \left(\frac{C_m - C_p}{C_b - C_p} \right) \quad (7)$$

Where k_s is the overall mass transfer coefficient of the solute in the boundary layer, C_m is the concentration at the membrane surface, C_p is the concentration in the permeate and C_b is the bulk concentration. The overall mass transfer coefficient is usually obtained from correlations of the form of the equation (8).

$$Sh = \frac{k_s d_h}{D} = K Re^a Sc^b \left(\frac{d_h}{L} \right)^c \quad (8)$$

Where the constants K , a , b , c vary with the flow regime.

The most important consequence of the concentration polarisation effect is the limit that it causes on the permeate flux when the pressure is increased. At low operating pressures, the permeate flux increases almost linearly with the applied pressure. However, at higher pressures, the permeate flux increases slower and finally the pressure reaches a point beyond which no further increase in flux is observed, as it is showed in Figure 2.12[31].

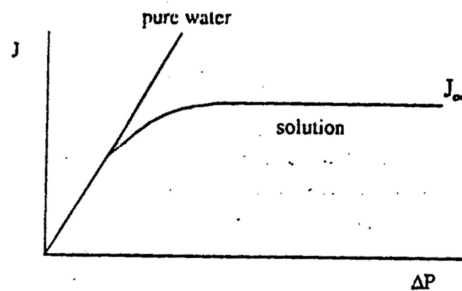


Figure 2.12 - Schematic drawing of the relationship between flux and applied pressure in ultrafiltration [28].

The effects of this phenomenon on the membrane can be described, among others, for two models: gel-polarisation model and osmotic pressure model.

vi. Effect of Concentration Polarisation on Retention

The phenomenon of concentration polarisation has influence in how pressure affects retention. It may cause the rejection to decrease with increasing pressure. The reason is that, increasing the pressure,

the concentration of solute at the surface of the membrane (C_s) increases over that in bulk stream (C_b). As the pressure is increased, the solvent flux is increased and the convective transport of solute ($J_w C$) to the membrane is increased. If the solute is retained by the membrane, it accumulates at the surface of the membrane until the back diffusive mass transport, $D_s(dc/dx)$, is equal to the forward convective transport. Even if a steady state is maintained, there must be a concentration gradient (dc/dx) to remove solute from the membrane. Thus, C_s will increase with pressure resulting in a decrease in solute retention. The pores large enough to pass solute, at higher pressures, pass more solvent, carrying a higher concentration of solute [9].

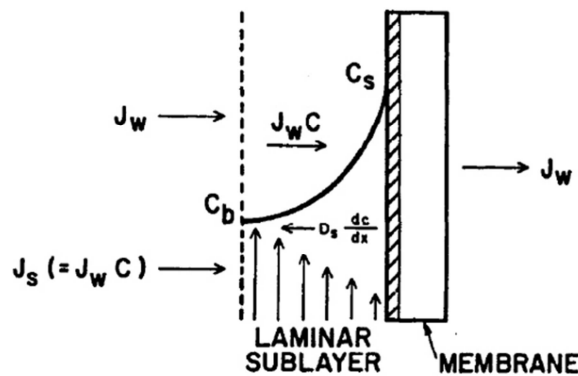


Figure 2.13 - Concentration polarisation in ultrafiltration.

Further increases in pressure will increase the solute concentration at the surface of the membrane to a limiting concentration. The incipient gel precipitates and the solute passage occurs at a constant rate [31]. Under these conditions, further increases in pressure will not increase C_s . Therefore, once the membrane is “gel-polarised”, the retention should be independent of pressure.

vii. Effect of Concentration Polarisation on the Membrane Flux

Likewise in the concentration polarisation effect on the retention, it can also severely limit the flux. The thin skin of the UF membranes minimizes the resistance to flow and the asymmetry of the pores virtually eliminates internal pore fouling. However, the hydraulic permeability of these membranes also increases the convective transport of solutes to the membranes surface. Consequently, the polarisation modulus increases as well.

This accumulation of the solute at the membrane interface can limit the flux when the applied pressure is increased. In the case of RO, the salts retained have a significant osmotic pressure and the effective pressure gradient is reduced by the osmotic pressure difference across the membrane, reducing the flux. But in the case of UF, the macromolecules have negligible osmotic pressures. Although the

osmotic pressure model is used by some researchers, the gel polarisation model seems to suit better the flux prediction [9]. The following description of the pressure effect on the membrane flux is based on the gel polarisation model.

At the beginning of the pressure increase, or at low concentrations in the bulk stream, the flux increases with the pressure. However the flux does not increase monotonically with pressure and it often becomes independent of pressure in the steady state.

Increasing the transmembrane pressure, a higher rate of convective transport of solute to surface of the membrane is achieved. If the system is not “gel-polarised”, the solute concentration at the surface (C_s) increases resulting in an increase in the concentration driven back by the diffusive transport away from the membrane. In this case, an increase of the flux is still observed.

$$J_v = \frac{\Delta P}{R_c + R_m} \quad (9)$$

Where R_m is the membrane resistance and R_c is the resistance of the cake.

The concentration on the membrane surface (C_s) will increase until the back diffusive transport of solute just equals the forward convective transport. So the steady state is showed by the equation (10).

$$J_v C = -D \frac{dc}{dx} \quad (10)$$

Where C is the concentration of the membrane retained solutes, D is the solute diffusivity and x is the distance from the membrane surface.

Eventually, the concentration at the membrane surface will be high enough for a gel to form ($C_s = C_g$). Further increases in the pressure will again temporarily increase the convective transport (J_c) to the membrane surface. However, since the surface concentration is at a maximum, the back diffusive transport will be fixed (assuming no changes in the fluid dynamics in the boundary layer) and solute will accumulate on the membrane. The gel will thicken or compact just compensating for the increased driving force by an equal increase in the resistance of the cake (R_c). Therefore, in the “gel-polarised regime”, flux is independent of pressure or membrane permeability, and is solely determined by the back diffusive transport, which is obtained by solving equation (10) [9].

$$J_v = k \ln \left(\frac{C_g}{C_b} \right) \quad (11)$$

Where $k = (D/\delta)$ is the mass transfer coefficient and δ is the boundary layer thickness.

Equation (11) describes the maximum flux, called limiting flux, which depends on the concentration in the bulk of the feed, C_b , and the mass transfer coefficient. Increasing the feed concentration, but keeping the mass transfer mass coefficient and the concentration at the membrane constant, the value of the limiting flux decreases [28].

The pressure effects described above are represented on Figure 2.14, and the Figure 2.15 illustrates the tangential flow on a polarised membrane surface.

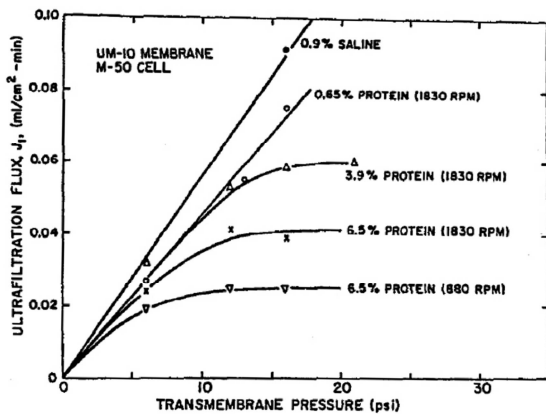


Figure 2.14 – Effect of pressure on ultrafiltration flux for bovine serum albumin solutions [31].

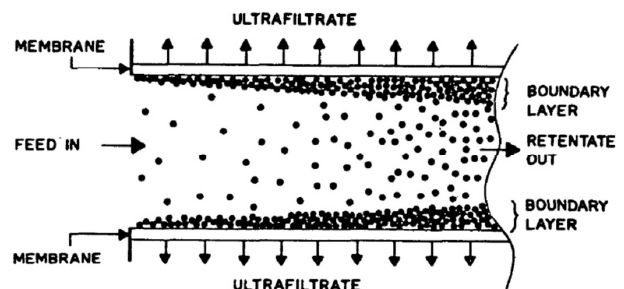


Figure 2.15 – Cross-flow ultrafiltration system [9].

viii. Diafiltration

In order to obtain more complete separations, the retentate is diluted with solvent (water) so that the salts and low molecular weight solutes are washed out. This type of operation is called diafiltration. It is not another membrane process but it is a design to achieve a better purification or fractionation [28].

Diafiltration is used to increase the percentage concentration of the retained components. During the UF process, water is added to the retentate to remove the unwanted species. Diafiltration is practiced both as a discontinuous and as a continuous process.

Discontinuous diafiltration is when the process of repetitive dilution is followed by a brief concentration. The addition of water to the retentate reduces the concentration of permeable solids in the retentate. The volume of retentate is reduced through filtration and water is then added to dilute the retentate to a certain volume. The retentate is then processed again by concentration.

Continuous diafiltration is generally more efficient. In this case, a batch of the solution to be processed is maintained at constant volume by adding pure water at the same rate permeate is removed. In the way, the macromolecules retained by the membrane remain at their initial concentration while the

salt (or low molecular weight solutes) decreases continuously. This process can be called “constant volume molecular washing” because the salts are washed out of the solution.

When micro solute exchange is desired, it can be done through diafiltration, if the water added contain the micro solute intended to replace the one in the starting solution [9].

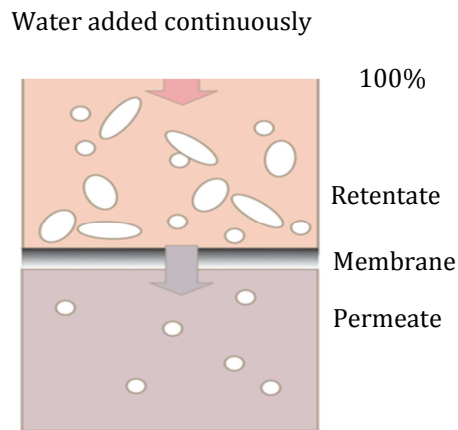


Figure 2.16 - Schematic continuous diafiltration operation.

2.2.1.4 Microfiltration

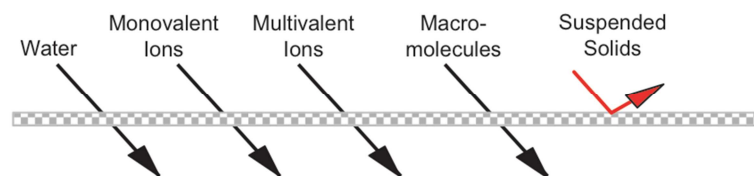


Figure 2.17 - Relative size exclusion for microfiltration [27].

Microfiltration is the membrane process that is closer to conventional filtration. As pore sizes of MF membranes range from 10 to 0.1 μm , the process is suitable for retaining suspensions and emulsions. Thus, microfiltration falls between ultrafiltration and conventional filtration. In most applications, MF membranes remove particles from already clean solutions.

Microfiltration can operate in three different process designs: dead-end filtration, cross-flow filtration and semi-dead-end filtration, which is an operation that combines both process designs.

MF membranes were firstly used in laboratories, but their applications became much more varied with the introduction of pleated membrane cartridges, which today dominates the market in general. MF membranes are used in biological and pharmaceutical manufacturing, in electronic processes, food and beverage industries and more recently they are also utilized in water treatment [24].

2.2.1.5 Applications of Pressure Driven Membrane Processes

Table 2.4 - Examples of Applications of pressure driven membrane processes ^{[9][33]}.

Membrane Process	Industry /Area	Examples of Applications
Microfiltration	Metal	MF of oil-polluted industrial effluents
	Dairy	- Bacteria removal and casein fractionation - MF of whey
	Pharmaceutical/Beverage	Sterilisation and particle removal
	Semiconductor Fluids	Particle removal
Ultrafiltration	Metal	UF of oil-water emulsions
	Dairy	Milk concentration
	Pulp and Paper	- Treatment of spent liquors - Treatment of bleach effluents - Wash water
	Textile	- UF of latex-contaminated effluents - UF of effluents from dyeing processes
	Food/Beverage	- Concentration of protein solutions - Recovery, purification of fruit juice/wine - Diafiltration to recover sugar from concentrate
	Pharmaceutical/ Biotechnology	- Cell harvesting - Enzyme/Virus concentration and purification - Blood plasma Processing - Enzyme reactors
	Dyes	- Dye recovery and purification - Diafiltration and concentration in pigment production
Reverse Osmosis	Pulp and Paper	Treatment of paper-machine effluents
	Pharmaceutical/Electronics	Production of pure water
	Food/Beverage	Concentration of protein solutions/fruit juice
	Refinery	Wastewater treatment
	Pollution Control	- Wastes treatment - Removal of toxic substances prior discharge
	Seawater/Brackish water	- Desalination - Removal of nitrates, fluorides, heavy metals
	Medicine	Artificial kidneys

2.2.2 System Design

Several simple filtration processes use a dead-end technique in which the flow of liquid to be filtered is directed perpendicular to the filter surface. This is effective whenever the concentration of particles to be removed is low, or the packing tendency of the filtered material does not produce a large pressure drop across the filter medium. Some common examples of dead-end filtration are home water filters, vacuum cleaners and oil filters in automobiles. Typically industrial uses include the sterile filtration in pharmaceutical, food and beverage industries (for example in microfiltration processes).

On the other hand, there are many process streams that have high concentrations of particles or macromolecules that rapidly compact on the filter surface when operated in a dead-end mode. Consequently, the filtration rate drops quickly to an unacceptable level. A cross-flow membrane system provides the means to maintain stable filtration rates, by using a membrane geometry that suits the physical characteristics of the fluid.

In cross flow, the fluid to be filtered is pumped across the membrane, parallel to its surface. By maintaining velocity across the membrane, material retained is swept off the membrane surface. Thus, there is a smaller tendency for the retained material to obstruct the membrane. Even so, there is a general decline in flux rate during continued operation due to the fouling [5].

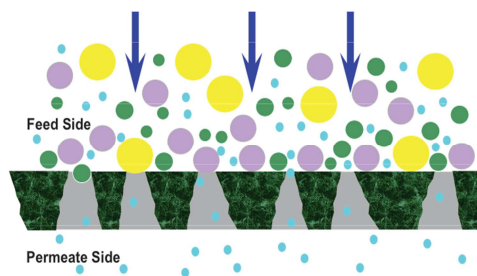


Figure 2.18 – Filtration operating in dead-end flow.

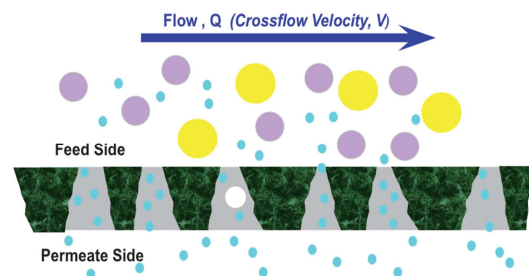


Figure 2.19 – Filtration operating in cross-flow.

Cross flow technology has primarily evolved in step with the advancement of polymer chemistry. The fact that polymers are durable and chemically resistant makes cross flow a cost-effective technology.

The theoretical principles of cross-flow filtration are derived from Fick's Law of Diffusion, which addresses the migration of suspended solids/macromolecules in a flowing stream towards a filtration surface and the potential back-diffusion into the bulk stream. This forms the basis for cross-flow design: the concentration of macromolecules at the membrane surface can be controlled as a function of the velocity of the fluid flowing parallel to that surface. The design of a successful cross flow system relies on choosing a membrane geometry that can be installed and operated economically, providing consistent predictable results and can be effectively cleaned [27].

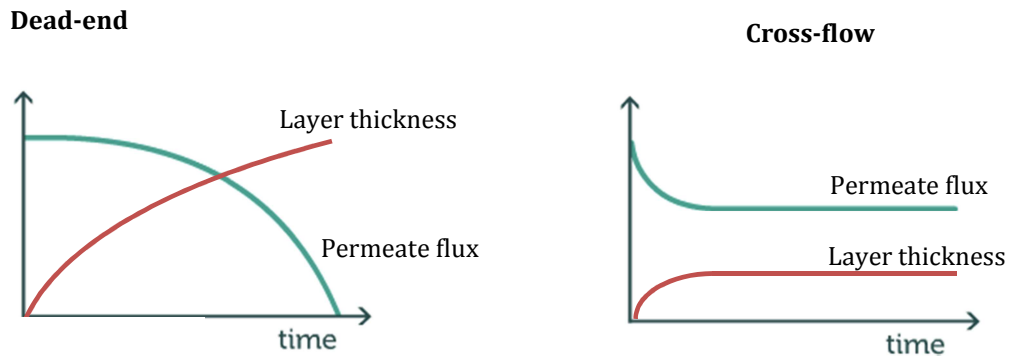


Figure 2.20 – Comparison of flux rates and layer thickness.

2.2.3 Membrane Types and Materials

Membrane material science has produced a wide range of materials of different structure and with different ways of functioning. Generally these materials can be classified into three types: synthetic products (polymers and elastomers), modified natural products (cellulose based) and inorganic (ceramic and metals).

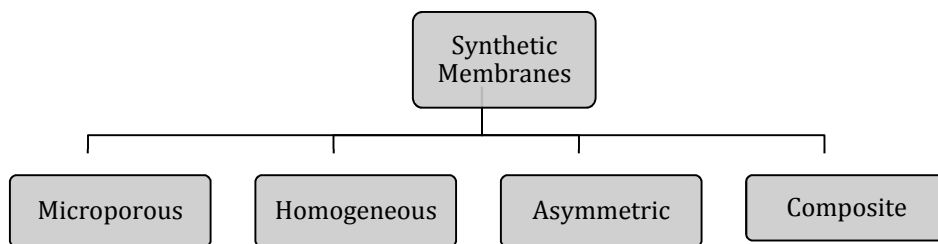


Figure 2.21 - General classification of synthetic membranes.

To be effective for separation, membrane material should ideally have certain properties, such as chemical resistance, mechanical and thermal stability, high permeability, high selectivity and stable operation [5].

2.2.3.1 Microporous Membranes

A microporous membrane is very similar in structure and function to a conventional filter, separating by a sieving mechanism. The pores vary from 0.01 to 20 μm . The membrane has a rigid, highly voided structure with randomly distributed and interconnected pores. The microporous membranes are further classified as isotropic, in which the pores are of uniform size throughout the membrane, and anisotropic, in which the pores change in size from one surface of the membrane to the other [25].

There are the following types of microporous membranes based on their structure: sintered membranes, stretched membranes, capillary pore membranes, and microporous phase inversion membranes.

Microporous membranes can be made from various materials such as ceramics, graphite, metal or metal-oxides and various polymers [31].

Most applications for these membranes are a microfiltration process.

2.2.3.2 Homogeneous Membranes

Homogeneous membranes are constituted by a dense film, through which a mixture of molecules is transported by pressure, concentration or electrical potential gradient. These membranes perform separation of species of similar size and different diffusivity in the membrane matrix. The mass transport in homogeneous membranes is always strictly by diffusion, thus permeabilities are quite low.

There are the following materials types of homogeneous membranes: polymer membranes, metal and glass membranes, liquid membranes and ion exchange membranes [31].

The most important applications of these membranes are gas permeation and pervaporation. Electrodialysis membranes are also homogeneous but with special characteristics of ion exchange [34].

2.2.3.3 Asymmetric Membranes

Asymmetric membranes are one of the most important membranes used today in separations processes. These membranes have two basic properties requested for all membrane processes: high mass transport rates for certain components and physical strength. These properties are physically separated, as an asymmetric membrane consists of a very thin polymer layer (which is the actual membrane) on a high porous thick sub layer.

The separations characteristics are determined by the nature of the polymer or pore size and the mass transport rate mainly by the thickness. The highly porous sub layer provides the support for the very thin polymer and it almost has no effect on separation characteristics.

The asymmetry of the porous sub layer allows the removal of the rejected materials at the surface by shearing forces applied by the feed solution. This is an important advantage comparing with the symmetric membranes, where most particles are retained within the porous, plugging the membrane and reducing the flux [31].

UF membranes are usually prepared by phase inversion. Some of the materials used to prepare UF membranes are typically polysulphone, polyethersulphone and polyacrylonitrile [23]. Figure 2.22 shows the molecular structure of polyethersulphone polymer⁵.

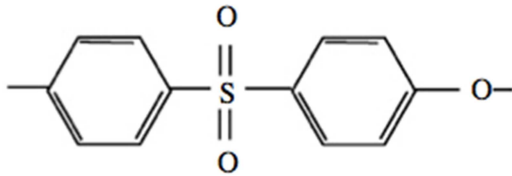


Figure 2.22 – Polyethersulphone molecular structure [23].

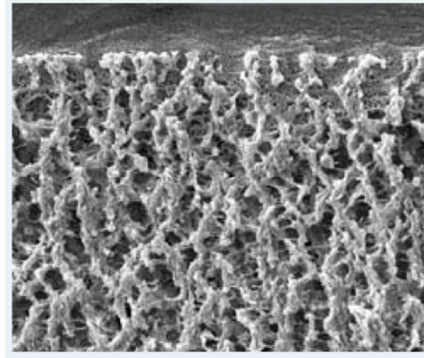


Figure 2.23 - Cross-section of ultrafiltration membrane. Asymmetric membrane [35].

The applications of asymmetric membranes are essentially the pressure driven processes, RO, UF or gas separation.

2.2.3.4 Composite Membranes

Composite membranes are in general an improvement over asymmetric phase inversion membranes. The composite technique allows production of support and active (skin) layers from different materials, which are selected for optimum function in each case. In addition, the skin layer may also be coated in order to produce a biocompatible membrane. The performance of a composite membrane is determined for both selective surface film and microporous support structure [33].

The usual materials to prepare composite membranes are cellulosic esters, polyamide, polysulphone and polyimide.

Composite membranes are used in RO, gas permeation and pervaporation.

2.2.4 Membrane Modules

The central part of any membrane plant is the module, i.e. the technical arrangement of the membranes. From the mass transfer studies it is known that hydrodynamics are of major importance in module design. In any case, areas of stagnant feed fluid in the module should be avoided. However, there

⁵ The membranes used in the work developed are polyethersulphone membranes.

are various aspects to take in account for an efficient module design, such as: high packing density, cost-effective manufacture, easy access for cleaning, cost-effective membrane replacement and power consumption [33].

A number of module designs are possible and all are based on two types of membranes configuration: flat and tubular. Plate and frame and spiral wound modules involve flat membranes, while tubular, capillary and hollow fibre modules are based on tubular configurations. The difference between the latter types of modules arises mainly from the dimensions of the tubes employed. Their basics features are briefly described in the next sections.

2.2.4.1 Plate and Frame Modules

In a plate and frame module, sets of two membranes are placed in a sandwich-like fashion with their feed sides facing each other. Feed and permeate compartment are separated by a spacer. Thus, membrane, feed spacers and product spacers are layered together between two end plates. The feed mixture is forced across the surface of the membrane. A portion passes through the membrane and enters the permeate channel and makes its way out from each membrane sheet.

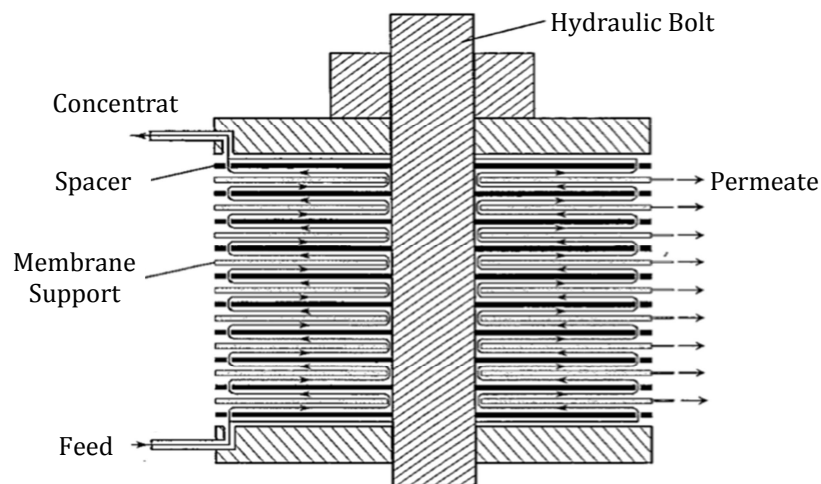


Figure 2.24 - Plate and frame module [34].

Plate and frame units have been developed for some small scale applications, but these units are expensive compared to other alternatives and leaks through the gaskets required for each plate are a potential problem.

These membrane modules are used in electrodialysis and pervaporation systems and in a limited numbers of RO, UF and MF applications [24].

In modules used for UF the membranes sheets are stacked either one on top of one another or side by side. The sheets are either in the form of circular discs, elliptical sheets or rectangular plates.

2.2.4.2 Spiral Wound Modules

Spiral wound modules consist of a series of sheets wrapped around a central permeate collecting tube. Feed solution passes axially along the sandwich in the channels formed by the spacers. This channel is of order of 1.0 mm in thickness and the cross flow velocities used generally give a laminar flow, although the spacer material may act as a turbulence promoter and thus reduce concentration polarisation. The permeate flows through the membrane in cross flow with the feed solution, i.e. radially inwards towards the central collecting tube. The diameter of this tube is small to maximise specific areas [36].

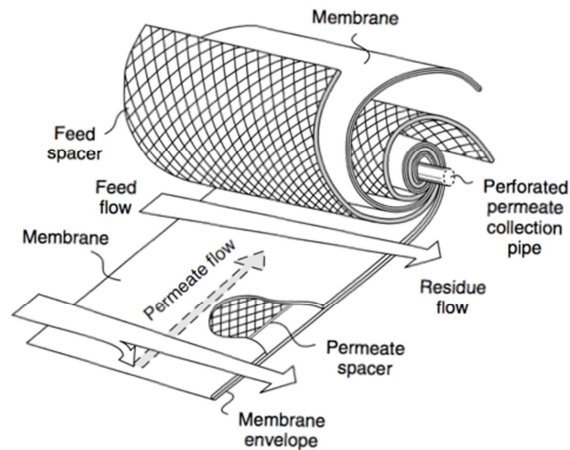


Figure 2.25 - Spiral wound module [24].

In practice two or more modules are fitted in series, and connected via the central permeate tubes, that is suitably sealed into a pressure housing into which feed solution is introduced at one end and retentate collected at the other. In common with hollow fibre modules, spiral wound modules can not be mechanically cleaned and thus have a low tolerance to particulate material. So these membranes limit the UF applications.

Spiral modules have potential applications in pervaporation and gas permeation and less widely in RO and UF. Also used widely for water purification.

2.2.4.3 Tubular Modules

The basic concept of a tubular module is a straight membrane tube surrounded by a porous support layer and support tube. Feed flows internally along the tube and permeate passes through the membrane into the porous support layer and through suitable holes in the support tube. In a typical tubular membrane system a large number of tubes are manifolded in series, to increase the module productivity. The permeate is removed from each tube and sent to a permeate collection header. The feed solution is pumped through all the tubes connected in series. The system resembles shell and tube heat exchangers.



Figure 2.26 – Tubular membrane module [8].

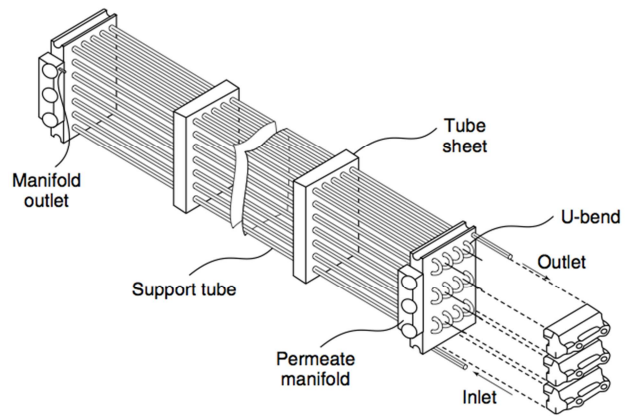


Figure 2.27 – Tubular ultrafiltration system with 30 tubes in series [24].

Developments in inorganic membrane materials in tubular form are particularly important in UF applications. They enable aggressive conditions of cleaning and generally extend the range of applications [24]. Tubular modules are a good option for UF because they have a high resistance to membrane fouling due to good fluid hydrodynamics, which outweighs the cost [24]. As tube diameters are relatively large, it allows in situ mechanical cleaning methods.

Principal applications are in UF and MF and also applications in RO.

2.2.4.4 Hollow Fibre Modules

Hollow fibre module consists of a bundle of very fine membrane packed into a cylindrical housing or shell. The individual fibres are placed in the module with both open ends fixed to the permeate head plate to facilitate easier manufacture. Feed is external to the fibres, as is the active membrane surface, and permeate flows internally along the fibres. Generally module performance is better when permeate and retentate are in countercurrent flow [36].

A major requirement of these modules is that feed stream should be clean, as they are particularly susceptible to fouling, and the restoring cost of a plugged module is high. Usually modules are manufactured with polyamide fibre, cellulose triacetate and sulphonated polysulphone. Main applications are RO and gas permeation and more recently pervaporation.

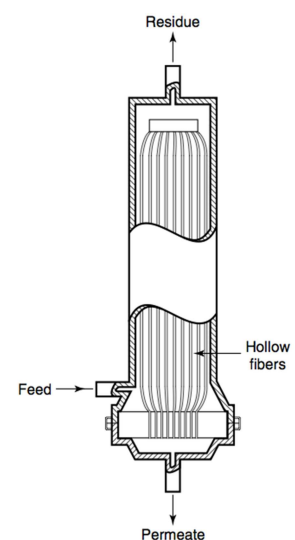


Figure 2.28 - Hollow fibre module [24].

3 Experimental Apparatus

The processing of aqueous inkjet colorant, which the experiments for this thesis were made, was carried out on the PCI unit. It is a pilot scale unit that uses a tubular module membrane module. This operation composes the filtration stage of aqueous inkjet production and is one of the last operations of the production process. It aims to purify and concentrate a sample in order to improve the final quality of the product, ensuring the required specifications are met.

The aqueous colorant processing was carried out by ultrafiltration with diafiltration, obtaining a permeate stream that is mostly water, solvent and inorganic impurities (with low molecular weight), but also metal ions and salts (such as chloride and sulphate) and a final product of colorant.

3.1 Experimental Description

3.1.1 Material Processed

The material processed was an aqueous inkjet dye, named Cyan – X⁶, based on copper phthalocyanine. CuPc is a complex of copper with phthalocyanine and is from the group of the phthalocyanine dyes.

3.1.2 Membranes and Module

The membranes used for the experiments are cross flow tubular membrane, and the module has 18 membranes with a total area of 0.425 m². This kind of membrane is suited to fluids with high viscosity and/or suspended solids, which is the case of the samples processed.

Table 3.1 - Membranes characteristics.

Membrane Type	ES-209
Material	Polyethersulphone
Maximum pH Range	1.5 – 12
Maximum Pressure (bar)	30
Maximum Temperature (°C)	80
Apparent Retention Character	9,000 MW
Hydrophilicity	2 (1 low, 5 high)
Solvent Resistance	2 (1 low, 3 high)



Figure 3.1 - Cross flow tubular membranes.

⁶ Due to confidential reasons.

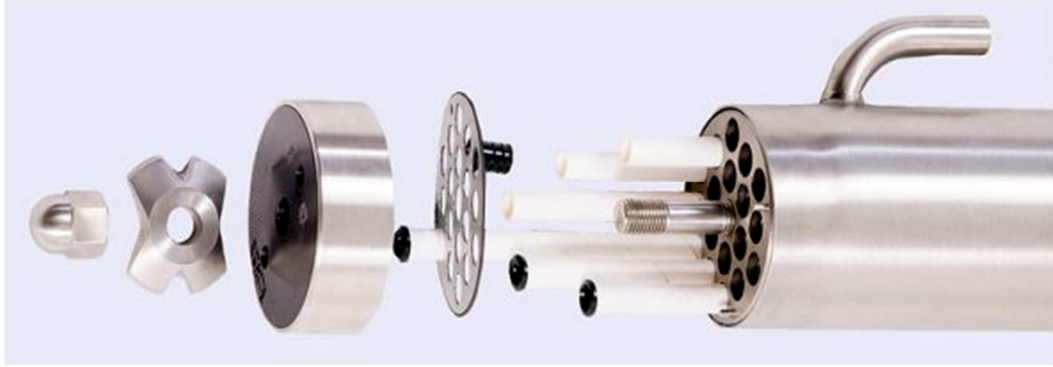


Figure 3.2 – Module and membranes used in the ultrafiltration experiments.

The module is of stainless steel construction, with the 12.7mm diameter tubular membranes, fitted into 18 perforated support tubes. It is possible to connect modules in series or parallel flow, to allow operation at different flow rates to suit crossflow and pressure drop requirements for individual applications.

The module has a turbulent flow design. All the experiments were carried out with a cross flow velocity of 5 m/s, which correspond to a Reynolds Number of 63310 for pure water flow.

Due to the robust design, the module can be used in systems designed for operation at up to 64 bar at 80°C [8].

3.1.3 Membrane Unit

The central part of the unit is mounted in a frame and includes a 25L feed tank, a centrifugal pump, the tubular membrane module, the concentrate and permeate lines and the control panel. The latter has a flowmeter and displays the permeate flow rate. No agitator is needed on the feed tank because the cross flow velocity is high enough to keep the feed solution fully agitated.

The control and indicator devices are: a level control in the feed tank, a pH meter that monitors pH and temperature of the feed solution, a pressure control valve and a conductivity meter that displays the permeate conductivity.

The auxiliary equipment includes a 50L permeate tank, 2 x 25L DI water tank, a smaller centrifugal pump that pumps the DI water and a DI cylinder connected to a biofilter.

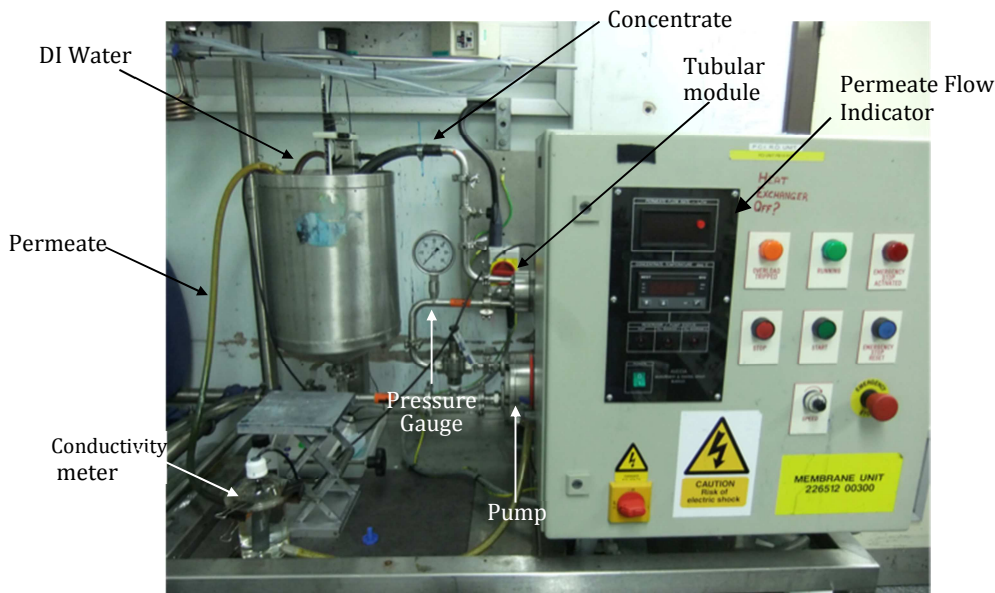


Figure 3.3 - PCI unit.

The unit has no heat exchanger, so the temperature of the feed solution varies during the ultrafiltration process. Although the maximum temperature defined by the membranes supplier is 80 °C, during the experiments it was kept under 50 °C.

The material is processed at 30 bar pressure, but for the thesis experiments, 40 bar pressure will be also studied.

Figure 3.3 shows the membrane unit in recirculation mode, where both permeate and concentrate are recycled to the feed tank. As there is no addition of DI water in this configuration the temperature increases.

To carry out the concentration of the aqueous dye, the level tank is set up at the desired volume and the permeate line is directed out of the system while the concentrate is recycled to the feed tank. There is no DI water added until the set level is reached, thus the temperature increases during the initial concentration process.

During the diafiltration, the permeate is taken out of the system while the concentrate is recycled to the feed tank and DI water is continuously added to the system. The DI water is fed to the system at the same rate as the permeate is collected, so the tank level is kept constant. During the diafiltration process, as the temperature of DI water is lower, the system temperature initially decreases and then tends to stabilize.

Figure 3.4 displays the flow diagram of the ultrafiltration process carried out on the PCI unit.

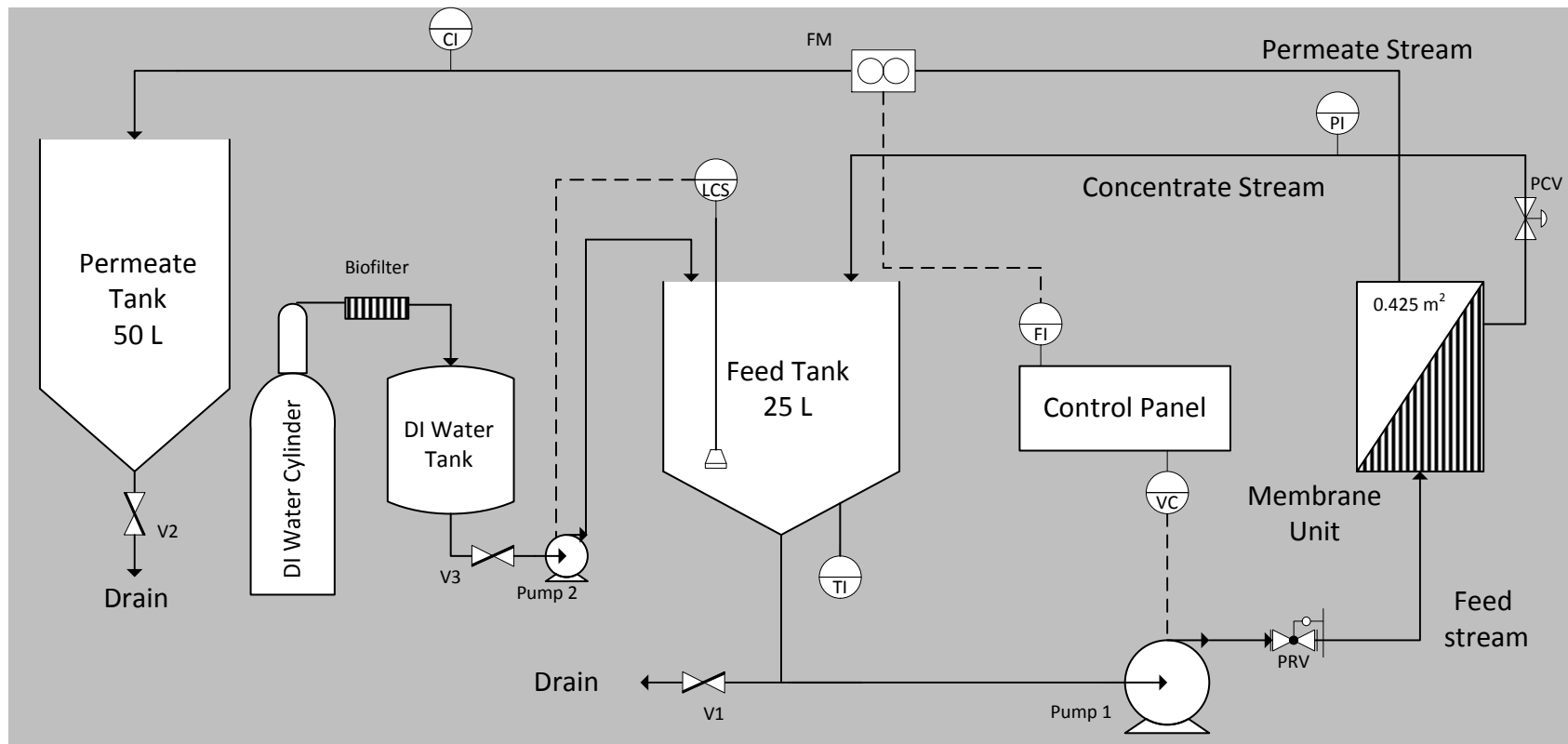


Figure 3.4 – Flow diagram of membrane filtration process in the PCI unit.

Instrument	Description
PI, FI, TI, CI	Pressure, permeate flow rate, temperature and permeate conductivity indicator.
VC, LCS	Cross flow velocity control. Level control and sensor.
PCV, PRV, V1, V2, V3	Pressure control valve, Pressure relief valve, ball-valve, gate valve, butterfly valve.
FM	Flowmeter.

3.2 Experimental Procedure

The experimental procedure for processing the samples includes several steps, related with either the material processing or the membrane performance.

Cold water flux measurements are made and recorded before and after the run in order to track the membrane performance. This procedure measures the flux decay after each run and the membrane performance during its lifetime. CWF measurements must be made at same temperature and pressure so that they can be compared afterwards.

The Cyan-X ultrafiltration process includes the following ordered steps: concentration from 3.37% to 5% dye strength, diafiltration, concentration from 5% to 8% dye strength, diafiltration, concentration from 8% to 15% dye strength and displacement. Procedures are detailed in the sections below.

i. Initial cold water flux (CWF) measurement

1. Make sure the tank valve is closed and fill up the feed tank with DI water until the set level.
2. Position both permeate and concentrate line to the feed tank. For the CWF measurements the system must be in recirculation.

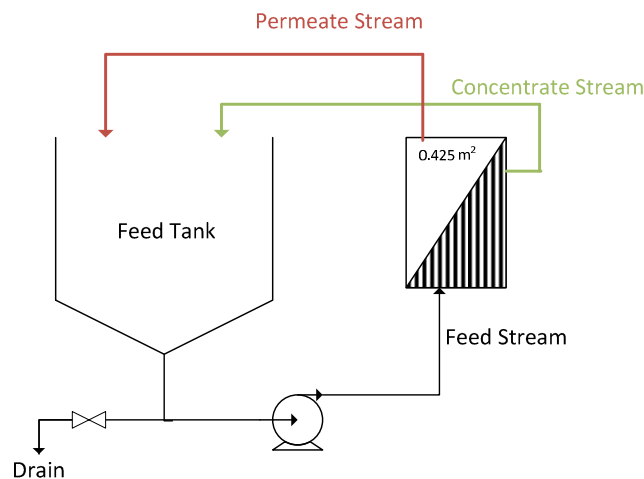


Figure 3.5 – Flow diagram of the system in total recirculation mode.

3. Switch on the pump and start running by setting the pump speed. Adjust the pressure applied to the desired value, through the pressure control valve.
4. When the temperature reaches 25 °C the permeate flow rate is recorded.
5. Take off the pressure and the pump speed, switch off the pumps and the system.
6. Discharge DI water by opening the tank valve.

ii. Ultrafiltration and Diafiltration Process

1. Load the sample to the feed tank. Dilute the sample by setting the tank level to the required dye strength, 3.37%. Switch on the DI water pump.
2. Switch on the feed pump and starting the run by setting the pump speed. Adjust the pressure to the desired value. The system should be in recirculation mode while the permeate conductivity is monitored. Once this parameter is steady the first concentration can be carried out. Readings of time, temperature, pH, flow rate, pressure, conductivity and permeate volume are taken.
3. The tank level is adjusted to the value which volume corresponds to 5% dye strength and the permeate hose is directed to the permeate tank. The concentration ends when the feed solution reaches the set level.

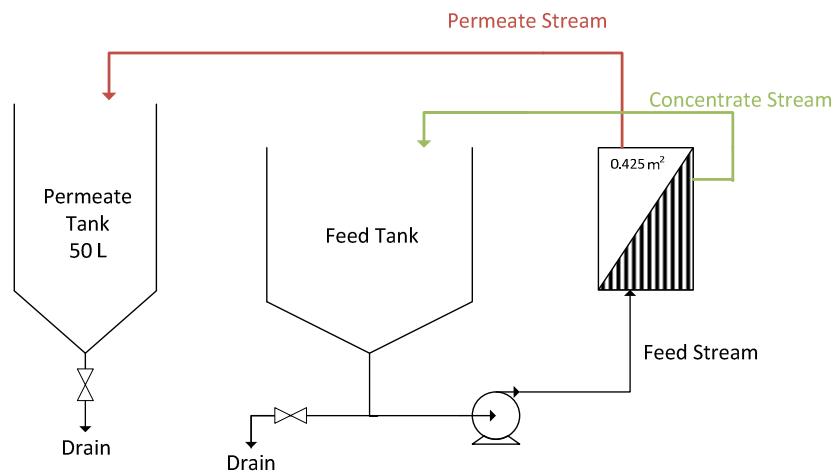


Figure 3.6 - Flow diagram of the system in concentration mode.

4. Diafiltration is automatically started through the feed of DI water to the system. The diafiltration is carried out until the permeate conductivity falls to approximately 500 μ S. Readings of the monitored parameters are taken frequently during the washing as well as samples of permeate and concentrate.

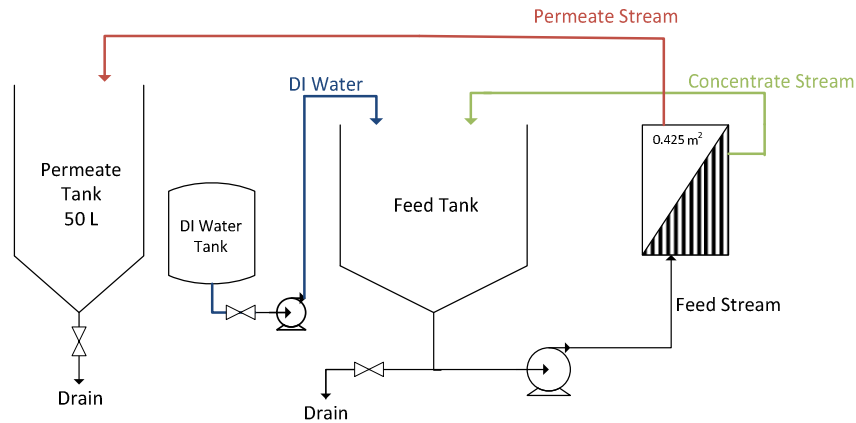


Figure 3.7 - Flow diagram of the system in diafiltration mode.

5. A further concentration is carried out in order to increase the dye strength to 8%. The level tank is set to a lower level and the concentration ends when the feed solution reaches that level. Reading and samples are taken.
6. Diafiltration is restarted and the batch is washed until the permeate conductivity is less than 90 μS .
7. The final concentration is carried out to obtain the final dye strength of 15%.
8. Switch off the DI water pump, take the pressure off and the pump speed. The concentrated product is discharged by opening the tank valve. Add DI water to the feed tank and turn on the feed pump to collect the concentrate product from membrane pipework. This is approximately 1.5L.
9. Take a 1L displacement.
10. Add DI water and run the system in recirculation to avoid residual ink from drying on the membrane surface.

When the system is in diafiltration mode, the number of wash volumes is determined during the processing. Wash volume is defined as the volume of permeate removed (volume of DI water added), that is equivalent to the total volume of solution in the system (feed tank + hold-up volume).

iii. Final CWF measurement

1. Clean the feed tank as well as the permeate and concentrates lines with DI water and discharge the remaining coloured water to drain. Repeat the procedure until the water is clean.

2. Fill up the feed tank with DI water until the set level and direct the permeate hose to the feed tank.
3. Start running the unit in recirculation and adjust the pressure.
4. When the temperature reaches 25 °C the permeate flow rate is recorded.
5. Take off the pressure and shut off the pump speed. Switch off the pumps and the system.

iv. Cleaning

The best method to remove the retained material from the membrane surface is through a chemical cleaning by circulating an appropriate cleaning solution through the membrane module for about 1 hour. The chemicals used to clean the membranes are alkaline solutions that can be followed by hot detergent solutions.

However, even after the cleaning, the flux may be not always be restored to the initial value. This result is an overall long-term decay [24].

1. Flush the system in recirculation mode several times and allow the temperature to reach 50°C.
2. Restart the flushing with fresh DI water and add 5% NaOH to obtain a pH between 11 – 11.5.
3. Take the pressure off and keep a high cross flow velocity, in order to clean the membrane surface.
4. Discharge the solution and flush the system with fresh DI water until the pH reaches DI water average values (~5.5).

3.3 Analytical Methods

3.3.1 Determination of Dye Strength by UV/Vis Spectroscopy

The dye strength is determined by measuring the optical density (absorbance) of a diluted solution.

Absorbance is a quantitative measure expressed as a logarithmic ratio between the radiation failing upon a material and the radiation transmitted through a material, equation (12). The absorbance is directly proportional to the concentration of the absorbing material in the sample, and these parameters are related according to the Beer-Lambert law, equation (13). Thus, the dye strength is obtained applying this relationship and considering the dilutions, equation (14).

Table 3.2 – Method of dye strength determination.

<p>Absorbance</p>	$A_{\lambda} = \log_{10} \left(\frac{I_0}{I_1} \right) \quad (12)$ <p>Where A_{λ} – absorbance at a certain wavelength (λ) I_0 – incident radiation I_1 – transmitted radiation</p>
<p>Beer-Lambert Law</p>	$A = \epsilon_0 CL \quad (13)$ <p>Where ϵ_0 - extinction coefficient C - concentration of absorbing species L - pathlength through the sample</p>
<p>Dye Strength</p>	$Strength (g / L) = \left(\frac{V_1 \times V_2}{m_1 \times m_2} \right) \left(\frac{A_{max}}{\epsilon_0} \right) \quad (14)$ <p>Where V_1, V_2 – dilutions volumes m_1, m_2 – masses diluted A_{max} – maximum absorbance</p>

The procedure to determine dye strength is described below.

1. Prepare a final 10,000 dilution by the following steps: weigh mass m_1 accurately and dilute in volume V_1 ; from this solution weigh m_2 and dilute in volume V_2 .
2. Fill up both of the spectrophotometer cells with DI water and determine the baseline.
3. Fill up one of the cells with the diluted coloured solution and run the spectrophotometer.
4. Read the maximum OD (absorbance) and calculate the dye strength by equation (14).

3.3.2 Determination of Metal Content by HPLC

The metal content in the concentrate and permeate samples was determined by high-performance liquid chromatography.

Liquid chromatography is a technique used to separate a mixture of compounds in order to identify or quantify them and also to purify the individual components. It involves passing a dissolved mixture in a mobile phase through a stationary phase. The mobile phase is a solvent that transports the mixture to be analyzed through a column that holds a solid stationary phase. The mixture is loaded onto

the top of the column, and their different components pass through the column at different rates because of the different chemical and physical interactions.

HPLC is a highly improved form of liquid chromatography. The solvent is forced through the column under high pressure, making the process much faster. Metal content is obtained by equation (15). A brief procedure is described below.

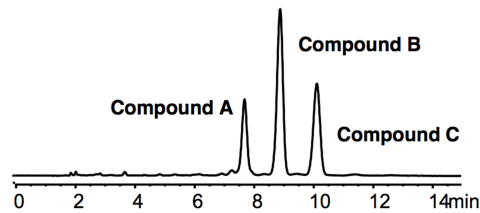


Figure 3.8 - Schematic chromatogram.

$$C_i(\text{ppm}) = \text{peak area of compound } i / \text{peak area of standard} \times \text{dilution rate} \quad (15)$$

1. Prepare the eluent and place it in a flask, checking that it is properly connected to the pump. Prepare the standard solution and the diluted solution of the sample to analyse.
2. Place the standard and the solution in the vials and run the HPLC.
3. Read the peak area that corresponds to the metal. Calculate the concentration by equation (15).

3.3.3 Water Analysis

Monitoring the quality of the DI water is crucial to ensure a high efficiency of the ultrafiltration stage, as DI water is used in the diafiltration process to wash the product and also in the membrane cleaning. As shown on the flow diagram, Figure 3.4, DI water is obtained by passing water through a cylinder, that contains an ion exchange resin and then through a biofilter. Both cylinder and biofilter have a limited lifetime, so it is necessary to monitor the physical parameters of the DI water on a weekly basis. Otherwise, the use of low quality DI water can lead to failures in the final product specifications. Thus, the pH, the conductivity and the bacterial growth of DI water are measured on a weekly basis. The Table 3.3 summarizes the DI water specifications.

Table 3.3 - Specifications of DI water.

pH	5.5 – 6.5	Mg (ppm)	< 0.005
Conductivity (µS)	~1µS	Si (ppm)	< 0.05
Na (ppm)	< 0.002	Fe (ppm)	< 0.0005
Ca (ppm)	< 0.005	Cl (ppm)	< 0.01

4 Results and Discussion

The membranes used in the Cyan-X processing were characterised. Additionally, in order to study how the filtration process at high pressure affects the membrane performance, the membrane characterisation was made before and after a Cyan-X processing at 40 bar. The objective was to quantify the membrane performance drop and to verify if the initial flux rate could be restored.

In order to gather data that allows an evaluation of the pressure effects on the filtration stage, several runs were carried out in the PCI unit at 30 and 40 bar pressure. The runs were carried out under the same conditions and from the same start material, so that the result comparisons are as reliable as possible. The general objective is to check any potential improvements in the overall filtration process, by increasing the pressure from 30 to 40 bar. The evaluation is based on the comparison of several process parameters, such as the permeate conductivity, the temperature, the flux rate, the cycle time and the wash volumes. The pressure effect on the product quality is tested by comparing the impurities removal rate and the rejection. The mass balance and the permeate colour losses are also compared in order to conclude about the pressure effect on the process yield.

4.1 Membrane Characterisation

i. Membrane Performance before and after Cyan processing

As mentioned on the section 2.3.1.3, the parameter that characterises a membrane is the hydraulic permeability coefficient, L_p . By equation (2), L_p is the slope of the linear variation of the permeate flux with the applied pressure. Three runs with DI water were carried out at three different pressures, 30, 35 and 40 bar, and the permeate flow rate was read at 25, 30, 35, 40 and 45 °C for each pressure (appendix A).

These trials were carried out before and after a Cyan-X sample processing at 40 bar pressure, and the variation of the flux as function of the applied pressure is plotted below. The membrane was also characterised after the chemical cleaning to quantify the percentage of membrane recovery.

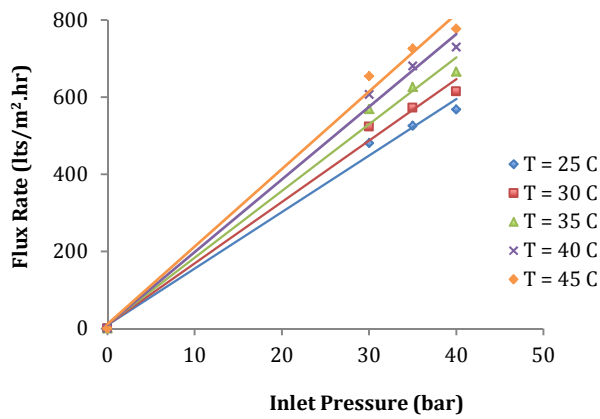


Figure 4.1 - Linear representation of the water flux rate versus applied pressure, at constant temperature, before the Cyan-X processing.

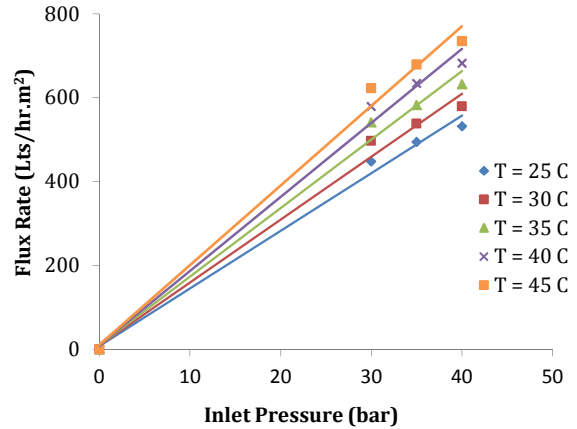


Figure 4.2 - Linear representation of the flux rate versus applied pressure, at constant temperature, after the Cyan-X processing, before the chemical cleaning.

Table 4.1 - Hydraulic permeabilities at different temperatures, and R-squared for each linear relation.

T (°C)	Before Cyan-X Run		After Cyan-X Run	
	L_p (Lts/m ² .hr.bar)	R ²	L_p (Lts/m ² .hr.bar)	R ²
25	14.66	0.991	13.75	0.991
30	15.91	0.990	14.99	0.989
35	17.31	0.989	16.32	0.989
40	18.85	0.993	17.64	0.990
45	20.11	0.991	18.97	0.990

Figure 4.1 and Figure 4.2 show that the results observed correspond to the expected results for the water permeability i.e. at constant temperature, the flux rate increases linearly when the pressure is increased.

Regarding the membrane performance before and after the Cyan-X run, the results show that the performance decreases, as the hydraulic permeability values decrease after the run.

The flux rate values pre and post run indicate that there is flux decay, which is due to the membrane fouling as consequence of residual product on the membrane surface or in the pores. Despite this flux decay, known in many membrane processes, membrane fouling can be reversible and, depending of the cleaning applied to the membrane, the flux can sometimes be recovered to the initial levels. Figure 4.3 shows the fluxes obtained for pure water before the run, after the run and after the chemical cleaning, measured at 30, 35 and 40 bar pressure at different temperatures.

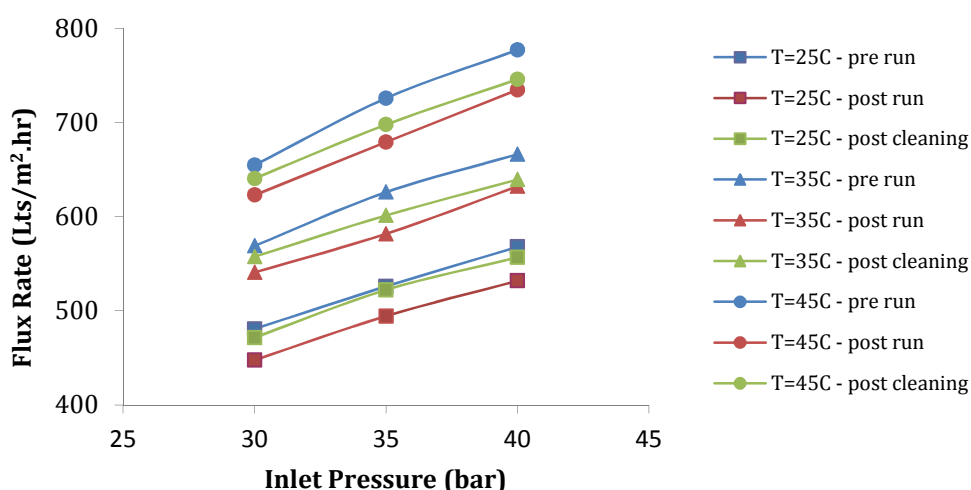


Figure 4.3 - Comparison of the flux rates for pure water before and after (including after cleaning) a run of Cyan-X.

The figure above shows in a clear way the decrease of the flux after each run and the correspondent recovery achieved after the cleaning. The graph shows that the decrease of the flux after the run is more significant at higher pressures and consequently the recover of the flux is less successful at higher pressures. Operating at 30 bar pressure, the flux rate almost return to the initial value. There are also differences regarding the temperature. Operating at lower temperatures will recover the initial flux.

These results confirm that the initial flux cannot always be restored. As mentioned before, it can be a consequence of membrane fouling, but the compaction of the membrane can also contribute to this result. Compaction occurs specially under high pressure conditions and it is the mechanical deformation of a polymeric membrane matrix during the filtration process. During the process, the porous structure densifies and, as result, the flux declines. After the pressure reduction, the flux generally does not return to its original value, since the deformation process is irreversible. The cleaning was carried out using 5% NaOH. Thus, it is important to mention that a more aggressive chemical cleaning could have been carried out.

As referred, the membrane characterisation was carried out after the run and after the cleaning to measure the performance decrease and recovery. In order to obtain relevant results to the thesis objective, it was determined the decrease of the membrane performance at both 30 and 40 bar pressure, which is showed on Figure 4.4.

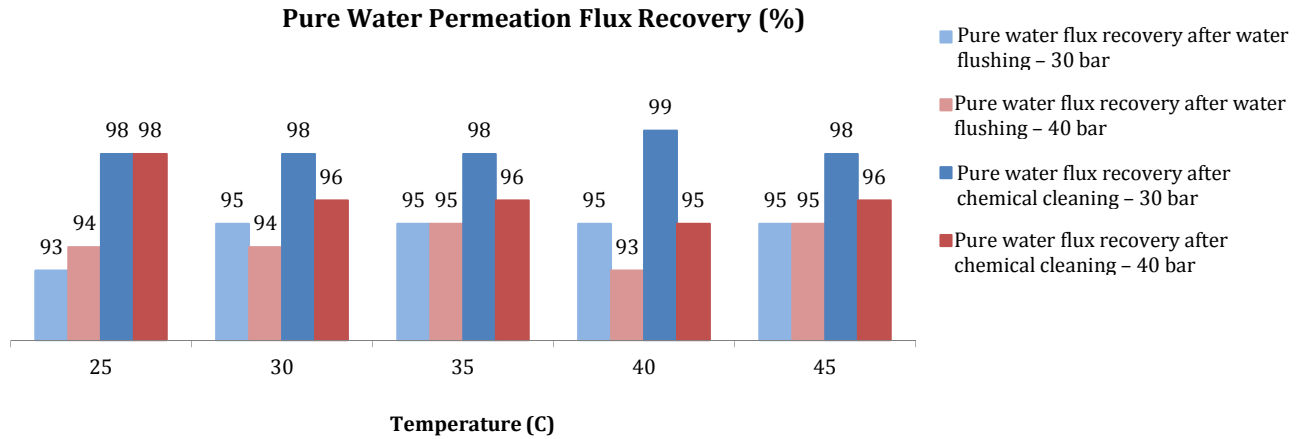


Figure 4.4 - Percentage of membrane performance obtained after the run and after the cleaning at 30 and 40 bar.

The graph above shows the percentage values of membrane performance for which the membrane performance drops after a run of Cyan-X, considering the pre run performance as 100%. The results are compared for 30 and 40 bar pressure at several temperatures. It also shows the recovery percentage of membrane performance achieved after the chemical cleaning.

It is observed that, at most temperatures, the decrease of membrane performance is higher at 40 bar than at 30 bar pressure. Operating at 30 bar, the membrane performance drops, on average, 5%. At 40 bar the percentage is, on average, 6%.

There are also differences regarding the recovery of performance. While operating at 30 bar the chemical cleaning yields 98% recovery of the initial performance, at 40 bar, the recovery achieved is only on average 96%.

ii. Temperature Effect on the Flux Rate

Analysing Figure 4.1 at constant pressure, one can see that the flux rate increases with temperature. Thus, Figure 4.5 displays the flux rates obtained to several temperatures at constant pressure.

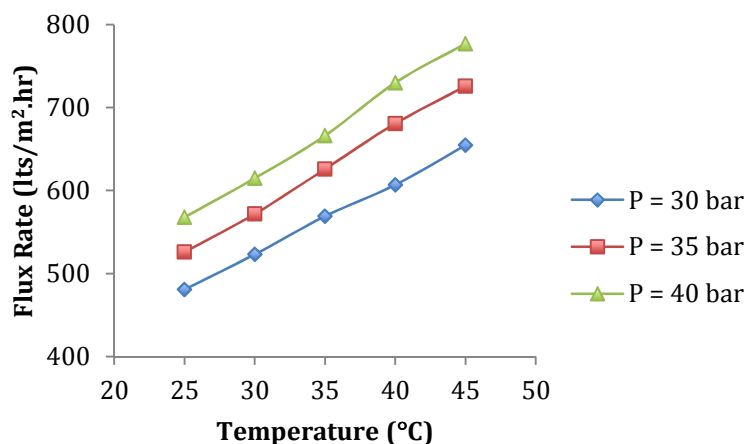


Figure 4.5 – Representation of the flux rate versus temperature, at constant pressure.

The flux rate increases with temperature due to the effect of the reducing viscosity. According to equation (3), the permeate flux is directly proportional to the inverse of the viscosity, which is lower at higher temperatures. Analysing the data presented (appendix A – Table A.1) it was calculated the percentage of flux increase per unit of temperature. For the three different pressures, it is observed that the flux rate increase, on average, 1.5% per °C. However, the potential flux increase based on temperature is only achieved with pure water, as this percentage decrease.

4.2 Cyan Trials

The Cyan-X dye processed is based on copper phthalocyanine, Figure 4.6. The dye is originally in form of paste and is dissolved to 8% strength in the processed samples.

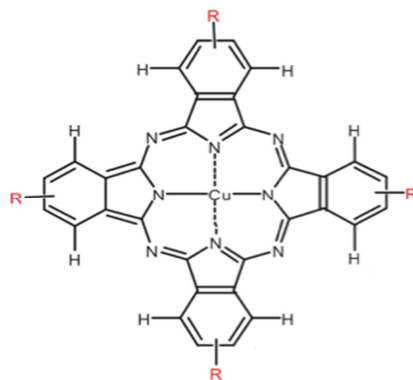


Figure 4.6 - Molecular structure of CuPC [37].

Section 4.2.1 describes and explains the profile of the monitored parameters during the cyan processing. In the section 4.2.2 the main parameters of the trials carried out at 30 and 40 bar pressure will be compared.

4.2.1 Monitored Parameters and Mass Balance of a Cyan Trial

Cyan-X was processed by ultrafiltration with diafiltration and during each run all the data was gathered on a datasheet. The datasheet contains information about the start material, project, colour, sample identification, initial strength, pH, volume and run number. The membrane type and area and the monitored parameters (time, flow rate, permeate conductivity, temperature, pressure, pH, permeate volume, tank level, wash volumes and any additional comments. It is also used to record the CWF before and after the run.

Project	Cyan	Membrane:	ES-209
Colour:	Cyan-X	Area:	0.425 m ²
Sample:	NBZ 6476/17/8	Strength:	6.54 %
Date :	27/01/2012	pH:	9.16
Plant:	Membrane Suite	Starting Volume:	5.20 litres
Run No:	PCU1356	Final Volume:	2.00 litres
		1st. Disp. Volume:	1.00 litres
		2nd. Disp. Volume:	litres

Initial Data:		
Cold Water Flow:	202.3	litres/hr
Pressure:	40	Bar
Temperature:	25	°C
pH	5.72	0.5 µS
Final Data:		
Cold Water Flow:	187.2	litres/hr
Pressure:	40	Bar
Temperature:	25	°C
pH	5.84	0.6 µS

Average temperature	40.7	°C
Average Pressure	40.0	Bar
Wash Volumes	20.48	

Clock Time	Time (mins)	Flow rate (lts/hr)	Flux Rate (lts/m ² .hr)	Conduct. (µS)	T (°C)	P (Bar)	pH	Permeate Vol. (lts)	Cumulative Vol. (lts)	Tank Level (lts)	Comments	Wash Volumes	Operation
12:50	0	6.7	15.76	0.7	23.1	40	9.22	0	0	9	3.37%	0.000	Recirculate
13:05	15	18.6	43.76	16000	40.1	40	8.88	0	0	9	C1/P1 3.37%	0.000	Recirculate
13:10	20	20.8	48.94	17500	45.5	40	8.75	1	1	5.5		0.095	Concentrate
13:17	27	21.3	50.12	18130	53.7	40	8.56	3	4	5.5	C2/P2 5%	0.524	Concentrate
13:30	40	38.7	91.06	12470	48.2	40	8.76	7	11	5.5	C3/P3	1.524	Wash
13:45	55	49.4	116.24	4650	40.7	40	8.88	10	21	5.5	C4/P4	2.952	Wash
14:00	70	52.8	124.24	1518	37.4	40	8.77	13	34	5.5	C5/P5	4.810	Wash
14:20	90	53.9	126.82	520	35.2	40	8.54	16	50	5.5	C6/P6	7.095	Wash
14:24	94	38.6	90.82	552	41.4	40	8.32	3	53	2.9	8%	7.524	Concentrate
14:36	106	39.3	92.47	414	40.4	40	8.16	7	60	2.9	C7/P7	9.115	Wash
14:49	119	39.4	92.71	296	40.3	40	7.97	8	68	2.9	C8/P8	10.933	Wash
15:02	132	40.1	94.35	210	40.2	40	7.76	8	76	2.9		12.751	Wash
15:17	147	40.2	94.59	145.6	39.8	40	7.51	10	86	2.9	C9/P9	15.024	Wash
15:42	172	39.4	92.71	86.6	39.3	40	7.21	16	102	2.9	C10/P10	18.660	Wash
15:51	181	39.8	93.65	74.8	39.5	40	7.13	6	108	2.9		20.024	Wash
15:53	185	24.3	57.18	105.5	46.9	40	6.93	2	110	1		20.478	Concentrate

Figure 4.7 - Spreadsheet of a typical run.

In order to have a profile of the most important parameters of the run, the spreadsheet displays a chart with the representation of the permeate conductivity, temperature and flux rate as a function of time.

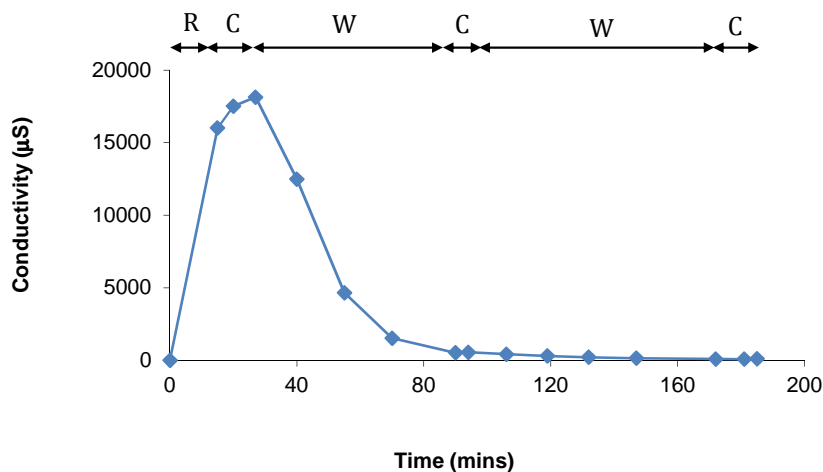


Figure 4.8 - Permeate conductivity profile versus time, of a Cyan-X run at 40 bar.

As Figure 4.8 shows, the permeate conductivity increasing during the recirculation (R) stage and it peaks after the first concentration (C). The high initial value is related to the presence of impurities, either metal ions, salts, solvent and a small amount of dye itself. When the diafiltration/washing (W) is started, DI water is added to the sample and the washing causes the permeate conductivity to decrease very quickly. This happens as the sample is diluted and the impurities are washed out. During the second concentration, the permeate conductivity does not increase, as all the solvent and most of the impurities are removed during the first washing. The second stage of diafiltration takes approximately as long as the first one, but the permeate conductivity decreases much more slowly because, at this point, the concentration of impurities is very low. It is considered that the product is purified enough when the permeate conductivity is very low, in this case less than 90µS, and thus the final concentration is carried out until a higher strength than the final specification is achieved. During this final stage, the conductivity usually increases slightly and this is due to the fact that, during the concentration, the permeate dye losses are slightly higher and some residual conducting species are removed.

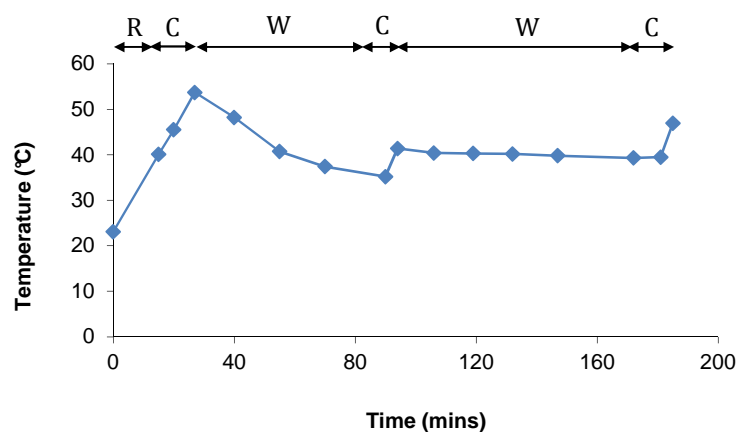


Figure 4.9 - Temperature profile versus time, of a Cyan-X run at 40 bar.

The temperature is an important parameter to monitor, as there is a limiting value above which one should not operate, due to the risk of damage to the membranes and consequent loss of efficiency. In fact, regarding membrane damage, high temperatures are more dangerous than high pressures.

As Figure 4.9 shows, the temperature increases during the recirculation because the cross velocity on the membrane is high and this causes the batch to heat up. During the first concentration, the temperature continues increasing, and it occurs at a faster rate as the flux rate is very low at this point and it takes slightly longer to reach the desired concentration. The diafiltration water reduces the temperature and it decreases continually until the start of the second concentration. There is an increase of temperature at this stage as no water is being added and the flux rate is higher at this point, the concentration stage is quick. During the second washing the temperature reduces and tends to remain fairly constant. As the flux is higher, the DI water flow is also higher. The temperature increases again with the final concentration and usually this final stage leads to temperatures very close to the limit. The volumes processed on the PCI unit are usually small and this requires greater attention at this stage to the tank level.

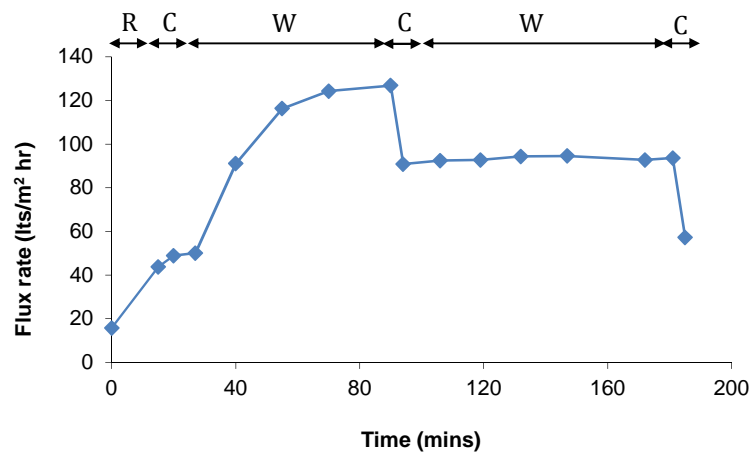


Figure 4.10 - Flux rate profile versus time, of a Cyan-X run at 40 bar.

Figure 4.10 shows that the flux rate starts at a very low value, under 20 lts/m².hr during recirculation, and that it increases moderately. This behaviour is mainly due to the presence of the solvent Y⁷, which causes high viscosity to the sample. During the first concentration, the increase of flux rate slows, being almost constant, as both dye and the impurities are more concentrated causing a decline in flux rate. When the diafiltration is started, the water dilutes the sample making the transport of impurities easier through the membrane and it results in a significant increase of the flux. As most solvent Y is removed in the first two wash volumes, the viscosity reduces, increasing the flux rate until the point that the second concentration is started. The increase of both impurities and polymer ratios causes the flux decline during the second concentration. During the second wash, the flux tends to be steady until the final concentration,

⁷ Due to confidential reasons.

when there is a further reduction of the flux. Depending on the sample, the last concentration can reduce the flux to a very low level, about 40 lts/m².hr.

In order to do the mass balance of the filtration process, the dye strength of the concentrate and permeate are measured, at several points during the ultrafiltration process. Through the mass balance is possible to quantify the process yield and the losses either to the permeate or to the unit.

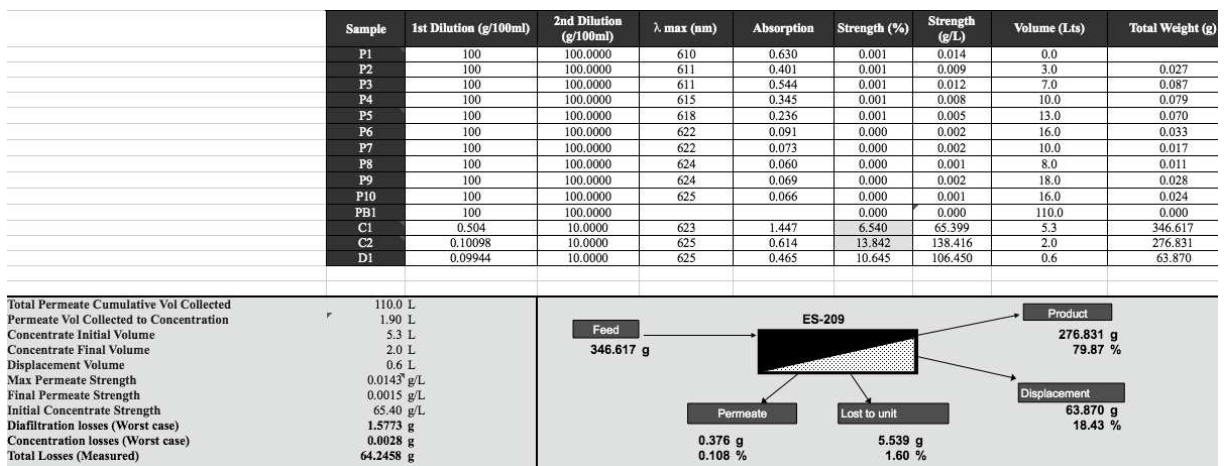


Figure 4.11 - Mass balance of the dye for the Cyan-X processing at 40 bar.

During the run, several small samples were taken and labelled as P1 – P10 and C1 – C10, permeates and concentrates respectively. By measuring the OD and applying the equation (14), the dye strength per unit of volume is obtained. The permeate volume is also recorded, thus it is possible to calculate the weight of dye that is lost in the permeate. As can be observed, the permeate losses are not significant, representing 0.1% of the initial amount of dye.

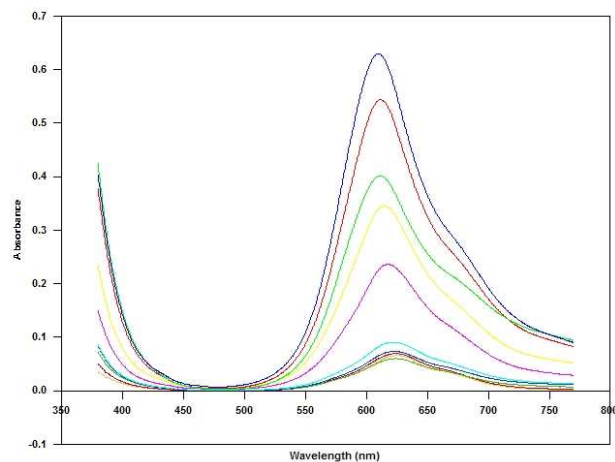


Figure 4.12 - Measurements of the optical density of the permeate samples of a typical trial.

The initial and final strength of the concentrate is determined and it is possible to calculate the actual weight of dry dye present in C1 (start material) and in C2 (final product). Applying the same method, the amount of dye present on the displacement (D1) is determined. Often, when the product is over concentrated, the displacement is strong enough to be used as product, which increases the amount of dye recovered.

Although this mass balance is not very accurate, gathering all the data, the yield of the process can be determined. In this example, the yield was 79,9%. Usually it is possible to achieve reasonable high yields using the PCI tubular unit.

4.2.2 Comparison Between Trials at 30 and 40 bar Pressure

Two samples of Cyan-X were processed under different pressure conditions, in order to understand the benefits or disadvantages of operating at a higher pressure. Both samples came from the same batch production, so that the dye composition and physical characteristic were the same. The volume of both samples was very similar in order to process the same amount of dye at 100%. The spreadsheets of the runs are in the appendix B.

4.2.2.1 Permeate Conductivity Profile

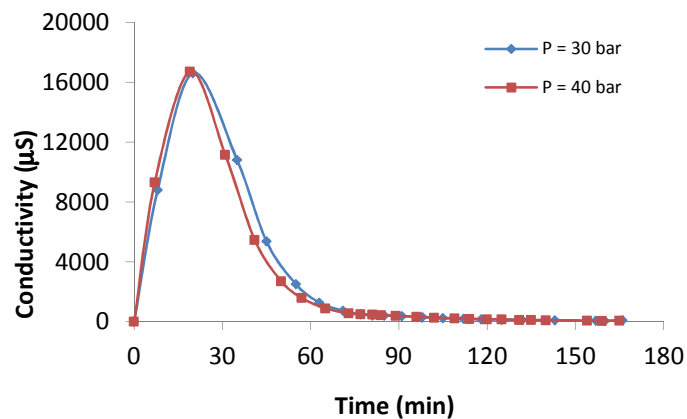


Figure 4.13 - Permeate conductivity profiles at 30 and 40 bar pressure.

Comparing the trials at 30 and 40 bar, it is observed that there is no significant difference in respect to the permeate conductivity. In both trials the permeate conductivity peaks roughly at the same time. Despite a slight faster decrease after it peaks (during the diafiltration), at 40 bar pressure, both profiles are similar. Apparently, a higher pressure does not lead to a faster decrease of conductivity, since

it is necessary to allow approximately the same time for the permeate conductivity to achieve the same desired values for both trials. As mentioned, the permeate conductivity is a good indicator of impurities present.

4.2.2.2 Temperature Profile

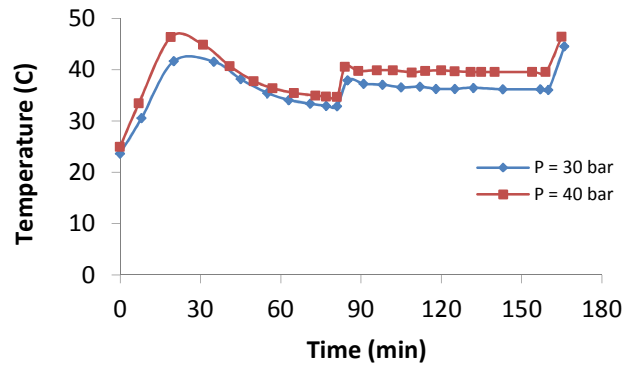


Figure 4.14 - Temperature profiles at 30 and 40 bar pressure.

Comparing the trials at 30 and 40 bar, it is observed that temperature increases faster when the unit operates at 40 bar pressure, which is expected because the velocity of the permeation flux through the membrane is higher. While operating at 40 bar the temperature gets closer to the limit (50°C) when the first and the last concentrations are carried out. Small volumes of samples achieve higher temperatures faster, and in some cases it is necessary to complete the final concentration before the desired strength is reached.

4.2.2.3 Flux Rate Profile

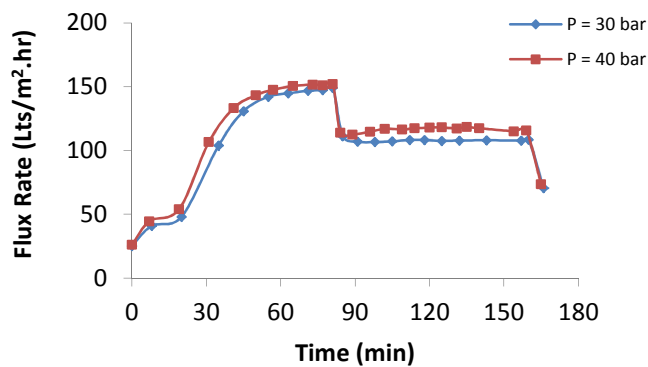


Figure 4.15 - Comparison of the flux rates at 30 and 40 bar pressure.

The comparison between both flux rates shows that, in most stages of the processing, the run at 40 bar pressure leads to fluxes slightly higher. This result is observed from the beginning of the run, in recirculation and it continues with the same profile until the second concentration occurs, which corresponds to the concentration from 5 to 8%. The increase of the flux with increased pressure is the expected result.

The concentration polarisation is an important phenomenon that has effects on the flux. The increase of the hydraulic permeability with pressure, also increases the convective transport of solutes to the membranes surface. Consequently, the polarisation increases as well.

According to the gel polarisation model, at low concentration in the bulk stream, the flux increases with the pressure, because higher pressure leads to higher rate of convective transport of solute to the membrane surface. Thus, the solute concentration at the surface increases and it results in an increase of the concentration driven back by diffusive transport and away from the membrane surface. As a result, the flux through the membrane increases. However, it is important to notice that the increase in the flux is not very significant, as it is shown in Figure 4.16.

During the first concentration, there is also an increase of flux at 40 bar. At this point, the high temperatures, which makes the viscosity decrease, combined with the low concentration (3.37 to 5%) causes a slight increase in flux rate.

It is observed that, during both second and final concentrations, the difference in the flux is very small, which suggest that at higher concentrations of the dye, the applied pressure does not have a significant effect on the flux. This result can be explained by the gel polarisation model. Increases in the pressure increase the convective transport (concentration polarization) to the membrane surface. However, a maximum value of concentration on the surface is reached and at this point it is considered that the concentration of solute on the membrane surface is equal to the concentration of the gel formed, caused by the effect of concentration polarisation. In this case, the back diffusive transport is fixed, and the solute accumulates on the membrane. Therefore, from this point on, the flux (called limiting flux) is independent of the pressure, and it depends of feed concentration. Taking the model in account, the results obtained suggest that operating at 40 bar and higher concentrations, the limiting flux can be achieved and the pressure does not increase the flux significantly through the membrane, as it is shown in Figure 4.17.

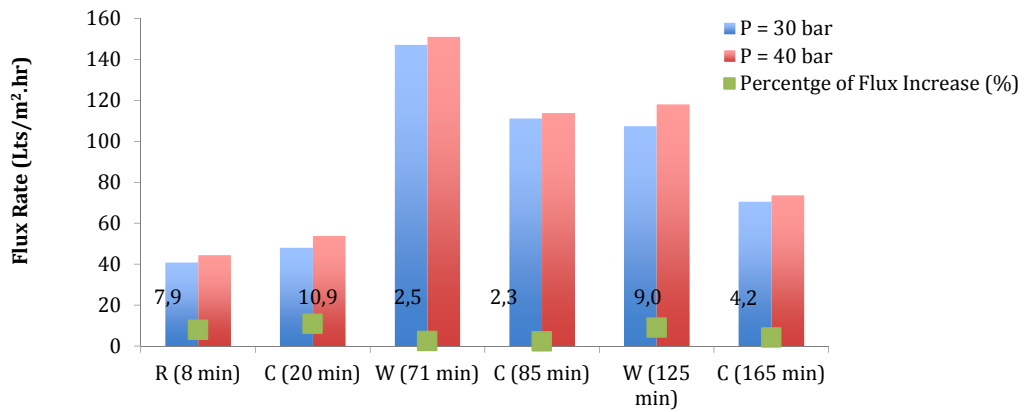


Figure 4.16 - Comparison of the flux rates distinguishing the different stages of the filtration. R – recirculation, C – concentration, W – washing.

Figure 4.15 and Figure 4.16 show that, the stages where a greater flux increase occurs, by operating at 40 bar pressure, are during the first concentration and the second washing. During the first concentration, at 40 bar, the temperature is higher and it leads to a higher flux due the reduction of viscosity. During the second diafiltration, even though the concentration at this point is 8%, most of the solvent Y and the impurities are already removed. Solvent Y causes a high viscosity to the solution, so when it is removed the viscosity is lower and the flux is higher.

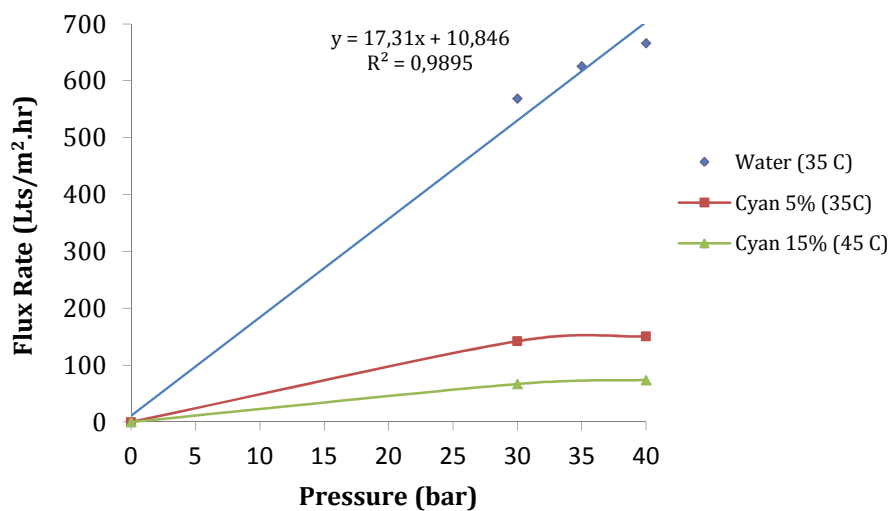


Figure 4.17 - Effect of pressure on Cyan - X ultrafiltration.

Figure 4.17 compares the flux profile between the water and the Cyan-X solutions at two different concentrations. The water permeate flux comes from the membrane characterization described in the previous section and the Cyan-X permeate flux rates come from the experiments carried out at 30 and 40

bar. As mentioned previously, the water flux is directly proportional to the applied pressure and the only resistance is the hydrodynamic resistance of the membrane. When the fluid processed is a solution, the behaviour observed is completely different when the pressure is increased. Regarding the Cyan-X, it is observed that, initially the flux increases with pressure, but after a certain point, the flux increase is very small and has different values for different concentrations of feed stream. There is no data of further pressures, but it seems that the flux profiles tend to stabilise, becoming independent of the pressure.

The table below shows the differences of the percentage of flux increase observed between pure water and the Cyan-X.

Table 4.2 - Percentage of flux increase, from 30 to 40 bar, registered for pure water and for the Cyan-X.

T (°C)	Percentage of Flux Increase (%)	
	Water	Cyan-X
25	15.3	3.6 (at 3.37% dye strength)
35	14.6	5.6 (at 5% dye strength)
45	15.7	9.3 (at 15% dye strength)

4.2.2.4 Mass Balance to the Dye

The mass balance was determined for both runs at 30 and 40 bar, in order to check the pressure effect on the process yield. It is calculated by measuring the OD of the initial and final concentrate samples (C1 and C2), the displacement (D1) and the permeate samples collected during the run. The strength (g/L) is obtained by applying the equation (14), which is multiplied by the volume gives the amount of dry dye present in each sample. Thus, it is possible to know how much product was lost to unit, permeate and displacement and the process yield.

Table 4.3 – Measurements for the mass balance of the Cyan-X run, at 30 bar.

Sample	Strength (g/L)	Volume (L)	Dry Weight (g)
C1	82.01	5	410.02
C2	138.8	2.5	346.99
D1	112.69	0.5	56.34
Sum Permeates	Appendix C – Table C.4		0.126
Total Permeate Cumulative Volume			115 L
Permeate Volume Collected to Concentration			9 L
Concentrate Initial Volume			5 L
Concentrate Final Volume			2.5 L
Displacement Volume			0.5 L

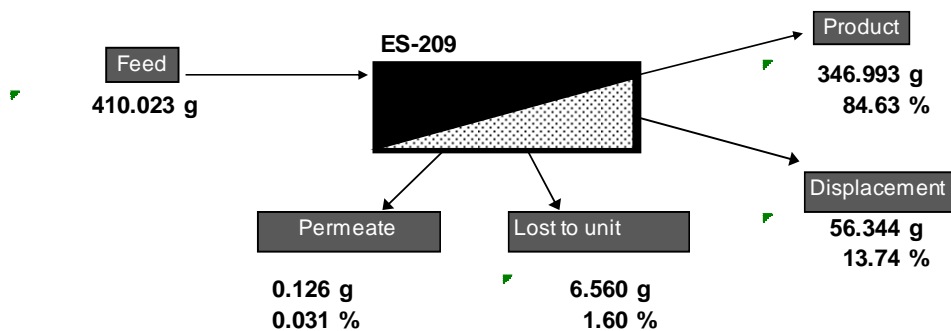


Figure 4.18 - Mass balance of Cyan-X run at 30 bar.

Table 4.4 – Measurements for the mass Balance of Cyan-X run at 40 bar pressure.

Sample	Strength (g/L)	Volume (L)	Dry Weight (g)
C1	82.01	4.8	393.62
C2	126.68	2.6	329.36
D1	93.16	0.5	46.58
Sum Permeates	Appendix C – Table C.4		0.167
Total Permeate Cumulative Volume			120 L
Permeate Volume Collected to Concentration			8.5 L
Concentrate Initial Volume			4.8 L
Concentrate Final Volume			2.6 L
Displacement Volume			0.5 L

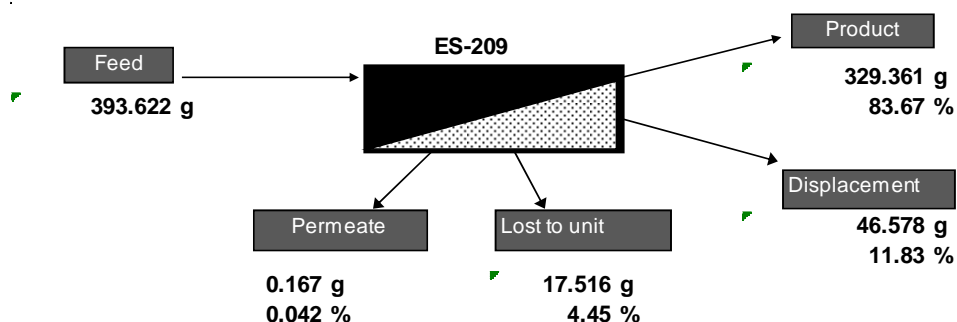


Figure 4.19 - Mass balance of Cyan-X run at 40 bar pressure.

Comparing the results, operating at 30 bar the percentage of product recovered is 84.63%, while at 40 bar it is 83.67%. In the trials carried out in the laboratory, the losses in the unit and in the displacement are not related to the process efficiency itself, but with the unit operation. Using the pilot membrane unit, additional losses arise from the discharging, sampling and system hold-up volume. The hold-up volume is the volume that corresponds to the piping and the tubular module and it is 1.5 litres for this unit. For this reason, it is not accurate to compare these losses. However, the permeate losses were

measured accurately and the results show that the permeate losses are slightly higher when the increased pressure is applied. Despite the small difference, the permeate losses increase from 0.031% at 30 bar, to 0.042% at 40 bar. Even though these are estimates, it suggests that higher pressure leads to a very slight decrease in the process yield.

4.2.2.5 Permeate Colour Losses

Following the mass balance results, the permeate colour losses are discussed in detail. In order to determine the amount of dye present in the permeate, samples were collected during the runs. The objective was to see how the permeate colour losses vary with increased pressure. The colour loss rate as function of the wash volumes is displayed in Figure 4.20.

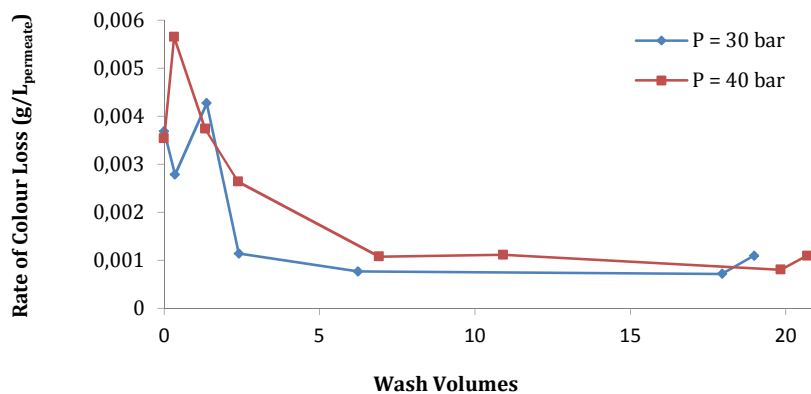


Figure 4.20 - Colour loss rate through the permeate of the runs at 30 and 40 bar.

The chart above shows that the trial carried out at 40 bar pressure leads to slightly higher colour losses in the permeate. This result can be related with the fact that, at 40 bar, there is a higher convective flux to the membrane, resulting in a slightly higher concentration of dye on the membrane surface. Thus, as the flux is higher, a slightly larger amount of dye can be pushed through the membrane, which increases the colour loss in the permeate.

It is clear that for both runs that most of the colour loss occurs during the first 2.5 wash volumes. However, the colour loss rates obtained does not show the same profile on the 30 and 40 bar pressure. In the run at 30 bar, the colour loss initially decreases, from the recirculation stage to the first concentration stage and then increases when the diafiltration is started, peaking at 1.4 wash volumes. After this point, the colour loss keeps at a low level and constant during the rest of the filtration. There is a slight increase corresponding to the final concentration to 15%. In the run at 40 bar, the colour loss increases as soon as the recirculation is started, and it peaks during the first concentration, before the diafiltration be started. After this point, the colour loss decreases continually, and remains constant after 7 wash volumes. It also increases slightly during the final concentration.

Figure 4.21 shows the difference of the colour losses between both runs, at the different stages of the process. Most significant differences are observed during the first concentration and at 2.4 wv, with an increase of colour loss higher.

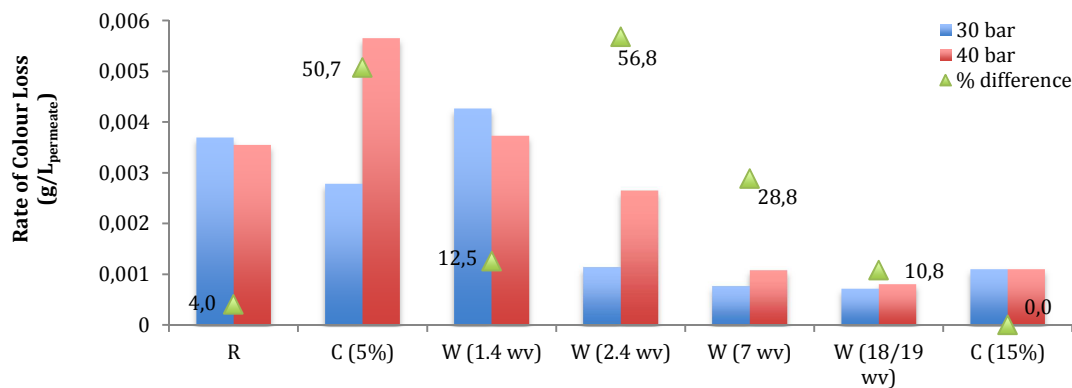


Figure 4.21 - Colour loss rate at 30 and 40 bar, showing the different stages of the filtration process.

4.2.2.6 Impurities Removal

The removal of impurities is the primary objective of the filtration of this aqueous cyan dye, as there are specifications that the final product must meet. Metal ions, salts and solvent are considered impurities.

i. Metal Ion Removal

Metal ions are one of the most important impurities to remove from the dye, as its presence can compromise the high purity of the final product. For this reason it is important to trace the metal rejection during the filtration process. The rejection of a compound is related with its size and with the type of interaction that exist between it and the membrane, which affects its adsorption.

In order to trace the metal rejection, the metal content was tracked in both concentrate and permeate during the runs at 30 and 40 bar pressure. Figure 4.22 shows the metal content profile obtained from the run at 30 bar, which is similar to the one obtained at 40 bar. It matches with the typical metal content profile in the concentrate and in the permeate obtained during the cyan purification on large scale. It was obtained measuring the amount of metal as solution and then calculating the correspondent amount as dry, by equation (16).

$$ppmFreeMetalasDry = \frac{1000}{ColourStrength} \times ppmFreeMetalasSolution \quad (16)$$

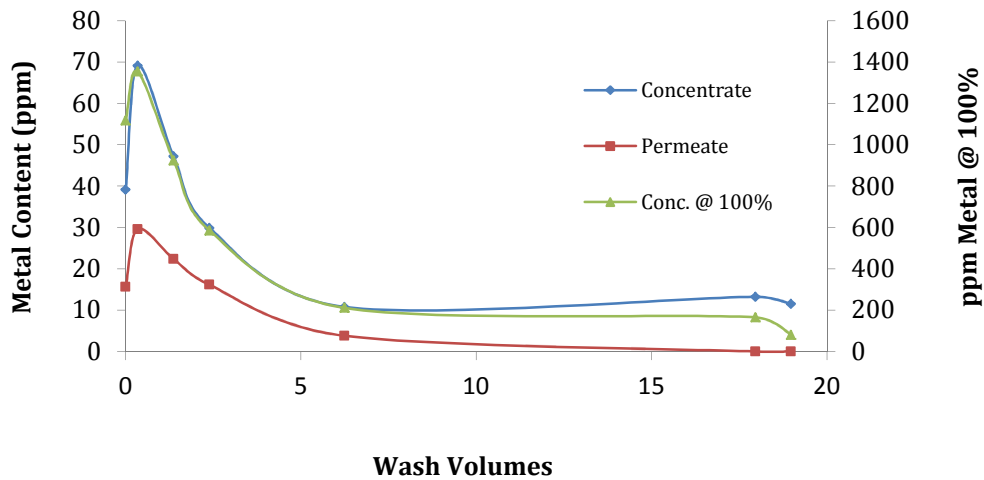


Figure 4.22 - Metal content profile in the concentrate and permeate, during UF process.

It is observed that the amount of metal present on the concentrate side is higher than on the permeate side during the whole processing, and this is because the metal is part of dye molecule itself. With cyan there are aggregation effects of the dye molecule.

The metal is detected in both concentrate and permeate from the beginning of the filtration, and there is a peak of that corresponds to the first concentration, from 3.37% to 5%. After this point, the removal continues and is mostly observed during the first 7 wv, which is roughly the moment when the second concentration, from 5% to 8%, is due. At 18 wv, there is a further decrease of metal in the concentrate, caused by the final concentration, to 15%.

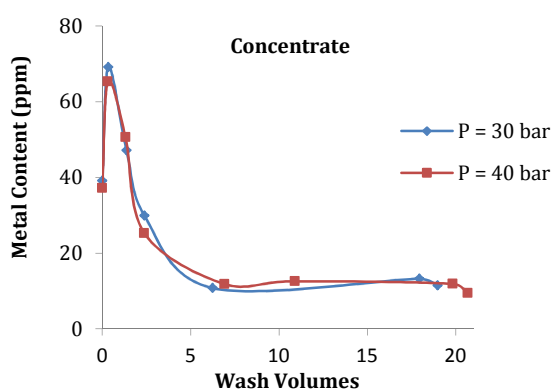


Figure 4.23 - Metal content profile in the concentrate.

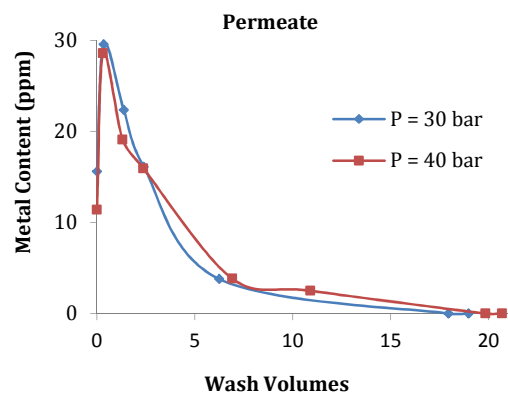


Figure 4.24 - Metal content profile in the permeate.

The figures above show the metal content comparison between 30 and 40 bar. It is observed that the pressure increase does not change the metal removal significantly. The concentrate profile

comparison suggests that the final content of metal is slightly lower in the run at 40 bar, however the initial content is lower. Observing the results in appendix C, the difference between the initial and final metal content in the concentrate, i.e. the metal removed (plus the metal lost to the unit), is exactly the same for both pressures.

In order to check the differences between the metal removal in the two runs, the metal rejection was tracked during the filtration process, applying equation (6).

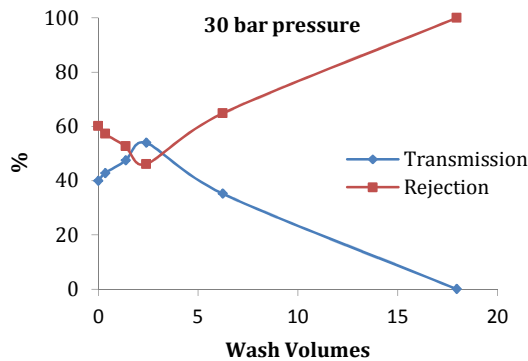


Figure 4.25 - Metal rejection and transmission at 30 bar pressure.

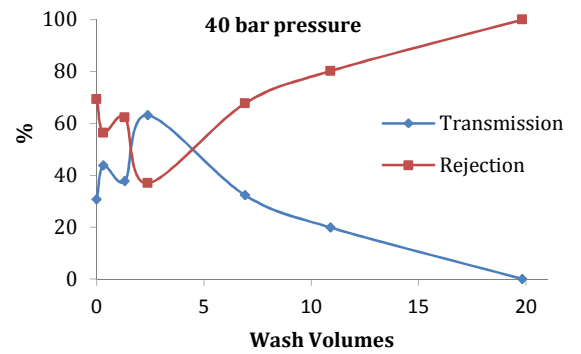


Figure 4.26 - Metal rejection and transmission at 40 bar pressure.

Despite the previous results suggesting that the overall rejection is similar for both pressures, the figures above show that there are slight differences in the metal rejection profile during the two experiments. Again, after 7 wv, the metal rejection increases quickly to 100%.

In order to understand the effect of the pressure on the metal retention, Figure 4.27 compares the retention factor between 30 and 40 bar pressure, for different points of the ultrafiltration process.

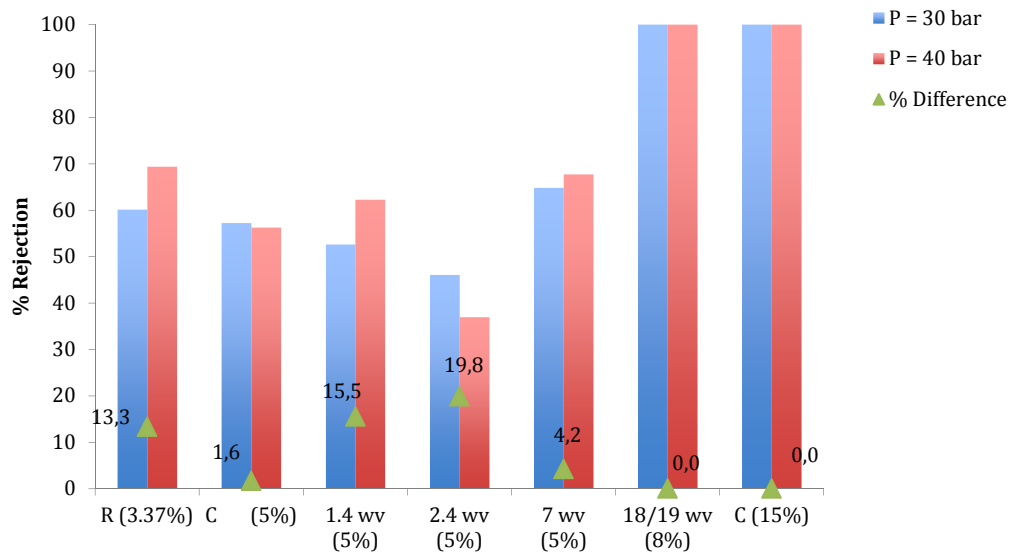


Figure 4.27 - Metal rejection at 30 and 40 bar pressure, showing the different stages of the filtration process.

The effect of concentration polarisation is to reduce the membrane flux, but it also affects the retention of macromolecules. According to the gel-polarisation model, described in section 2.2.1.3, with macromolecular solutions, the concentration of retained macromolecules at the membrane surface increases with increased pressure, so permeation of the macromolecules also increases, lowering the rejection. This effect is more noticeable at low pressures and under these conditions increasing the applied pressure produces the largest increase in the flux and hence concentration polarisation at the membrane surface. At high pressure, the change in flux with increased pressure is smaller, so the decrease in rejection by the membrane is less apparent. However, concentration polarisation can interfere with the ability of an ultrafiltration membrane to separate a mixture of dissolved macromolecules.

Observing the comparison of the metal rejections obtained for both pressures, it is clear that the results do not match the gel-polarisation explanation. Figure 4.27 shows that during the most part of the ultrafiltration, the increased applied pressure leads to an increase of the metal rejection, which happens during the recirculation (R) and during the washing/diafiltration at 1.4 and 7 wash volumes. During the first concentration (C), the metal rejection decreases slightly at 40 bar and the only measurement that shows a significant decrease of metal rejection with high pressure is at 2.4 wash volumes, during the washing/diafiltration. At the end of the processing, at 19 wash volumes, both trials at 30 and 40 bar present a metal rejection of 100%.

It is expected that an ultrafiltration membrane, in this case with a 9000 MW cut-off, would allow easy passage of a metal ion, however, the explanation of the general increase of the metal rejection with increased pressure might be related with the dye molecule itself. The cyan dye tends to aggregate, forming

macromolecules that change what would be the expected interaction between the membrane and the metal ion.

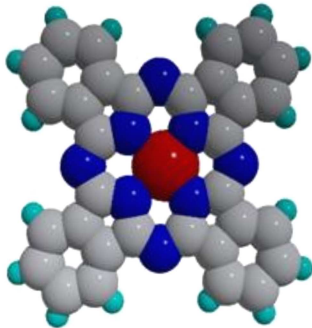


Figure 4.28 - Model of the CuPc molecule, $\text{CuC}_{32}\text{N}_8\text{H}_{16}$.

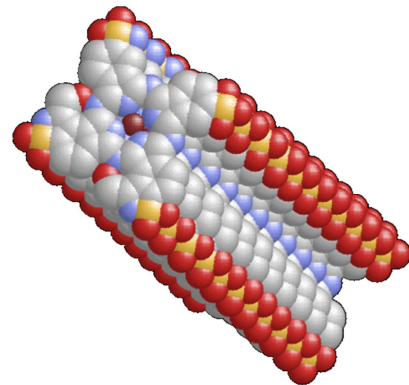


Figure 4.29 - Model of the aggregate formed by the dye molecules ^[38].

The actual MW of the dye molecule is about 1200 Da, but the aggregates formed are much greater than the 9000 MWCO membrane. The increased rejection observed suggests that the aggregates formed can constitute a secondary barrier layer, blocking the passage or trapping the metal ions.

Analysing the different stages represented in Figure 4.27, it is observed that the pressure effect on the retention is different during the process.

During the recirculation the increased pressure makes the metal rejection increase. Despite the concentration being very low at this point, the high viscosity caused by the solvent presence contributes, along with the aggregation effect, to this result.

Immediately after the concentration to 5%, the effect of the second layer is not so noticeable and there is a slight decrease of the metal rejection at 40 bar. This might be related with the fact that the sample is less viscous and the flux is higher at this point.

When the diafiltration is started, the first measurement indicates that, at 40 bar, the rejection is higher than at 30 bar. With higher pressure there is a higher concentration of dye (aggregates) on the membrane surface, retaining the metal ion. At 2.4 wv, the rejection at 40 bar is lower than at 30 bar, and it might be due to the effect of the diafiltration and the increased flux rate, allowing an easier passage of the metal ions at 40 bar. At 7 wv the measurements indicate a new increase of the rejection with pressure, and at this point most of free metal ions are already removed. More measurements between the previous points would help to understand the change observed on the rejection during the diafiltration stage. At 19 wv both trials have a metal rejection of 100%.

ii. Solvent Removal

During the Cyan-X processing the removal of the solvent Y takes place, which is used during the dye synthesis. The solvent needs to be removed totally, in order to obtain the final product specification, and the filtration process is able to achieve this target. Figure 4.30 shows the typical solvent content profile in the permeate and concentrate during the filtration process.

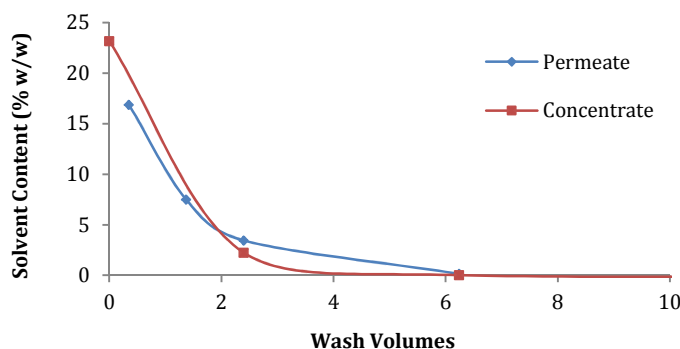


Figure 4.30 - Solvent content profile in the permeate and concentrate, during UF process.

As the chart above shows, the samples have an initial solvent Y content of around 20 - 25 % w/w. Initially, the solvent content, in both permeate and concentrate, decreases very quickly. In fact, most of the solvent is removed during the first two wash volumes and after this point the removal continues at a slower rate. It is observed that after 6 wash volumes, the amount of solvent in the concentrate and in the permeate is very low.

Running the samples at an increased pressure does not change the solvent removal profile, but the results of solvent removal were compared at 30 and 40 bar pressure, in order to check the pressure effects in terms of required wash volumes to perform the removal.

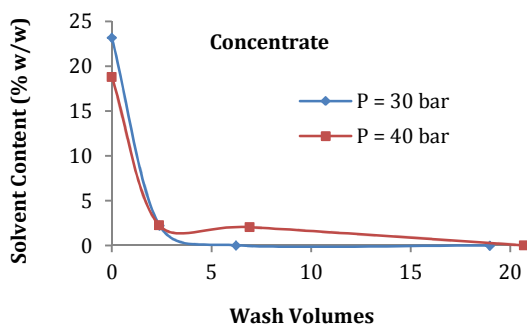


Figure 4.31 - Solvent content in the concentrate, at 30 and 40 bar.

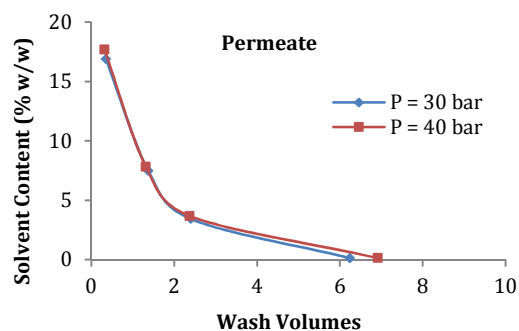


Figure 4.32 - Solvent content in the permeate, at 30 and 40 bar.

The charts above are not conclusive about the effect of the pressure, as they represent the content of solvent as function of the number of wash volumes, but the initial amount of solvent was not exactly the same in both experiments. However, it is possible to observe that in both concentrate and permeate, the increase of the pressure does not lead to significant differences.

The results of the concentrate show that initially the solvent content decreases in a similar way at both pressures. At 2.5 wash volumes, the solvent content is roughly the same at 30 and 40 bar, but after this point it seems that the removal does not have the same profile. At 30 bar pressure, the solvent content in the concentrate decreases quickly, while at 40 bar pressure the decrease of solvent content is slower, and the results show that the solvent is present in the concentrate for longer at 40 bar pressure.

The results of the permeate show that both solvent content profiles are identical. However, initially there is a slight difference, where the amount of solvent present in the permeate is higher in the run at 40 bar pressure. Between 6 and 7 wash volumes, the solvent content is insignificant.

In order to evaluate only the rate of solvent removal, rather than its content, Figure 4.33 shows the amount of solvent removed per litre of permeate collected.

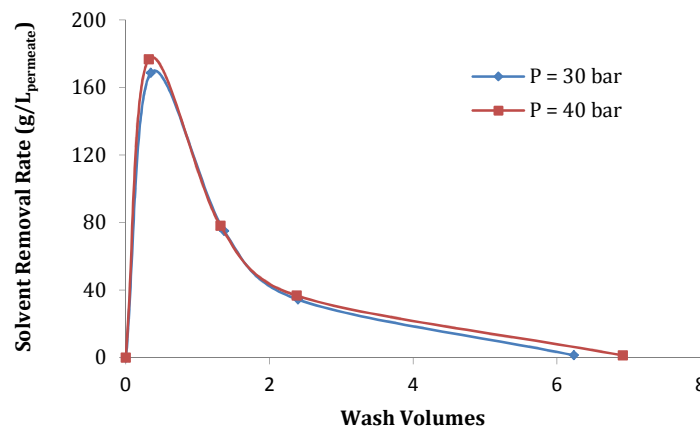


Figure 4.33 - Solvent removal rate, at 30 and 40 bar pressure.

It is observed initially that, the amount of solvent removed per unit of volume of permeate is slightly higher in the run at 40 bar pressure and this point correspond to the first concentration stage and the beginning of the diafiltration. At 2.5 wash volumes, during the diafiltration, the removal rate is almost identical, and a higher rate is not observed in the run at 40 bar pressure. At the end of the diafiltration stage, before the second concentration is performed (7 WV), the removal of solvent is very low for both pressures. The lack of measurements between 2.5 and 6 wash volumes does not allow a check of the exact point of the end solvent removal.

iii. EDTA Removal

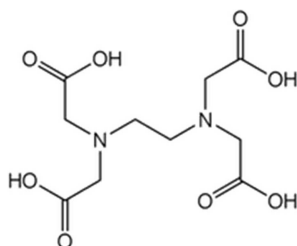


Figure 4.34 - Molecular structure of EDTA.

EDTA belongs to the aminocarboxylic acid group and it is used with the dye solution as a chelating agent, forming stable complexes with the metal ion. EDTA is used to sequester the metal ion in the aqueous dye solution, preventing metal ion impurities from contaminating the final product.

The results of free metal removal were described previously, but it is also important to know if there is any effect of pressure on the removal of EDTA and consequently the removal of the metal sequestered. Figure 4.35 shows the profile obtained for the EDTA removed in the permeate during both trials at 30 and 40 bar.

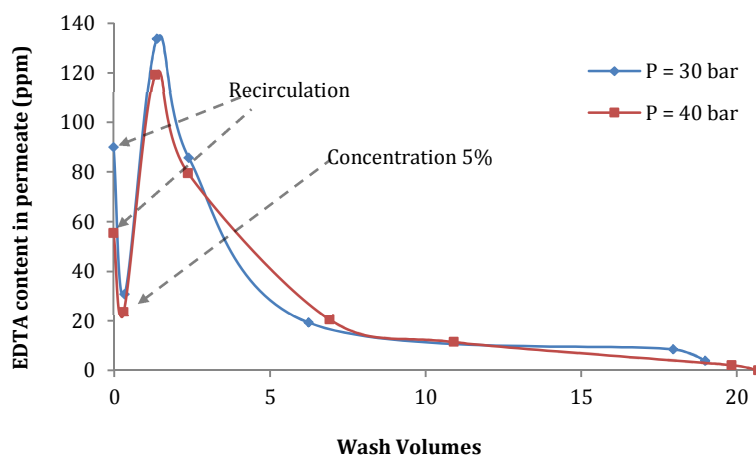


Figure 4.35 - EDTA content profile in the permeate, at 30 and 40 bar.

The figure above shows that the difference of the pressure does not affect the profile obtained for the EDTA content in the permeate. The fact that the initial volume of both samples was not exactly the same may have some influence on the results. The EDTA content removed to the permeate at the beginning of the run, during recirculation, is a considerable amount. Its concentration decreases significantly during the first concentration to 5%, and that is probably due to the increase of aggregation of the dye on the membrane surface and to the fact that the flux rate at this point is very low as a

consequence of the high viscosity. After this point, the EDTA content peaks at 1.4 wash volumes, decreasing afterwards until the end of the washing/diafiltration, where it is negligible. Similar to what happens with the free metal removal, most of the EDTA is removed during the first 7 wash volumes.

In order to evaluate the pressure effect on the EDTA removal, Figure 4.36 shows the rate of removal, expressing the concentration removed per litre of permeate collected.

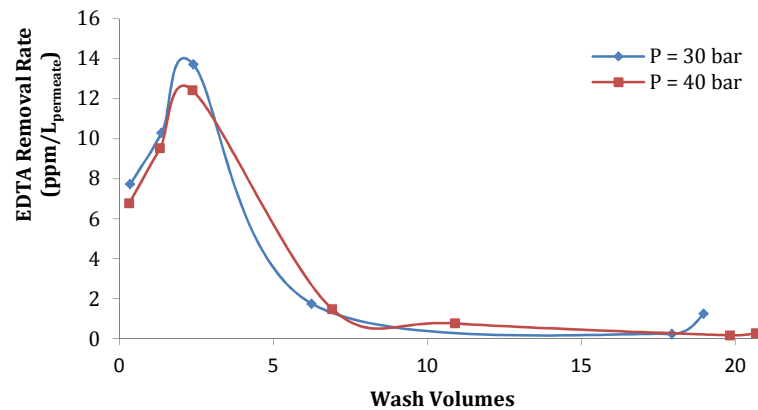


Figure 4.36 - Rate of EDTA removal at 30 and 40 bar.

It is observed that the removal of EDTA is higher at 30 bar pressure during the process. Similarly to what happens with the free metal removal, the results suggest that the increased pressure does not lead to a higher removal of EDTA. The explanation lies in the same phenomena described previously, the dye aggregates enlarge the effect of concentration polarisation on the membrane surface, which does not allow a higher removal with higher pressure.

4.2.2.7 Cycle Time and Wash Volumes

In order to evaluate the overall effects due to an increase of pressure, it is also important to study the variation of other parameters, not related with the separation itself. Therefore, the cycle time and the number of wash volumes are important factors, mainly from the economical point of running the membrane process.

The cycle time is not the most relevant factor in a laboratorial scale, but it becomes much more relevant in a large scale production, where the time of loading, discharging and cleaning are added to the cycle time of the filtration process. In the experiments carried out on the laboratory, the cycle time corresponds only to the period of time during which the unit is operating.

The cycle time depends of the volume of the sample to process i.e. depends on the total amount of the dye present in the sample. It also depends of the level of impurities present. Thus, the values of the cycle time have to be compared carefully.

In order to have an overview of the typical cycles time to the Cyan-X processing, the cycle time obtained for some runs was adjusted to the same amount of initial dye, 400g at 100% strength, and the results are plotted on Figure 4.37.

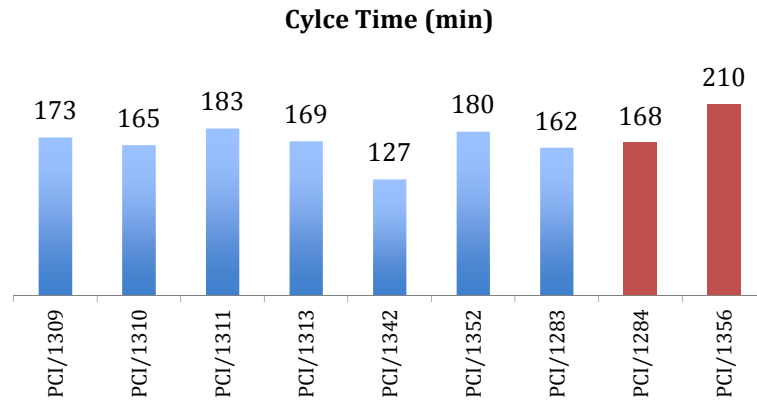


Figure 4.37 - Overview of the cycle time of some runs of Cyan-X, at 30 and 40 bar.

The red bars correspond to trials carried out at 40 bar, and the results suggest that those runs tend to have slightly higher cycle times. It could be expected a lower cycle time operating under higher pressure, but as it was described, the increase of applied pressure does not seem to accelerate the rate of the impurities removal (the conductivity decrease does not seem to be faster). However, the most important factor related to the cycle time is the impurities content.

The trials PCI/1283 and 1284 are from the same batch production (are the ones that have been compared during the evaluation) and it is observed that when the dye weight is adjusted to the exact same amount, the run at 40 bar pressure takes slightly longer than the run at 30 bar. Figure 4.38 show the actual times obtained for both of these trials, showing the time that each filtration stage takes.

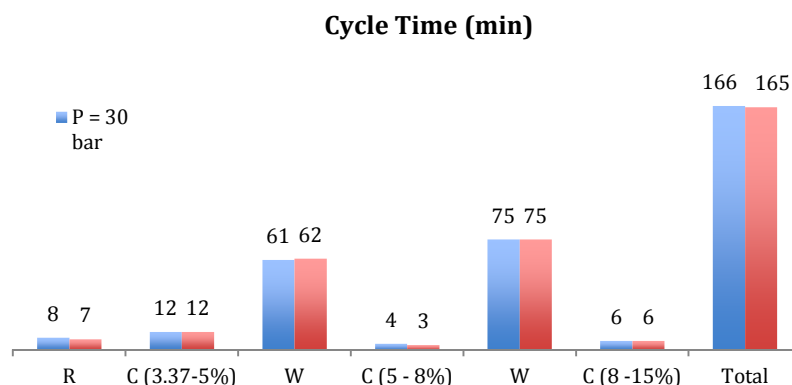


Figure 4.38 - Comparison of the cycle time, showing the different filtration stages, at 30 and 40 bar, runs PCI/1283 and 1284.

The chart above shows the actual times obtained of the recirculation (R), concentrations (C) and washing/diafiltration (W), at 30 and 40 bar. It is observed that in all the stages, the times are equivalent equals for both pressures. Thus, the increase of applied pressure does not have a significant effect on the cycle time.

However it is important to mention that, if the results were scaled up to the production unit, the conclusions could be different because the cycle time is related with the number of wash volumes required. While on the laboratory scale, one wash volume was around 8 litres, on plant scale this is 15,000 litres. Thus, if more wash volumes are required there might be a significant effect on the cycle time.

Wash volume is the volume of permeate removed equivalent to the total volume of the sample in the system, including the hold-up volume. When the system is in recirculation, the volume of permeate is equal to the volume of DI water added to the system, thus wash volumes are the measure of the amount of necessary DI water. Figure 4.39 shows the number of wash volumes required for both runs, showing the number of wash volumes required for each stage (recirculation, concentration and washing/diafiltration).

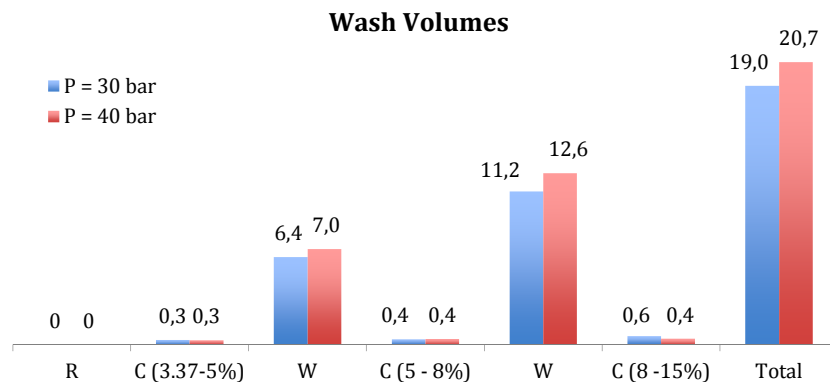


Figure 4.39 - Comparison of wash volumes required at 30 and 40 bar pressure, showing the filtration stages.

The results show that the run at 40 bar pressure required 1.7 wash volumes more than the one at 30 bar, mainly during the second stage of diafiltration. This fact is expected because, at 40 bar, the flux rate is higher, thus more permeate is collected and consequently more wash volumes are needed.

Comparing the wash volumes with the cycle time and the conductivity, the results suggest that, supplying more DI water to the system does not lead to a faster decrease of the conductivity (which means that it does not increase the removal rate of the impurities), and as result, the cycle time does not decrease significantly.

4.2.2.8 Membrane Performance and Limitations

The cold water flow is measured before each trial carried out on the PCI unit, at a constant temperature (25 °C) and at the pressure that will be applied to the trial. There is a natural decrease of the CWF measured with time, as a consequence of membrane fouling and depending of the samples characteristics, the contribution to the membrane fouling will be less or greater. These measurements allow the membrane performance to be tracked over time, to determine when a chemical clean should be done and the end of the membrane lifetime. Figure 4.40 shows the initial CWF measurements of some Cyan-X runs with time.

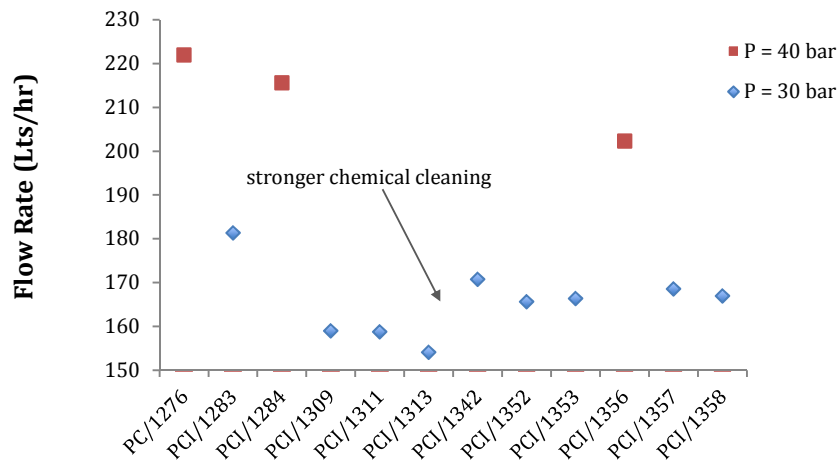


Figure 4.40 - Initial CWF measurements of several runs on PCI. Experimental conditions: 30 or 40 bar pressure, temperature of 25°C, pump speed 5.

The graph shows the decrease of membrane performance and also the recovery achieved when a cleaning agent is used. The lack of data and the fact that only a few trials were carried out at 40 bar, does not allow an accurate conclusion about any greater membrane damage at 40 bar. However, the run PCI/1356 was performed at 40 bar and the initial CWF of the following runs (1357 and 1358) are not different on the graph. This evidence suggest that running the membrane unit at 40 bar does not reduce the membrane performance more than the current runs at 30 bar.

On the other hand, it might be sensible to consider the effect of the pressure on the membrane compaction. As mentioned previously, the membrane compaction is the name given to the irreversible “flattening” of a membrane due to pressure. It is function of pressure and temperature and it can be an important factor that affects membrane performance and lifetime. There are no rules available but, according the literature [39], the guidelines to avoid or minimize compaction, described on Table 4.5, can be applied to the experimental conditions.

Table 4.5 - Guidelines to avoid or minimise compaction applied to the experimental conditions.

Literature	Pressure (bar)	x	Temperature (°C)	< 1200	Safe operation. Standard elements.
				1200 - 2000	Difficult. Special element design.
Trials	30	x	35.6	1068	< 1200
	40	x	38.7	1548	> 1200

The experimental conditions are 30 and 40 bar pressure and the average temperatures during the runs (appendix B). Using this method and operating at 40 bar pressures and at higher temperatures, can lead to a less safe operation where special element design is needed.

On the evaluation of the high pressure effects on the membranes performance, it is necessary to take into consideration the temperature effect on the membranes damage. The current processing has no temperature control, whereby, at 40 bar, the membranes operate under high pressure and temperature, and it can lead to greater permeate reduction over the time. Using the same literature guidelines ^[39], processing at temperatures between 15 and 50°C should be restricted to a maximum pressure of 30 bar to avoid compaction.

4.2.2.9 Summary of Results Obtained at 30 and 40 bar

Table 4.6 - Summary of the results compared at 30 and 40 bar pressure.

Parameter Evaluated	Result	More Advantageous to the Process		
		30 bar	40 bar	No Relevant Difference
Permeate Conductivity	The permeate conductivity peaks and decrease mostly equally under both pressures, taking roughly the same time to achieve low values.			√
Temperature	Operating at 40 bar pressure, the temperature of the feed solution increases faster, and it gets closer to the limit during the first and final concentrations.	√		
Flux Rate	Higher flux rates obtained for the run at 40 bar, with an average of increase of 6.1%. During second and last concentrations, the increase is not significant.		√	
Process Yield	Higher percentage of product recovered operating the system at 30 bar pressure.	√		
Permeate Colour Losses	Higher permeate colour losses during most run, operating at 40 bar pressure. The biggest differences occur during the first concentration and at 2.4 wv, with an increase of permeate colour losses at 40 bar of more than 50%.	√		
Metal Rejection	Comparing the runs at 30 and 40 bar, the results vary depending the stage of the run. However, in average, there is an increase of metal rejection of 3% operating at 40 bar pressure.	√		
Solvent Removal	Not significant difference on the solvent removal.			√
EDTA Removal	It was observed a decrease of 16% of EDTA removed in the permeate, operating at 40 bar.	√		
Wash Volumes	An additional 1.7 wash volumes were required to the run at 40 bar.	√		
Cycle Time	Not relevant difference on the time required to carry out the filtration.			√
Membrane Damage	According to literature, with no heat control, operating at higher pressure and temperature can lead to reduction in the membrane performance.	√		

5 Conclusions

The results discussed intend to evaluate and explain how an increase of pressure affects the productivity and the quality of the product studied. The conclusions are supported by the comparison of the main parameters involved in the filtration process and also for the membrane characterisation.

The membrane characterisation was carried out before and after a run of Cyan-X at 40 bar, and it was observed that the hydraulic permeability of the membrane decreased, on average by 6% after the run, 3% is recovered with a chemical clean. Although a more aggressive cleaning could have been carried out, these values were obtained by carrying out the usual cleaning procedure. Using the hydraulic permeability coefficients and the fluxes measured, it is concluded that the initial membrane performance is not restored to 100%, which is due to the membrane fouling and some to compaction of the membrane. Regarding the operating pressure it is concluded that, operating at 30 bar, the membrane performance is restored to 98%, while operating at 40 bar the recovery is about 96%.

The data from the runs of Cyan-X at 30 and 40 bar and the analysis of the product was gathered to evaluate the variation of main parameter with pressure.

It is shown that the temperature of the feed solution increases quicker at 40 bar, and consequently it gets closer to the limiting temperature of 50°C, during the concentration stage than at 30 bar. This is an important parameter that contributes to the reduction in membrane performance.

The combination of the increase of pressure with the higher temperature, that lowers the viscosity, leads to increase of the flux rate, on average, in 6% at 40 bar. This increase is mainly noticeable during the diafiltration stages, because during the concentration stages the flux rate decay is similar for both pressures. The 6% of flux increase observed for Cyan-X is much lower than the value recorded, at the same temperature, for pure water - 15% of flux increase. This expected difference, is related with fouling and concentration polarisation phenomena and with the dye molecular structure itself. The fact the flux does not increase significantly leads to the conclusion that the limiting flux is close to being achieved, which means that it becomes independent of the pressure.

Concerning the permeate conductivity, the results show that despite the permeate flux being slightly higher at 40 bar, it does not significantly affect the profile of the permeate conductivity. As the conductivity indicates the presence of ionic species, it means that there is not a big difference of impurities removed between 30 and 40 bar. It is shown that it requires the same diafiltration time to achieve the desired low level of permeate conductivity.

On the process yield evaluation, the increased pressure does not improve the product recovery. At 30 bar the process yield is higher than at 40 bar.

The pressure increase has a significant effect on the permeate colour losses, the run at 40 bar presents higher colour losses than the run at 30 bar. The higher fluxes observed at 40 bar, lead to a bigger loss of the dye, which has an impact on the mass balance. Although the amounts of dye measured in the permeate samples are not high, operating at 40 bar does cause an increase of colour loss of 25%.

The removal of impurities represents a crucial part of the filtration process, in order to achieve a high level of purity of the product. Therefore, it is important to find the ideal operating conditions to optimise the filtration. It is shown that, an increase of pressure does not guarantee a higher removal of impurities. Due to the concentration polarisation phenomenon and the fact that the dye molecules tend to form aggregates of macromolecules on the membrane surface, higher fluxes does not lead to higher removal of impurities, because the resistance on the membrane surface increase. Concerning the metal ion removal, the results show that the rejection increases during most stages of the filtration process, operating at 40 bar.

Another impurity to remove is the solvent present in the sample, this causes a very high viscosity to the product. It was observed that the increase in the pressure does not significantly change the amount of solvent removed or the rate at which the removal is effected.

Regarding the complexing agent, EDTA, in which is attached the metal ion in the feed, is removed during the process. The increase of pressure does not yield higher removal. Operating at 40 bar pressure, gives an average decrease of agent removal of 16 %, comparing with the run at 30 bar.

Finally, two parameters important to the process optimisation are the cycle time and the number of wash volumes required during the diafiltration. These parameters are very important on a large scale production, as they are considerable economical factors. The diafiltration is performed with deionised water, which means that there are significant costs in the water consption. The diafiltration is carried out at constant volume, thus operating at higher pressure (higher permeate fluxes) means higher volume of DI water required. The results show that the run at 40 bar required more 1.7 wash volumes than the run at 30 bar.

As a consequence of the increase in the impurity rejection at 40 bar, the cycle time of the operation does not change significantly, despite the higher fluxes. Both trials offer a similar cycle time.

The overall conclusion of the thesis, considering all the parameters, is that increasing the operation pressure from 30 to 40 bar does not provide clear benefits to the process, nor does it improve or reduce the product quality and process yield. The purity of the final product seems to depend more on the components that are initially present in the samples, than to the applied pressure during the filtration process. The results also suggest that operating at 40 bar and consequently higher temperatures, might lead to a faster reduction in the membrane performance.

5.1 Further Work Proposals

FUJIFILM Imaging Colorants is a leading global supplier of high performance aqueous inks, offering technological performance that has enabled aqueous ink jet dyes to be used in many new markets sectors including, photography, commercial printing, packaging, labels, textiles, etc. With the appearance of new products and a growing competitive market, FFIC continue the development to improve the product quality and to minimise the production costs.

In particular, concerning this evaluation, it is important to quantify on a longer term, the membrane performance decay at 40 bar, as the membranes cost is a very important factor. It is also important to know how much it is possible to recover of the membrane performance, by applying a more aggressive chemical cleaning by tracking the CWF.

The aqueous inkjet solutions can be produced from variable material (different impurities present), thus it is important to study how the pressure applied affects the filtration of different production batches. It would be important to study how the pressure affects different samples with different initial compositions. In order to have a wider range of data, which would allow more reliable comparisons, more experiments at 30 and 40 bar pressure would be necessary, keeping the initial volume and strength constant.

The filtration process performed on the pilot membrane unit is the same of the one carried out on the production plant, it would be useful to try to reproduce exactly the plant operating conditions, to facilitate the pressure change. An increase of 10 bar does not have a significant impact on the energy costs on the laboratory scale but it would be crucial to study the impact of a higher pressure on the costs related with the feed pumps and with the DI water consumption.

References

- [1] – <http://www.fujifilm.com/> (May 2012);
- [2] - <http://www.sdi.co.uk/resources/case-studies/chemical-sciences/fujifilms-imaging-colorants.aspx> (May 2012);
- [3] – <http://ffukhx09/online/default.htm> (FFIC Intranet)
- [4] - <http://www.fujifilmic.com> (May 2012)
- [5] – Scott, K., Hughes, R., *Industrial Membrane Separation Technology*, 1st ed., Blackie Academic & Professional, 1996;
- [6] - Strathmann, H, Giorno, L., Drioli, E., *An Introduction to Membrane Science and Technology*, Institute of Membrane Technology, CNR-ITM at University of Calabria, Italy, 2006;
- [7] - *How the Dye Industry is Benefiting from Membrane Technology*, Filtration+Separation, June 2002;
- [8] – <http://www.pcimembranes.pl/>; (September 2012)
- [9] - Porter, M. C., *Handbook of Industrial Membrane Technology*, Noyes Publications, New Jersey, 1990;
- [10] – Dynapol, Palo Alto, Calif., *Salt Addition in Ultrafiltration Purification of Solutions of Polymeric Colorants*, Booth, R. G., Cooper, A. R., US 4,189,380, Feb. 19, 1980;
- [11] – www.pall.com (September 2012)
- [12] - *Protein Concentration and Diafiltration by Tangential Flow Filtration*, Millipore, 2003;
- [13] - Z. Kovácsa, M. Discacciatib, W. Samhabera, Numerical simulation and optimization of multi-step batch membrane processes, *Journal of Membrane Science* 324, 50–58, July 2008;
- [14] – D. Sen, A. Roy, A. Bhattacharya, D. Banerjee, C Bhattacharjee, Development of a knowledge based hybrid neural network (KBHNN) for studying the effect of diafiltration during ultrafiltration of whey, *Desalination* 273, 168–178, November 2010;
- [15] – Y. Priscilla Lai, M. Mondor, C. Moresoli, H. Drolet, M. Gros-Louis, D. Ippersiel, F. Lamarche, Y. Arcand, Production of soy protein isolates with low phytic acid content by membrane technologies: Impact of the extraction and ultrafiltration/diafiltration conditions, *Journal of Food Engineering* 114, 221–227, August 2012;
- [16] - C. Baldasso, T.C. Barros, I.C. Tessaro, Concentration and purification of whey proteins by ultrafiltration, *Desalination* 278, 381–386, June 2011;
- [17] - M. Yazdanshenas, A.R. Tabatabaenezhad, R. Roostaazad, A.B. Khoshfetrat, Full scale analysis of apple juice ultrafiltration and optimization of diafiltration, *Separation and Purification Technology* 47, 52–57, June 2005;
- [18] – Z. Lia, A. H-Kittikuna, W. Youravongb, Purification of protease from pre-treated tuna spleen extract by ultrafiltration: An altered operational mode involving critical flux condition and diafiltration *Separation and Purification Technology* 66, 368–374, December 2008;
- [19] - *A Hands-On Guide to Ultrafiltration/Diafiltration Optimization using Pellicon Cassettes*, Millipore, 2008;
- [20] – S. Loeb, L. Titalman, E. Korngold, J. Freiman, Effect of porous support fabric on osmosis through a Loeb-Sourirajan type asymmetric membrane, *Journal of Membrane Science* 129, 243-249, 1997;
- [21] – <http://www.engineer.ucla.edu/explore/history/major-research-highlights/first-demonstration-of-reverse-osmosis> (July 2012);

- [22] – Ridgway, H. F., PhD, *Advanced Membrane Technologies*, Stanford University, May 2008;
- [23] – Nunes, S. P., Peinemann, K. V., *Membrane Technology in the Chemical Industry*, WILEY-VCH, Weinheim, 2001;
- [24] – Baker, R. W., *Membrane Technology and Applications*, 2nd ed., John Wiley & Sons, California, 2004;
- [25] – Nath, K., *Membrane Separation Processes*, PHI Learning, 2008;
- [26] - <http://www.geafiltration.com> (August 2012);
- [27] - <http://kochmembrane.com/Learning-Center> (September 2012)
- [28] - Mulder, M., *Basic Principles of Membrane Technology*, 2nd ed., Kluwer Academic Publishers, 2003;
- [29] - Norman N. Li, Anthony G. Fane, W. S. Winston Ho, and T. Matsuura, *Advance Membrane Technology and Applications*, John Wiley & Sons, Ltd, 2008;
- [30] - Caetano, A., Pinho, M.N, Drioli, E., Muntau, H., *Membrane Technology Applications to Industrial Wastewater Treatment*, Kluwer Academic Publishers;
- [31] - P.M. Bungay, H.K. Lonsdale, M. N. de Pinho, *Synthetic Membranes: Science, Engineering and Applications*, D. Reidel Publishing Company, 1983;
- [32] - W. Richard Bowen, F. Jenner, Theoretical descriptions of membrane filtration of colloids and fine particles: An assessment and review, *Advances in Colloid and Interface Science* 56, 141-200, 1995;
- [33] - R. Rautenbach, R. Albrecht, *Membrane Processes*, John Wiley & Sons, 1989;
- [34] - M. N., Pinho, V. Geraldes, L. M. Minhalma, *Integração de Operações de Membranas em Processos Químicos*, Lisboa, 2002;
- [35] - www.millipore.com (September 2012);
- [36] - K. Scott, *Handbook of Industrial Membranes*, 1st ed, Elsevier Science Publishers, 1995;
- [37] – Y. Fujie, N. Hanaki, T. Fujiwara, S. Tanaka, M. Noro, K. Tateishi, K. Usami, A. Hibino, N. Wachi, T. Taguchi, Y. Yabuki, Development of High Durability Cyan and Magenta Dyes for Ink Jet Printing System, *Fujifilm Research & Development*, No.54, 2009;
- [38] – Sesta, N., *Evaluation and Optimisation of Spiral Membranes for Purification of Inkjet Colorants*, 2006;
- [39] – Wagner, J., *Membrane Filtration Handbook – Practical Tips and Hints*, 2nd ed., B. Sc. Chem. Eng., 2001.

Appendix A - Experimental Results of Membrane Characterisation

Table A.1 - Water characterisation at three different pressures, before a run of cyan.

Pressure (bar)	Flux rate (Lts/m ² .hr)				
	T = 25 C	T = 30 C	T = 35 C	T = 40 C	T = 45C
30	480.71	523.06	568.94	606.82	654.59
35	525.88	571.765	625.88	680.71	725.65
40	567.76	614.82	666.12	729.88	776.94

Table A.2 - Water characterisation at three different pressures, after a run of cyan.

Pressure (bar)	Flux rate (Lts/m ² .hr)				
	T = 25 C	T = 30 C	T = 35 C	T = 40 C	T = 45C
30	447.53	496.47	540.71	579.06	622.82
35	494.35	537.41	581.65	633.88	679.06
40	531.76	579.06	632.00	681.65	734.59

Table A.3 - Water characterisation at three different pressures, after the chemical cleaning.

Pressure (bar)	Flux rate (Lts/m ² .hr)				
	T = 25 C	T = 30 C	T = 35 C	T = 40 C	T = 45C
30	471.53	511.76	557.412	597.88	640.47
35	522.12	556.24	601.18	650.82	697.65
40	556.71	591.29	639.29	693.88	745.65

Appendix B – Experimental Results of Cyan-X trials

Table B.1 - Experimental results of the Cyan-X run carried out at 30 bar pressure, used for the comparison in section 4.2.2.

Colour	Cyan-X	Initial Strength	8.2%	Initial Data					
Sample	ex. 26 / Bx. 603	pH	9.08	CWF	181.3 Lts/hr				
Run No.	PCI/1283	Starting Volume	5 L	Pressure	30 bar				
Membrane	ES – 209	Final Volume	2.1 L	Temperature	25.0 C				
Area	0.425 m ²	1st Disp. Volume	1 L	pH	4.05				
Results				Final Data					
Average Temperature		35.6 °C		CWF	-				
Average Pressure		30 bar		Pressure	-				
Wash Volumes		18.98		Temperature	-				
				pH	-				
Readings									
Time (min)	Flux Rate (Lts/m ² .hr)	Conductivity (µS)	Temperature (C)	pH	Cumulative Vol. (Lts)	Tank Level (Lts)	Comments	Wash Volumes	Operation
0	25.18	1.1	23.7	9.23	0	10.1	3.37%	0.00	R
8	40.94	8800	30.6	9.14	0	10.1	P1/C1	0.00	R
20	48.00	16620	41.7	8.89	4	6.3	P2/C2, 5%	0.34	C
35	104.00	10820	41.6	9.02	12	6.3	P3/C3	1.37	W
45	130.82	5370	38.2	9.05	20	6.3	P4/C4	2.40	W
55	142.12	2510	35.5	9.00	28	6.3	-	3.42	W
63	144.71	1276	34.1	8.94	36	6.3	-	4.45	W
71	146.82	731	33.4	8.82	44	6.3	-	5.47	W
77	147.29	500	33	8.72	50	6.3	P5/C5	6.24	W
81	149.18	415	32.9	8.65	54	6.3	-	6.76	W
85	111.29	408	38	8.46	57	3.4	8%	7.14	C
91	106.82	372	37.3	8.33	62	3.4	-	8.16	W
98	106.59	309	37.1	8.21	67	3.4	-	9.18	W
105	107.06	251	36.6	8.05	72	3.4	-	10.20	W
112	108.24	200	36.7	7.88	77	3.4	-	11.22	W
118	108.24	166	36.3	7.74	82	3.4	-	12.24	W
125	107.53	137	36.3	7.60	87	3.4	-	13.26	W
132	107.76	114	36.5	7.59	95	3.4	-	14.28	W
143	108.00	88.8	36.2	7.42	100	3.4	-	15.91	W
157	107.76	65.7	36.2	7.20	110	3.4	P6/C6	17.96	W
160	108.47	60.9	36.1	7.17	112	3.4	-	18.36	W
166	70.59	91.8	44.6	7.01	115	1.1	P7/C7	18.98	C

Table B.2 - Experimental results of the Cyan-X run carried out at 40 bar pressure, used for the comparison in section 4.2.2.

Colour		Cyan-X	Initial Strength		8.2%	Initial Data			
Sample		ex. 26 / Bx. 603	pH		9.27	CWF	215.6 Lts/hr		
Run No.		PCI/1284	Starting Volume		4.8 L	Pressure	40 bar		
Membrane		ES - 209	Final Volume		2.1 L	Temperature	25.0 C		
Area		0.425 m ²	1st Disp. Volume		1 L	pH	4.35		
Results						Final Data			
Average Temperature			38.7 C			CWF	216.3 Lts/hr		
Average Pressure			40 bar			Pressure	40 bar		
Wash Volumes			20.69			Temperature	25.0 C		
						pH	4.89		
Readings									
Time (min)	Flux Rate (Lts/m ² .hr)	Conductivity (mS)	Temperature (C)	pH	Cumulative Vol. (Lts)	Tank Level (Lts)	Comments	Wash Volumes	Operation
0	26.12	15.9	25	9.27	0	9.6	3.37%	0.00	R
7	44.47	9310	33.5	9.13	0	9.6	P1/C1	0.00	R
19	53.88	16710	46.4	8.82	3.5	6	P2/C2, 5%	0.32	C
31	106.59	11150	44.9	8.93	11	6	P3/C3	1.32	W
41	133.18	5470	40.7	8.96	19	6	P4/C4	2.38	W
50	143.29	2710	37.8	8.96	27	6	-	3.45	W
57	147.53	1590	36.4	8.90	34	6	-	4.38	W
65	150.59	895	35.5	8.79	42	6	-	5.45	W
73	151.53	569	35	8.70	50	6	-	6.52	W
77	151.06	500	34.8	8.65	53	6	P5/C5	6.92	W
81	152.00	477	34.7	8.61	56	6	-	7.32	W
84	113.88	442	40.6	8.41	59	3.2	8%	7.72	C
89	112.47	397	39.8	8.29	64	3.2	-	8.78	W
96	114.59	326	39.9	8.20	69	3.2	-	9.84	W
102	116.94	271	39.9	8.08	74	3.2	P6/C6	10.91	W
109	116.47	221	39.5	7.98	79	3.2	-	11.97	W
114	117.41	192	39.8	7.90	83	3.2	-	12.82	W
120	117.88	162	39.9	7.78	88	3.2	-	13.89	W
125	118.12	162	39.7	7.69	92	3.2	-	14.74	W
131	117.18	121	39.6	7.61	97	3.2	-	15.80	W
135	118.35	111.2	39.6	7.57	100	3.2	-	16.44	W
140	117.41	105.2	39.6	7.48	102	3.2	-	16.86	W
154	115.06	68.9	39.6	7.27	116	3.2	P7/C7	19.84	W
159	115.76	64.2	39.6	7.23	118	3.2	-	20.27	W
165	73.65	84.7	46.5	7.10	120	1	P8/C8, 15%	20.69	C

Appendix C – Results of samples analysis

Table C.1 - Results of free metal content in the permeate and concentrate samples collected during the runs.

Run	Permeate		Concentrate	
	Samples	Free Metal (ppm)	Samples	Free Metal (ppm)
PCI/1283 (30 bar)	P1	15.62	C1	39.15
	P2	29.57	C2	69.12
	P3	22.36	C3	47.17
	P4	16.11	C4	29.87
	P5	3.78	C5	10.75
	P6	0	C6	13.21
	P7	0	C7	11.47
PCI/1284 (40 bar)	P1	11.4	C1	37.19
	P2	28.56	C2	65.34
	P3	19.1	C3	50.6
	P4	15.92	C4	25.24
	P5	3.82	C5	11.83
	P6	2.49	C6	12.56
	P7	0	C7	11.86
	P8	0	C8	9.41

Table C.2 - Results of solvent content in the permeate and concentrate sample collected during the runs.

Run	Permeate		Concentrate	
	Samples	Solvent %(w/w)	Samples	Solvent %(w/w)
PCI/1283 (30 bar)	P2	16.88	C1	23.18
	P3	7.5	C4	2.24
	P4	3.44	C5	0.02
	P5	0.14	C7	0.00
PCI/1284 (40 bar)	P2	17.67	C1	18.82
	P3	7.8	C4	2.26
	P4	3.67	C5	2.04
	P5	0.13	C8	0.01

Table C.3 - Results of EDTA content in the permeate samples collected during the runs.

PCI/1283 (30 bar)		PCI/1284 (40 bar)	
Samples	EDTA (ppm)	Samples	EDTA (ppm)
P1	90	P1	55.5
P2	30.9	P2	23.7
P3	133.7	P3	119.1
P4	85.7	P4	79.5
P5	19.3	P5	20.5
P6	8.5	P6	11.4
P7	3.9	P7	2.1
		P8	0

Table C.4 - Measurements of strength of the permeate samples collected during the runs.

Run	Samples	Dilution	Absorbance	Strength (g/L)	Permeate Vol. (L)
PCI/1283 (30 bar)	P1	1	0.1617	0.0037	0
	P2	1	0.1222	0.0028	4
	P3	1	0.1874	0.0043	8
	P4	1	0.05	0.0011	8
	P5	1	0.0336	0.0008	30
	P6	1	0.0314	0.0007	60
	P7	1	0.048	0.0011	5
PCI/1284 (40 bar)	P1	1	0.1552	0.0035	0
	P2	1	0.2479	0.0056	3.5
	P3	1	0.1639	0.0037	7.5
	P4	1	0.1157	0.0026	8
	P5	1	0.0472	0.0012	34
	P6	1	0.0488	0.0011	21
	P7	1	0.0352	0.0008	42
	P8	1	0.048	0.0011	4

